

Structural Stability Properties of Antithetic Integral (Rein) Control with Output Inhibition

Corentin Briat¹ and Mustafa Khammash²

Department of Biosystems Science and Engineering, ETH-Zürich, Switzerland

Abstract

Perfect adaptation is a well-studied biochemical homeostatic behavior lying at the core of biochemical regulation. While the concepts of homeostasis and perfect adaptation are not new, their underlying mechanisms and associated biochemical regulation motifs are not yet fully understood. Insights from control theory unraveled the connections between perfect adaptation and integral control, a prevalent engineering control strategy. In particular, the recently introduced Antithetic Integral Controller (AIC) has been shown to successfully ensure perfect adaptation properties to the network it is connected to. The complementary structure of the two molecules the AIC relies upon allows for a versatile way to control biochemical networks, a property which gave rise to an important body of literature pertaining to mathematically elucidating its properties, generalizing its structure, and developing experimental methods for its implementation. The Antithetic Integral Rein Controller (AIRC), an extension of the AIC in which both controller molecules are used for control, holds many promises as it supposedly overcomes certain limitations of the AIC. We focus here on an AIRC structure with output inhibition that combines two AICs in a single structure. We theoretically demonstrate its superior properties, which are linked to the intrinsic properties of a specific AIC structure with output inhibition. This controller ensure structural stability and structural perfect adaptation properties for the controlled network under mild assumptions, meaning that this property is independent of the parameters of the network and the controller. The results are very general and valid for the class of unimolecular mass-action networks as well as more general networks, including cooperative and Michaelis-Menten networks. We also provide a systematic and accessible computational way for verifying whether a given network satisfies the conditions under which the structural property would hold. Finally, we also propose a possible implementation of such a regulation mechanism using an intein-based synthetic circuit.

1 Introduction

In his pioneering works, Walter B. Cannon laid the groundwork for studying biological and physiological regulation and coined the term “homeostasis”. This concept, which he introduced in 1929, describes the ability of living organisms to regulate their internal processes [21]. Homeostasis encompasses many physiological processes, such as the regulation of body temperature, blood sugar, and cholesterol [43,63] as well as neuronal function in neuroscience [78]. Similar ideas were later adapted and further developed in the seminal works of Jacob, Monod, and co-workers [42,49].

A stringent type of homeostatic regulation of particular recent interest is perfect adaptation. It refers to the ability of a network that is subjected to persistent stimuli (or perturbations) to adapt to that stimulus by

¹Corentin Briat is now with the School of Life Sciences, University of Applied Sciences Northwestern Switzerland, Switzerland. email: corentin@briat.info, url: www.briat.info.

²email: mustafa.khammash@bsse.ethz.ch, url: <https://bsse.ethz.ch/ctsb>

having the molecular concentration of one or more of its constituent species return to their pre-stimulus level. Robust perfect adaptation is achieved when the adaptation property still holds in spite of perturbations of the network’s parameters or topology. The phenomenon of robust perfect adaptation has been observed in biological networks [8, 79, 27, 2, 50], and the elucidation of its underlying mechanisms, design principles, and topological requirements has been extensively reported using both theoretical and computational approaches [79, 2, 26, 48, 52, 14, 6, 45, 39, 5, 41, 17, 12, 45], among others. It is important to note that the concept of robust perfect adaptation is not uniform across all scenarios, and variations exist depending on the exact class of perturbations to which adaptation is robust. It is therefore essential to specify the particular type of perturbations being considered, as this can influence the underlying conditions needed to achieve perfect adaptation.

The *perfect adaptation design problem*, is the problem of designing mechanisms that ensure perfect adaptation for a given biochemical network. This problem has recently attracted a lot of attention, partly due to its parallels with the so-called *regulation problem* and *disturbance rejection problem* in control engineering. These problems involve designing industrial controllers that enable the controlled system to compensate for unmeasured environmental variations and perturbations (disturbances), while keeping the controlled variables at a pre-defined, chosen level (set-point). A simple control strategy known to structurally solve the regulation and the disturbance rejection problems is the so-called *integral controller*, which forms the core of Proportional-Integral-Derivative (PID) controllers, a prevalent control algorithm found in a vast range of applications [1]. This connection between biology, control engineering, and mathematics echos Wiener’s Cybernetics [74], which proposed the existence of control motifs in living systems and suggested that they be studied using the same tools used to study man-made control systems.

The Antithetic Integral Controller (AIC) [14] is one such generic motif. It employs a simple strategy that ensures robust perfect adaptation properties in biochemical systems in both the deterministic and stochastic settings through the implementation of an integral feedback module. Its core mechanism is that of molecular sequestration [22], a method for comparing two molecular levels. The theoretical properties of the Antithetic Integral Controller and its leaky variants have now been well-studied, in both the deterministic [16, 58, 54, 55, 13, 17, 31, 32] and the stochastic [14, 15, 4] settings. Notably, the stochastic model of a specific AIC type – referred to in this paper as naAIC and illustrated in Figure 8 – exhibits structural stability properties under very mild conditions. Interestingly, this property is absent in its deterministic counterpart, which requires significantly stronger conditions to achieve stability. A key requirement for effective control is *set-point admissibility*, which ensures that the topology of the controlled network allows molecular levels of the controlled species to reach a desired set-point, potentially through appropriate tuning of the control parameters. As discussed in Box 1 for the specific case of a gene expression network and more generally in [14, 13], the original AIC – referred to here as naAIC and defined in (3.2) – is inherently limited to regulating the controlled species above its basal expression level. Sub-basal levels are unattainable, consistent with the fact that the naAIC structure influences the transcription rate of mRNA or, more broadly, acts as a direct or indirect activator of the controlled species. In contrast, a less explored AIC structure – denoted here as niAIC and defined in (3.3), also discussed in the context of gene expression regulation in Box 1 – operates as an inhibitor of the controlled species. This structure allows for regulation of protein levels below their basal expression level. This distinction highlights the critical impact of input selection and controller network topology on the set of admissible set-points for the controlled molecular species.

A natural question arises: can a controller topology be designed to both expand the set of admissible set-points and ensure the necessary stability properties of the controlled network? Developing a general strategy for this purpose would not only enhance the theoretical appeal of the design but also improve its practical robustness to changes in the process. For instance, one could easily envision scenarios where environmental or cellular context changes render a previously admissible set-point non-admissible. Such changes would inevitably destabilize the controlled network, potentially resulting in oscillations, saturations, or even cell death.

The Antithetic Integral Rein Controller (AIRC), introduced in [38], exploits the bimolecular structure of the AIC by utilizing its two controller species in separate channels for network modulation and giving rise to a wide variety of possible control topologies, as can be seen in Figure 1a. The specific AIRC considered in [38], which we refer here as an *aiAIRC with output inhibition* and depicted in Figure 1b, employs the first controller species as an indirect activator of the controlled species and the second as a direct inhibitor of the controlled species. This configuration offers certain advantages, including the possibility to reach a wider range of set-points, compared to the naAIC described above, and potentially improving the transient response of the network [38]. This controller network topology could potentially expand the range of admissible set-points – a possibility that, to date, has not been rigorously proven in general. Similarly, the analysis of its essential stability properties has largely been limited to the context of gene expression [38], providing only limited insight into more general network configurations. While set-point admissibility is an important prerequisite for adaptation, the central concern is stability. Stability ensures that the controlled network reliably converges to the steady state associated with the desired set-point for the controlled molecular species. Once again, both the choice of inputs to the controlled network and the controller topology play a crucial role in determining stability. These decisions must be made carefully, in accordance with the system’s property in order to ensure the desired properties for the controlled network.

Our aim in this work is to elucidate the properties of both the aiAIRC with output inhibition and its component, the niAIC with output inhibition. We first show that, for unimolecular networks, the aiAIRC with output inhibition yields nonnegative equilibria regardless of the value of the set-point, implying that, in contrast to the naAIC, all positive set-points are admissible for that controller. This finding is established here more broadly and simply than in previous studies [38, 56]. Additionally, we show that the aiAIRC with output inhibition exhibits an interesting equilibrium switching behavior in the strong sequestration regime, which corresponds to the regime where the controller species sequestration rate is large. This regime has been extensively studied in theoretical analyses of antithetic integral control structures [57]. In this regime, the AIRC toggles between activation and output inhibition of the controlled species based on the set-point’s relation to the basal expression level, behaving alternately like an naAIC or an niAIC with output inhibition. This behavior underscores the importance of studying the much less explored niAIC with output inhibition.

We first establish that the niAIC with output inhibition locally behaves like a filtered Proportional-Integral (PI) controller, in contrast to the naAIC’s sole integral control action, as discussed in similar context in [31, 32]. A key difference of PI controllers over purely integral controller, as implemented by the naAIC in [14, 13], is that the proportional action has the capacity of stabilizing the dynamics of a controlled system and improving its transient behavior, as also pointed out in [15]. We further demonstrate that this class of controllers solves the perfect adaptation problem and provide necessary conditions on the network for adaptation that are similar in flavor to those obtained for the naAIC in [13]. We then leverage ideas from control theory, dynamical systems, and linear algebra to show that when the network is unimolecular and stable, the closed-loop network will also be stable, provided that the set-point is admissible (i.e. below the basal expression level) for all possible values for the gain of the controller and its sequestration rate. Exploiting the stabilization properties of the controller, we then extend these results to a more general class of networks, which we refer to *output unstable networks*, for which the same result holds but with no restriction on the set-point value. These results are further extended to the AIRC with output inhibition.

Addressing general nonlinear networks presents a challenge due to their diversity and complex technical aspects. Despite these hurdles, we successfully establish structural stability principles applicable to these networks. These principles can be assessed on case-by-case manner using readily available computational methods, which we outline. Interestingly, we find that for certain significant subclasses, such as cooperative and Michaelis-Menten networks, those extensive additional analyses are unnecessary. Indeed, in these case we can directly apply general results similar to those established for the unimolecular case.

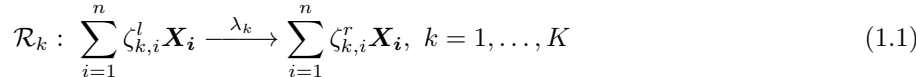
Concluding our study, we propose a feasible implementation of the controller using intein-based systems

[51, 73]. This approach draws on existing knowledge in synthetic biology and previous developments in intein-mediated controllers, most notably the work of Anastassove et al. [3].

The main takeaway of this paper is that AIRC networks offer a powerful framework for controlling reaction networks, possibly in the presence of non-monotonic reaction paths that may alternate between activation and inhibition depending on the network configuration. These controller networks address set-point limitations and ensure structural stability, both of which are critical for controlling highly uncertain systems using controllers that face similar constraints and for which fine-tuning may not be feasible. This paper further complete past works from the same authors and provides a mathematical foundation for these claims in the context of niAIC with output inhibition and its associated aiAIRC structure. We believe this work marks a significant step forward in advancing a robust mathematical control theory for reaction networks, systems biology, and synthetic biology.

Reaction Networks

Reaction networks are a very powerful modeling paradigm that can be used to represent any population system, such as those arising in biology, ecology, epidemiology, etc.[37]. A reaction network $(\mathbf{X}, \mathcal{R})$ consists of a set of n molecular species $\mathbf{X} = \{\mathbf{X}_1, \dots, \mathbf{X}_n\}$ that interact through K reaction channels $\mathcal{R} = \{\mathcal{R}_1, \dots, \mathcal{R}_K\}$ denoted as



where $\zeta_{k,i}^l, \zeta_{k,i}^r \in \mathbb{Z}_{\geq 0}^n$ are the left and right stoichiometric vectors. The stoichiometric vector of reaction \mathcal{R}_k is given by $\zeta_k := \zeta_k^r - \zeta_k^l \in \mathbb{Z}^n$ where $\zeta_k^r = \text{col}(\zeta_{k,1}^r, \dots, \zeta_{k,n}^r)$ and $\zeta_k^l = \text{col}(\zeta_{k,1}^l, \dots, \zeta_{k,n}^l)$. Each reaction \mathcal{R}_k is also described by its propensity function λ_k that describes, in the deterministic setting, the rate at which this reaction occurs. Such rates may take multiple forms such as mass-action, Hill, Michaelis-Menten, etc. [71, 2]. In particular, when the network only has mass-action kinetics, only the reaction rates are indicated on top of the arrow in (1.1). This will be explicitly mentioned when this is the case. In all those cases, we define \mathcal{P} to be the set of the network parameters, that is, the set of all parameters describing the reaction rates or, more generally, all the parameters of the propensity functions.

In the deterministic setting, reaction networks are quantitatively described in terms of a vector of molecular concentrations, denoted here by $x(t)$, which evolves on a state-space $\mathcal{S} \subseteq \mathbb{R}_{\geq 0}^n$. As a result, the propensity functions $\lambda_k : \mathcal{S} \mapsto \mathbb{R}_{\geq 0}$ are defined in such a way that \mathcal{S} is forward invariant; i.e. for all $x_0 \in \mathcal{S}$, we have that $x(t) \in \mathcal{S}$ for all $t \geq 0$. This will be tacitly assumed to be the case in the rest of the paper. The dynamical model representing the deterministic reaction network (1.1) is, therefore, given by the Reaction Rate Equation (RRE)

$$\begin{aligned} \dot{x}(t) &= \sum_{k=1}^K \zeta_k \lambda_k(x(t)), \quad t \geq 0 \\ x(0) &= x_0. \end{aligned} \quad (1.2)$$

The point x^* is said to be an equilibrium point for the above dynamics if $\sum_{k=1}^K \zeta_k \lambda_k(x^*) = 0$.

Perfect Adaptation

The perfect adaptation property is the property of a reaction network that certain molecular counts will return to the previous equilibrium levels after the appearance of environmental changes and network perturbations. This is one of the many types of homeostatic behaviors that can be found in living organisms [21] or that can be theoretically constructed [2, 48, 14, 36, 45, 39]. The version we consider in this paper is the one below:

Definition 1.1 (Perfect Adaptation) *Consider a reaction network $(\mathbf{X}, \mathcal{R})$ and a species $\mathbf{Y} \in \mathbf{X}$. The species \mathbf{Y} is said to exhibit the perfect adaptation property in the network $(\mathbf{X}, \mathcal{R})$ if*

1. the equilibrium point x^* is (locally) asymptotically stable for the dynamics of the network (1.2), and
2. the equilibrium value of the concentrations of the species \mathbf{Y} , denoted by y^* , is independent of all the parameters in a subset of \mathcal{P} .

The definition of perfect adaptation we consider consists of two components. The stability component is here to guarantee that the network goes back to the same equilibrium after a state perturbation. The second component is the equilibrium perfect adaptation property which indicates that if we perturb the parameters in some subset of \mathcal{P} , the equilibrium for \mathbf{Y} , denoted by y^* , remains the same. Note, however, that the equilibrium states may not be the same. Stronger definitions of perfect adaptation exist. For example, *robust perfect adaptation* requires that the perfect adaptation property remains valid under sufficiently small perturbations to certain network parameters. On the other hand, the property is termed *structural* when it holds for all positive values of specific network parameters. Structural perfect adaptation can be seen as the ultimate form of robustness, which is ensured by the structure of the network rather than by the values of its parameters. We will particularly focus on this latter variant as it is particularly desirable in biological contexts where network uncertainties are significant and fine-tuning is challenging, if not impossible.

Perfect adaptation and its variants are rather strong properties: endogenous and engineered networks may not immediately satisfy them by design. Analogously, industrial systems are not naturally self-regulating (e.g. robots) and require additional components to make them fully functional and reliable. The design of such components is the purpose of control engineering and, keeping that exact same state of mind, we may pose the following question: how to turn a non-adapting network into a perfectly adapting one? There are different possible ways to do so depending on how the problem is formulated and the different constraints. The version of the problem we consider is the one below:

Definition 1.2 (Perfect Adaptation Design Problem) Consider a reaction network $(\mathbf{X}, \mathcal{R})$ and a species $\mathbf{Y} \in \mathbf{X}$. The perfect adaptation problem consists of finding a controller network $(\mathbf{Z}, \mathcal{R}^c)$ such that

1. \mathbf{Y} exhibits the perfect adaptation property in the network $(\mathbf{X} \cup \mathbf{Z}, \mathcal{R} \cup \mathcal{R}^c)$, and
2. y^* is equal to a tunable set-point which is a known function of the controller parameters only (i.e. it is independent of the parameters of the network $(\mathbf{X}, \mathcal{R})$).

The above problem is a reaction network analogue of the more standard engineering control problems in which controllers are designed to ensure certain specifications for the controlled systems. In the present case, the controllers are to be implemented within cells using biological components, whence the name *in-vivo controller*, rather than in a computer. Due to the nature of the substrate, specific constraints and challenges, usually absent in more standard engineering problems, are to be considered to ensure the proper operation of the controllers; see e.g. [46, 18]. The requirement that the set-point be adjustable is facultative here but allows for an increased flexibility and the possible optimization of the overall controlled network, as discussed in [16] in the context of the control of metabolic networks.

When the set-point needs to be adjusted, the question of which set-point values are compatible with the network arises. This leads us to the concept of set-point admissibility:

Definition 1.3 (Set-point admissibility) Consider a reaction network $(\mathbf{X}, \mathcal{R})$ and a species $\mathbf{Y} \in \mathbf{X}$. Moreover, decompose \mathcal{P} as $\mathcal{P}_f \cup \mathcal{P}_t$ where \mathcal{P}_f is a set of fixed network parameters and \mathcal{P}_t is a set of tunable network parameters.

We say that a set-point r is admissible for the species \mathbf{Y} if, given the values for the parameters in \mathcal{P}_f , we can select values for the parameters in \mathcal{P}_t such that $x^* \geq 0$ and $y^* = r$ where x^* is an equilibrium point for the dynamics (1.2). The admissible set for the output \mathbf{Y} is the set of its admissible values.

The motivation for dividing the parameter set \mathcal{P} into two subsets, \mathcal{P}_t and \mathcal{P}_f , is to distinguish between parameters that can be actuated and those that are inherent to the network's structure. In this context,

the admissibility of a chosen set-point is a necessary condition for the proper functioning of the controlled network around that set-point. Setting a non-admissible set-point effectively asks the system to reach an unattainable value, potentially leading to unstable or diverging state trajectories.

Set-point admissibility depends on the network’s structure, the specific output considered, and the choice of tunable parameters. Selecting different tunable parameters results in different admissible sets for the output. This is illustrated in Box 1, where we examine a gene expression network first with the transcription rate as the tunable parameter and then with the protein degradation rate. In this paper, we use set-point admissibility as a preliminary criterion for deciding which parameters should be used to actuate the network. Once these parameters are selected, we can analyze the network’s properties and propose a suitable controller structure to solve the perfect adaptation design problem.

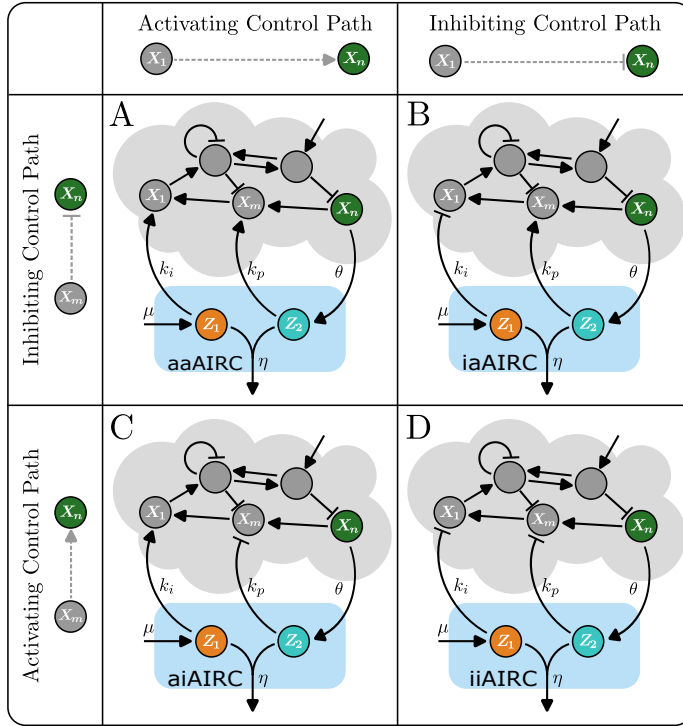
Finally, although set-point admissibility is essential for the perfect adaptation design problem, it is meaningless without stability. Set-point admissibility only indicates the possibility of attaining a certain value for the controlled species at steady state. For this to be meaningful, the state of the controlled network must also converge to that steady state. Without convergence, the system may exhibit diverging or oscillatory trajectories, rendering the concept of perfect adaptation meaningless, as no actual adaptation occurs in the controlled network. Establishing the conditions for stability and structural stability is therefore the main goal of this study.

Antithetic Integral (Rein) Controllers

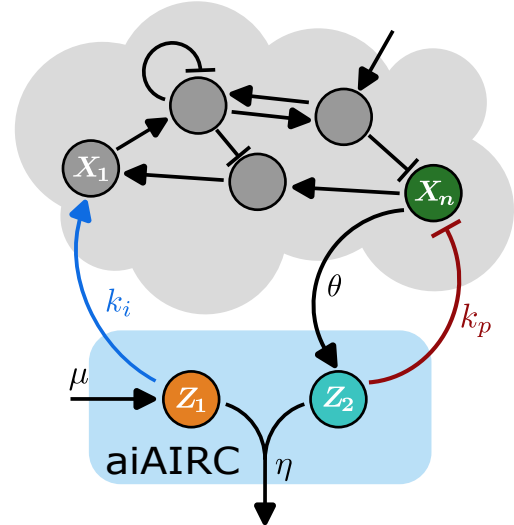
The Antithetic Integral Controller (AIC), introduced in [14] and further discussed in [13, 54, 55], is one of the few, structurally simple, integral controllers that can be implemented in terms of chemical reactions and that can operate in both the deterministic and the stochastic settings. Other integral controllers of course exist, such as zeroth-order integral controllers [52] and autocatalytic integral controllers [25, 19, 76, 13], but are unfortunately only functional in the deterministic setting. The AIC relies on molecular sequestration as core principle, which consists of two complementary molecular species strongly sequestering each other. Sequestration is a well-known mechanism that has been naturally selected to achieve certain pivotal functions within living organisms, such as bacterial stress response through the use of sigma-factors [68]. On a more theoretical level, the sequestration reaction plays an essential role in the solution of realization problems [53, 28] as it can be interpreted as a molecular implementation of a subtraction operator [14, 13, 24, 30]. The internal bimolecular structure of the AIC makes it a very flexible controller that can easily implement negative and positive feedback loops using both activation or inhibition interactions, as illustrated in Figure 8 in Box 1. More advanced structures built upon the AIC can be generated through a clever addition of reactions and species in order to achieve more complex behaviors and performance requirements; see e.g. [35, 33, 3]. The common denominator to all those designs is that the controlled species should repress itself through a sequence of reactions involving controller species, a mechanism that makes the AIC a member of the family of negative feedback controllers.

A particular extension of the AIC is the so-called Antithetic Integral Rein Controller (AIRC), which exploits the bimolecular structure of the AIC to implement a second actuation channel acting in opposition to the first one. The concept of rein control has been introduced by Saunders in [62] as a central mechanism for glucose regulation and was shown to have enhanced robustness properties over a unidirectional control mechanism. Therefore, it is expected that the AIRC benefits from the same advantages over the AIC which only acts on the controlled species in a unidirectional manner and may offer limited performance in some scenarios. As shown in Figure 1a, the AIRC admits multiple possible configurations depending on the role of the controller species (activator or inhibitor) and the reaction paths between the actuated and the controlled species. As AIRCs can be interpreted as the superposition of two AICs, the same rules apply and one must select roles for the controller species in a way that makes the controller a negative feedback controller.

The aiAIRC with output inhibition, shown in Figure 1b, is a special case of the aiAIRC, which consist of the superposition of an nAIC and an niAIC with output inhibition. This structure was considered in [38] in the special case of gene expression control, where some of its properties were discussed. The objective of this paper is to address this problem in a much more general setting.



(a) Example of possible AIRCs.



(b) The aiAIRC with output inhibition.

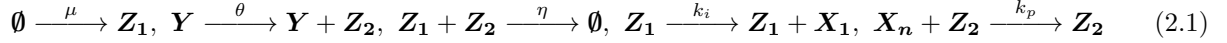
Figure 1: (a). Different possible structures of the AIRC depending on whether the controller species Z_1 and Z_2 act as activators or inhibitors on the actuated species X_1 and X_m and whether the actuated species act as activators or inhibitors for the controlled species X_n . In the first column, X_1 is an activator for X_n whereas it is an inhibitor in the second one. Similarly, in the first row X_m is an inhibitor of X_n where it is an activator in the second one. The roles of the controller species is chosen so that the overall feedback loop is a negative feedback loop and have opposite action on the controlled species. For instance, when X_1 activates X_n and X_m inhibits it, a suitable AIRC is given by the aaAIRC, since that $X_n \rightarrow Z_2 \rightarrow Z_1 \rightarrow X_1 \rightarrow X_n$ and $X_n \rightarrow Z_2 \rightarrow X_m \rightarrow X_n$, showing that Z_1 acts as an activator and Z_2 as a repressor, as required to make the topology a rein controller. One can also observe that the two feedback loops implemented by the aaAIRC are negative feedback loops. Analogous conclusions hold for all the topologies. (b) The aiAIRC with output inhibition consists of two AICs: an nAIC that activates the production of X_1 (blue pointed arrow) and an niAIC that directly inhibits the output X_n (red blunt head arrow).

2 Results

The aiAIRC with output inhibition allows for an arbitrary set-point.

As discussed in Box 1, the nAIC and niAIC induce mutually exclusive set-point admissibility conditions in line with their activatory or inhibitory nature and in the unidirectionality of their actuation mechanism. The intuition is that those mutually exclusive conditions could be perhaps made compatible through the consideration of a combination of those controllers, that is through the consideration of an aiAIRC with

output actuation described by the reaction network



where the reaction rates $\mu, \theta, \eta, k_p, k_i > 0$ are the parameters of the controller and are assumed to be freely adjustable. It is assumed here that the controlled species is \mathbf{X}_n . The closed-loop network consisting of the interconnection of a unimolecular mass-action network of the form (1.1) and the aiAIRC (2.1) is described by the dynamical system

$$\begin{aligned} \dot{x}(t) &= Ax(t) + e_1 k_i z_1(t) - e_n x_n(t) k_p z_2(t) + b_0 \\ \dot{z}_1(t) &= \mu - \eta z_1(t) z_2(t) \\ \dot{z}_2(t) &= \theta x_n(t) - \eta z_1(t) z_2(t) \end{aligned} \quad (2.2)$$

where $x \in \mathbb{R}_{\geq 0}^n$ is the vector of concentrations of the species of the network whereas $z_1, z_2 \in \mathbb{R}_{\geq 0}$ are the concentrations of the species of the controller. The matrix A is the matrix describing the dynamics of the network to be controlled whereas b_0 is the vector of basal rates which are obtained from applying (1.2) to the case of unimolecular networks, that is, we have $\sum_{k=1}^K \zeta_k \lambda_k(x) =: Ax + b_0$. Moreover, in that case, the set of all fixed parameters \mathcal{P}_f are those in the matrix A and the vector b_0 whereas the set of tunable parameters are those of the controller network, that is, $\mathcal{P}_t = \{k_i, k_p, \mu, \theta, \eta\}$. For the sake of convenience, we define $r := \mu/\theta$ which, as we shall see later, coincides with the set-point. The vector e_i is the vector of all zeros except at the index i where the entry is equal to one. Practically speaking, requiring that the network is unimolecular and mass-action is equivalent to saying that the dynamics of the network is linear. While their consideration may appear limited in scope, they have the benefits of being simple to introduce and to allow for a direct, explicit mathematical analysis which may be extrapolated to the more general nonlinear setting. More details about this are given in Section S4 of the SI.

The following result is a simplified version of Proposition S3.3 of the SI:

Proposition 2.1 *Assume that A is Hurwitz stable³ and that $e_n^T A^{-1} e_1 \neq 0$. Then, the equilibrium point (x^*, z_1^*, z_2^*) of the closed-loop system (2.2) is unique, nonnegative and such that $x_n^* = r := \mu/\theta$.*

This result indicates that under the assumptions regarding the matrix A , all set-points $r > 0$ are admissible for the system (2.2). This confirms our initial intuition, as these assumptions are independent of the set-point value r , and this value can be set through an appropriate choice of the tunable parameters μ and θ . The assumption that A is Hurwitz stable is equivalent to stating that the solution of the uncontrolled network dynamics $\dot{x} = Ax + b_0$ is stable and globally converges to its unique nonnegative equilibrium point $-A^{-1}b_0$. While such behavior is common in practice, some networks may exhibit sustained oscillations. In such cases, the proposed controller structure may not be adequate for solving the associated perfect adaptation problem. However, the above result can be adapted to address the more general case where A is not Hurwitz stable, as stated in Proposition S3.3 of the SI.

The aiAIRC with output inhibition behaves as a filtered proportional-integral controller

This controller locally acts as a filtered Proportional-Integral (PI) controller consisting of the combination of a proportional action, which depends directly on the output/error, and an integral action, which depends on the integral of the output/error. To show this, consider the linearized dynamics of (2.2) about the unique equilibrium point

$$\begin{aligned} \dot{\tilde{x}}(t) &= A\tilde{x}(t) - e_n k_p z_2^* \tilde{y}(t) + e_1 k_i \tilde{z}_1(t) - e_n k_p r \tilde{z}_2(t) \\ \dot{\tilde{z}}_1(t) &= -\eta z_2^* \tilde{z}_1(t) - \eta z_1^* \tilde{z}_2(t) \\ \dot{\tilde{z}}_2(t) &= \theta \tilde{y}(t) - \eta z_2^* \tilde{z}_1(t) - \eta z_1^* \tilde{z}_2(t) \end{aligned} \quad (2.3)$$

³A matrix is Hurwitz stable if all its eigenvalues have negative real part.

where $\tilde{x} = x - x^*$, $\tilde{z}_1 = z_1 - z_1^*$, and $\tilde{z}_2 = z_2 - z_2^*$. One can observe that the controller acts at three levels: the first one lies at the level of the dynamics of the output through the term $-e_n k_p z_2^* \tilde{y}(t)$, the second one at the level of the production of the species \mathbf{X}_1 through the term $e_1 k_i \tilde{z}_1(t)$, and the last one at the level of the degradation of the output through the term $-e_n k_p r \tilde{z}_2(t)$. The first term corresponds the proportional action as it depends proportionally on the output, the second and the third terms correspond to two integral actions with the difference that the former is activating whereas the latter is inhibiting. The presence of the PI action can be further emphasized by formulating the overall system into the interconnection of the network and the controller in the Laplace domain. In this domain, the network can be represented as a map from the input $\hat{u}(s)$ to the controlled output $\hat{x}_n(s)$ as

$$\hat{x}_n(s) = \underbrace{e_n^T (sI - A) \begin{bmatrix} e_1 & -e_n \end{bmatrix}}_{\text{Network}} \hat{u}(s), \quad (2.4)$$

while the control input can be expressed as

$$\hat{u}(s) = \left(\underbrace{\begin{bmatrix} 0 \\ -k_p z_2^* \end{bmatrix}}_{\text{Proportional Action}} + \underbrace{\frac{1}{(s + \eta(z_1^* + z_2^*))} \frac{1}{s} \begin{bmatrix} -k_i \eta \theta z_1^* \\ \theta k_p r (s + \eta z_2^*) \end{bmatrix}}_{\text{Filtered Integral Action}} \right) \hat{x}_n(s). \quad (2.5)$$

As previously mentioned, the controller comprises two components. The first is a proportional component that depends linearly on the output species \mathbf{X}_n and is present only in the second part of the control input – the channel that influences the degradation of the controlled species. Notably, this proportional term is absent in the naAIC architecture discussed in Box 1 and in earlier works on integral control of reaction networks [14, 13]. The second component is a low-pass filtered integral term, consisting of an integration operation – represented by $1/s$, which is the Laplace transform of the integration operation – followed by a low-pass filter operation, corresponding to $1/(s + \eta(z_1^* + z_2^*))$. The inclusion of the low-pass filter does not adversely affect the integral action, so zero steady-state error and, therefore, perfect adaptation are maintained provided that the dynamics of the controlled network is stable. We can observe that the filtered PI structure is preserved as long as $k_p \neq 0$. If $k_p = 0$, the controller reduces to an antithetic integral controller of the naAIC form, as discussed in [14, 13] and in Box 1. Conversely, when $k_i = 0$, the controller loses its naAIC arm but retains integral action through the arm associated with the niAIC, therefore preserving the perfect adaptation property under the assumption that the controlled network is stable.

The aiAIRC with output inhibition has a switching behavior in the strong sequestration regime.

A successful technique in the analysis of antithetic structures consists of letting the sequestration rate go to infinity, a regime we call here the *strong sequestration regime*. This procedure allows one to perform model reduction yielding a simplification of the dynamical and equilibrium equations from which insights could be more easily drawn from. In fact, it can be shown that in this strong sequestration regime yields the expressions $z_1(t) \approx \max\{0, I(t)\}$, $z_2(t) \approx -\min\{0, I(t)\}$, and $\dot{I}(t) = \mu - \theta y(t)$ in which we can observe the presence of the integral action.

However, we are more interested here in the behavior of the equilibrium point of the closed-loop network (2.2) in that regime. The following result, which is a simplified version of Proposition S3.2 in the SI, provides the description of this behavior:

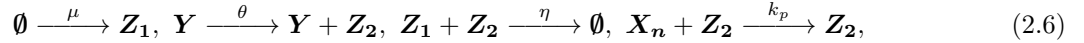
Proposition 2.2 *Assume that A is Hurwitz stable, then the basal output expression level g_0 for the system is given by $g_0 = -e_n^T A^{-1} b_0$. Assuming further $e_n^T A^{-1} e_1 \neq 0$ yields the following statements for the equilibrium point (x^*, z_1^*, z_2^*) of the closed-loop system (2.2):*

1. If the set-point r is larger than the basal output expression g_0 , then $(z_1^*, z_2^*) \xrightarrow{\eta \rightarrow \infty} (u_1^*/k_i, 0)$ where $u_1^* = (r - g_0)/g_1$.
2. If the set-point r is smaller than the basal output expression g_0 , then $(z_1^*, z_2^*) \xrightarrow{\eta \rightarrow \infty} (0, u_2^*/k_p)$ where $u_2^* = (g_0 - r)/(g_n r)$.

This result can easily be interpreted as follows: when the set-point r is larger than the basal level g_0 , only the naAIC component of the controller is active whereas in the opposite scenario only the niAIC component is active. As already mentioned, the naAIC has been extensively studied and the case where $r > g_0$ can be considered now as well-understood. However, the niAIC structure is much less understood and clarifying its properties will be one of the objectives of this paper.

The niAIC with output inhibition structurally stabilizes stable unimolecular mass-action networks under some set-point admissibility condition

The niAIC with output inhibition is described by the following reaction network



which yields the following model for the closed-loop network (1.1)-(2.6)

$$\begin{aligned} \dot{x}(t) &= Ax(t) - e_n x_n(t) k_p z_2(t) + b_0 \\ \dot{z}_1(t) &= \mu - k_p \eta z_1(t) z_2(t) \\ \dot{z}_2(t) &= \theta x_n(t) - k_p \eta z_1(t) z_2(t) \end{aligned} \quad (2.7)$$

where we have changed η into ηk_p . This latter modification does not change the nature of the results but dramatically simplifies their derivation [13]. The first part of the solution to the perfect adaptation problem stated in Definition 1.2 consists of establishing conditions under which a set-point is admissible. This is formulated in the following result:

Proposition 2.3 *Assume that A is Metzler⁴ and Hurwitz stable⁵, then the equilibrium point (x^*, z_1^*, z_2^*) of the closed-loop network (2.7) is unique, nonnegative and such that $x_n^* = r$ if and only if $r < g_0$.*

As previously mentioned, assuming that A is Hurwitz stable is equivalent to stating that the trajectories of the uncontrolled network globally converge to a unique equilibrium point. While this is a simplifying assumption to ease the exposition of the main results, Theorem S3.14 in the SI demonstrates that it can be relaxed to accommodate cases where A may exhibit a certain forms of instability.

The second part of the solution to the perfect adaptation problem consists of establishing conditions under which the equilibrium point (x^*, z_1^*, z_2^*) of the closed-loop network (2.7) is locally asymptotically stable. This can be achieved through the study of the asymptotic stability of the linearized system

$$\begin{bmatrix} \dot{\tilde{x}}(t) \\ \dot{\tilde{z}}_1(t) \\ \dot{\tilde{z}}_2(t) \end{bmatrix} = \underbrace{\begin{bmatrix} \bar{A} & 0 & -e_n k_p r \\ 0 & -\eta u_* & -\mu k_p / u_* \\ \theta e_n^T & -\eta u_* & -\mu k_p / u_* \end{bmatrix}}_{A_\ell} \begin{bmatrix} \tilde{x}(t) \\ \tilde{z}_1(t) \\ \tilde{z}_2(t) \end{bmatrix} \quad (2.8)$$

where $\bar{A} := A - e_n e_n^T u_*$, $\tilde{x} = x - x^*$, $\tilde{z}_1 = z_1 - z_1^*$, and $\tilde{z}_2 = z_2 - z_2^*$. This linearized system is asymptotically stable if and only if all the eigenvalues of the matrix A_ℓ have negative real parts. In order to formulate conditions in terms of the data of the problem (i.e. the matrix A of the network to be controlled) and the

⁴A real, square matrix is Metzler if its off-diagonal entries are nonnegative.

⁵A square matrix is Hurwitz stable if its eigenvalues have negative real part.

tunable controller parameters $\mu, \theta, k_p, \eta > 0$ under which the linearized dynamics is asymptotically stable, we rewrite the system as the interconnection depicted in Figure 10.B where

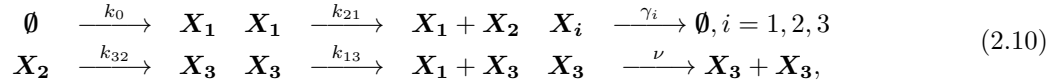
$$H_1(s) = \frac{k_p}{s}, \quad \text{and} \quad H_2(s) = e_n^T (sI - \bar{A})^{-1} e_n \mu + \frac{\mu s}{u_*(s + \eta u_*)}. \quad (2.9)$$

Using the concepts and tools described in Box 2 yields the following result

Theorem 2.4 *Assume that $\mu/\theta < g_0$ and that the matrix A is Metzler and Hurwitz stable. Then, the unique equilibrium point (x^*, z_1^*, z_2^*) of the system (2.7) lies in the nonnegative orthant, is such that $x_n^* = \mu/\theta$, and is locally exponentially stable for all $\eta, k_p > 0$.*

This result means that all state trajectories will converge to the equilibrium point provided that they start sufficiently close from it and that the conditions of the result are met. The fact that the conditions do not depend on the parameters $\eta, k_p > 0$ makes the implementation of the controller an easier task as fine tuning parameters in while implementation is usually not an option in synthetic biology. Note that those parameters do still have an impact on the dynamics of the system (2.7) and its quantitative properties such as speed of convergence, oscillations, overshoot, etc.

As an illustrative example, consider the following unimolecular mass-action gene expression network with protein maturation and positive feedback:



where $\mathbf{X}_1, \mathbf{X}_2$, and \mathbf{X}_3 are the mRNA, protein, and matured protein species, respectively, and where the parameters of the reactions of positive real numbers, which are in the set of fixed parameters \mathcal{P}_f . We assume here that we would like to control the matured species, that is, $\mathbf{Y} = \mathbf{X}_3$. The model of the system is given by

$$\begin{bmatrix} \dot{x}_1 \\ \dot{x}_2 \\ \dot{x}_3 \end{bmatrix} = \begin{bmatrix} -\gamma_1 & 0 & k_{13} \\ k_{21} & -\gamma_2 & 0 \\ 0 & k_{32} & \nu - \gamma_3 \end{bmatrix} \begin{bmatrix} x_1 \\ x_2 \\ x_3 \end{bmatrix} + \begin{bmatrix} k_0 \\ 0 \\ 0 \end{bmatrix} \quad (2.11)$$

where x_1, x_2, x_3 are the mRNA, protein, and matured protein concentrations, respectively. The matrix describing the dynamics of the network is Metzler, by construction, and is Hurwitz stable provided that $\gamma_1 \gamma_2 \gamma_3 - k_{13} k_{32} k_{21} > 0$ (Routh-Hurwitz criterion). We also have that

$$g_0 = \frac{k_0 k_{21} k_{32}}{\gamma_1 \gamma_2 (\gamma_3 - \nu) - k_{21} k_{32} k_{13}} > 0. \quad (2.12)$$

By virtue of Theorem 2.4, assuming that the network (2.10) is stable, we can conclude that the closed-loop network (2.10), (2.6) is locally exponentially stable for all $0 < \mu/\theta < g_0$ and all $k_p > 0, \eta > 0$.

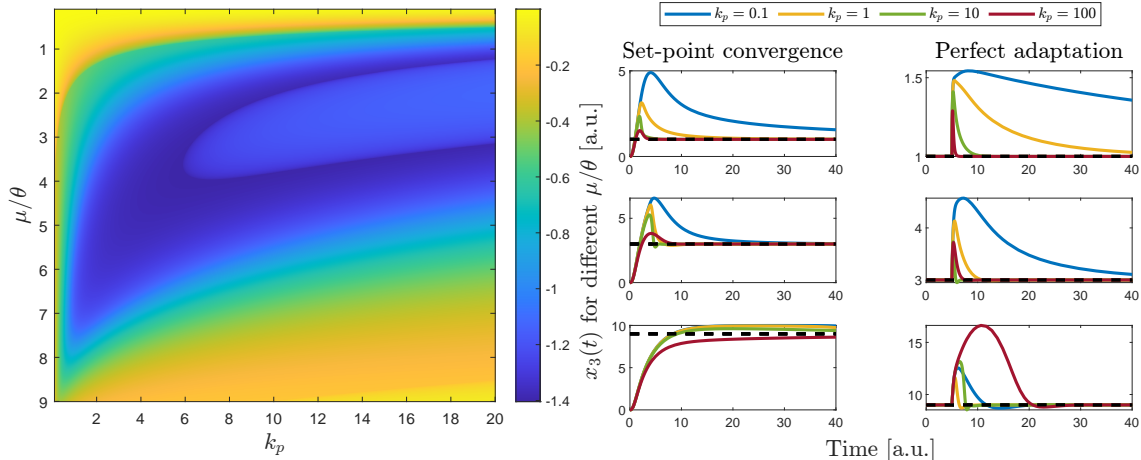


Figure 2: **Left.** Spectral abscissa (i.e. real-part of the rightmost eigenvalue) of the system associated with the (2.10), (2.6) with the parameters $\gamma_1 = 1$, $\gamma_2 = \gamma_3 = 2$, $k_{21} = 1$, $k_{32} = 2$, $k_0 = 10$, $k_{13} = 1$, $\nu = 0$, $\eta = 100/k_p$, and $\theta = 1$ and for various values for μ and k_p . We have that $g_0 = 10$ and calculations show that the spectral abscissa of A is -0.3044 while the spectral abscissa of the closed-loop system may reach smaller values, which indicates that this controller is able to improve the convergence properties of the system near the equilibrium point. **Right.** Time domain evolution of the concentrations of \mathbf{X}_3 for various values for the set-point μ/θ and controller gains k_p . The left column depicts simulation results for zero initial conditions (convergence properties) whereas the right column depicts the response of the closed-loop network when the parameter k_{32} changes from 2 to 3 at $t = 5$ (perfect adaptation property).

The niAIC with output inhibition structurally stabilizes a class of unstable unimolecular mass-action networks under no set-point restriction

In the previous section, we considered the case where the matrix A describes the dynamics of a stable network. In the present section, we relax this assumption by allowing a more general case where the network is allowed to be unstable in a very specific way, a property that we call "output instability". While the precise definition of output instability provided in the SI is rather technical, it can be intuitively motivated by analyzing the structure of the niAIC. Since the niAIC acts on the network by actively degrading the controlled species, it seems natural to believe that this controller could still achieve its goal even when the controlled species exhibits unstable behavior. Output instability of the matrix A is therefore a rigorous characterization of those matrices where only the controlled species is allowed to be unstable – hence the term "output unstable." The rest of this section demonstrates that relaxing the stability of the network is not only possible but also leads to surprising results, notably regarding set-point admissibility, as shown below:

Proposition 2.5 *Assume that A is Metzler and output unstable, then the equilibrium point (x^*, z_1^*, z_2^*) of the closed-loop network (2.7) is unique, nonnegative and such that $x_n^* = r$ if and only if $g_0 \neq 0$.*

We can observe here that, by relaxing the stability of the network, we allow for more flexibility at the level of the set-point, which is a dramatic change over the previous case for which the set-point value is more restricted. The reason for the emergence of this property is that, as opposed to the stable case, there is no equilibrium output basal level for the controlled species. In this regard, one can just let the output spontaneously increase beyond the set-point value before starting degrading it and making it converge to the desired set-point.

Having a suitable equilibrium point is only one part of the solution of the perfect adaptation problem. The second one is the stability of that equilibrium point, which is addressed in the result below:

Theorem 2.6 Assume that A is Metzler and output unstable, and that $g_0 \neq 0$. Then, the unique equilibrium point (x^*, z_1^*, z_2^*) of the closed-loop network (2.7) lies in the nonnegative orthant, is such that $x_n^* = \mu/\theta$, and is locally exponentially stable for all $\eta, k_p, \mu, \theta > 0$.

This result tells us that all state trajectories will converge to the equilibrium point provided that they start sufficiently close from it and that the conditions of the result are met. In the present case, the stability of the equilibrium point holds unconditionally of the controller parameters, which a drastic change over Theorem 2.4 where the set-point value is required to be smaller than the output basal expression level. In this case, the controller functions both as a stabilizer for the system dynamics and as a regulator for the controlled species. Specifically, the stabilization effect arises from the proportional action in the controller, as described in equation (2.5), while the regulation effect is due to the filtered integral action. This dual role is consistent with standard results in the literature on PID control [1].

To illustrate this discussion, consider back the network (2.10) with the model (2.11), which can be shown to be output unstable if and only if

$$\gamma_1\gamma_2(\nu - \gamma_3) + k_{21}k_{32}k_{13} > 0. \quad (2.13)$$

We also have the following expression for g_0

$$g_0 = \frac{-k_0k_{21}k_{32}}{\gamma_1\gamma_2(\nu - \gamma_3) + k_{21}k_{32}k_{13}} < 0, \quad (2.14)$$

and observe that it is negative. This is due to the fact that the network is output unstable, and that this value does not represent the output basal expression level anymore.

By virtue of Theorem (2.6), assuming that the network (2.10) is output unstable, we can conclude that the closed-loop network (2.10), (2.6) is locally exponentially stable for all $\mu, \theta, k_p > 0, \eta > 0$. This statement is illustrated by simulation in Figure S19 and Figure S20.

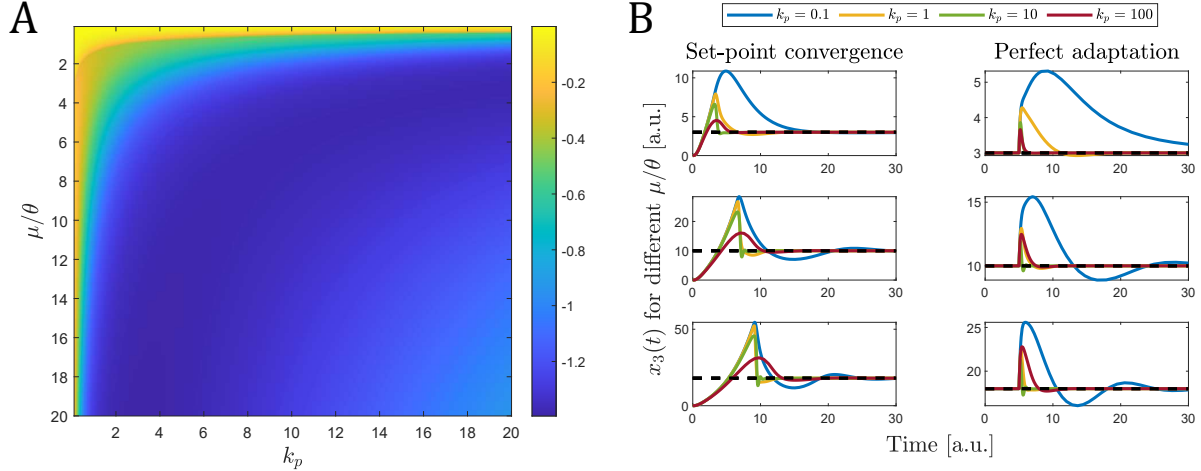


Figure 3: **A.** Spectral abscissa (i.e. real-part of the rightmost eigenvalue) of the system associated with the (2.10), (2.6) with the parameters $\gamma_1 = 1$, $\gamma_2 = \gamma_3 = 2$, $k_{21} = 1$, $k_{32} = 2$, $k_0 = 10$, $k_{13} = 3$, $\nu = 0$, $\eta = 100/k_p$, and $\theta = 1$ and for various values for μ and k_p . We have that $g_0 = -10$, $g_n = -1$, and calculations show that the spectral abscissa of A is 0.2188 while the spectral abscissa of the closed-loop system may reach smaller values, which indicates that this controller is able to stabilize the network and improve the convergence properties of the system near the equilibrium point. **B.** Time domain evolution of the concentrations of \mathbf{X}_3 for various values for the set-point μ/θ and controller gains k_p . The left column depicts simulation results for zero initial conditions (convergence properties) whereas the right column depicts the response of the closed-loop network when the parameter k_{32} changes from 2 to 3 at $t = 5$ (perfect adaptation property).

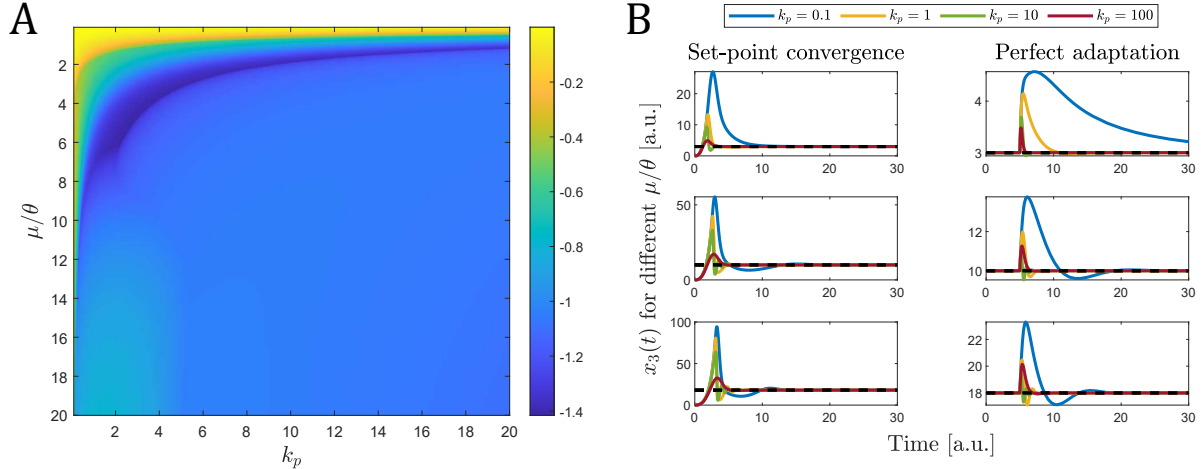


Figure 4: **A.** Spectral abscissa (i.e. real-part of the rightmost eigenvalue) of the system associated with the (2.10), (2.6) with the parameters $\gamma_1 = 1$, $\gamma_2 = \gamma_3 = 2$, $k_{21} = 1$, $k_{32} = 2$, $k_0 = 10$, $k_{13} = 1$, $\nu = 3$, $\eta = 100/k_p$, and $\theta = 1$ and for various values for μ and k_p . We have that $g_0 = -5$, $g_n = -1/2$, and calculations show that the spectral abscissa of A is 1.2695 while the spectral abscissa of the closed-loop system may reach smaller values, which indicates that this controller is able to stabilize the network and improve the convergence properties of the system near the equilibrium point. **B.** Time domain evolution of the concentrations of \mathbf{X}_3 for various values for the set-point μ/θ and controller gains k_p . The left column depicts simulation results for zero initial conditions (convergence properties) whereas the right column depicts the response of the closed-loop network when the parameter k_{32} changes from 2 to 3 at $t = 5$ (perfect adaptation property).

How restrictive are the stability conditions on the unimolecular networks?

A natural question is how strong the assumptions are on the considered class of unimolecular networks. As shown in the theoretical results and simulations above, imposing that A is Hurwitz stable is clearly a restrictive assumption, which was later relaxed to considering matrices A that are output-unstable. Therefore, the next question is, how restrictive is this assumption?

As proved in Section S3.4 and Section S3.5, structural stability with respect to the controller gain k_p requires that all non-actuated species X_2, \dots, X_n be stable. Nonnegative equilibrium points as well as an unstable behavior for the controlled network may also result from this assumption being not satisfied. The necessity of the natural stability of the non-actuated species can be easily explained by noting that the actuation affects only the degradation of the controlled species, while the controlled species can only act as an activator for the other species. This means that if any of the non-actuated species is unstable, there is no way to stabilize it through the degradation of the controlled species alone.

We consider now two simple case scenarios that illustrate the previously evoked technical problems. The first one is that of a unimolecular network described by the matrices

$$A = \begin{bmatrix} 1 & 0 \\ 1 & -1 \end{bmatrix}, \quad b_0 = \begin{bmatrix} 1 \\ 0 \end{bmatrix}. \quad (2.15)$$

This matrix is neither Hurwitz nor output-unstable as the first molecular species is unstable. The equilibrium concentrations for the species of the network controlled using an niAIC with output-inhibition is given by

$$x^* = -(A - k_p z_2^* e_n e_n^T)^{-1} b_0 = \begin{bmatrix} -1 \\ 1 \\ -\frac{1}{k_p z_2^* + 1} \end{bmatrix} \quad (2.16)$$

and unavoidably contains a negative equilibrium for the species \mathbf{X}_1 , which is not admissible. This means that the controlled network will necessarily be unstable.

For the second scenario, we slightly change b_0 to $b_0 = \begin{bmatrix} 0 \\ 1 \end{bmatrix}$, which yields the (now admissible) equilibrium point

$$x^* = \begin{bmatrix} 0 \\ 1 \\ \frac{1}{k_p z_2^* + 1} \end{bmatrix}. \quad (2.17)$$

Setting then $z_2^* := \frac{1}{k_p(1/r - 1)}$ yields $x_2^* = r$, $z_1^* = \mu/(\eta k_p z_2^*)$, and the Jacobian matrix

$$J = \begin{bmatrix} 1 & 0 & 0 & 0 \\ 1 & -\frac{1}{r} & 0 & -k_p r \\ 0 & 0 & -\eta \left(\frac{1}{r} - 1 \right) & \frac{k_p \mu r}{r - 1} \\ 0 & \theta & -\eta \left(\frac{1}{r} - 1 \right) & \frac{k_p \mu r}{r - 1} \end{bmatrix}, \quad (2.18)$$

which is not Hurwitz stable because of the presence of an eigenvalue equal to one. This proves that the unique equilibrium point of the controlled network is unstable in this situation.

Those two examples illustrate the two problems that may arise in whenever the matrix A is neither Hurwitz nor output-unstable: absence of a nonnegative equilibrium point or instability of the nonnegative equilibrium point.

Extension to the aiAIRC with output inhibition.

We may now ask the question of how this translates to the aiAIRC controller with output inhibition, as depicted in Figure 1a. This is, in fact, true and stated in the following result:

Theorem 2.7 *Assume that A is Metzler, output unstable, and nonsingular and that $g_0 \neq 0$. Then, the unique equilibrium point of the system (2.2) is locally exponentially stable for all $\eta, k_p, \mu, \theta > 0$ and all $k_i \in [0, \bar{k}_i]$ for some $\bar{k}_i > 0$.*

This result indicates that, within the context of the aiAIRC, the structural stability of the controlled network is preserved with respect to the parameters $\eta, k_p, \mu, \theta > 0$. However, the result does not address structural stability concerning the gain k_i of the naAIC arm of the aiAIRC. At first glance, this may seem conservative, as it is possible that the network is also structurally stable with respect to $k_i > 0$ in certain cases. This issue lies beyond the scope of this paper because the mathematical tools developed in the SI do not apply here due to technical reasons that we will not discuss here. This exciting open problem is left for future research.

We can, however, illustrate the above result and our claim about the structural stability of the network with respect to k_i through numerical simulations depicted in Figure 5. Consistent with the developed theory, the first panel shows that for the controlled network to be stable when $r > g_0$, it is necessary for k_i to be positive. This implies that the naAIC component of the aiAIRC is essential for the stability of the controlled network, aligning with previous works on the topic [14, 13]. Similarly, the third panel demonstrates that when $r < g_0$, a positive k_p is required for stability, indicating that the niAIC component is crucial. This finding is consistent with the results previously discussed in this paper.

In the special case when $r = g_0$, both arms of the aiAIRC are essential to ensure the stability of the controlled network. This scenario is particularly interesting because this equilibrium point is unstable for both the naAIC

and niAIC controller networks individually. Stability can only be achieved by combining both controllers into the unified aiAIRC structure.

In all these scenarios, we observe that the controlled network remains stable for values of both k_p and k_i that are significantly greater than zero. Although not displayed in Figure 5, this stability persists even for much larger parameter values. This suggests that the controlled network is structurally stable with respect to the controller parameters k_p and k_i .

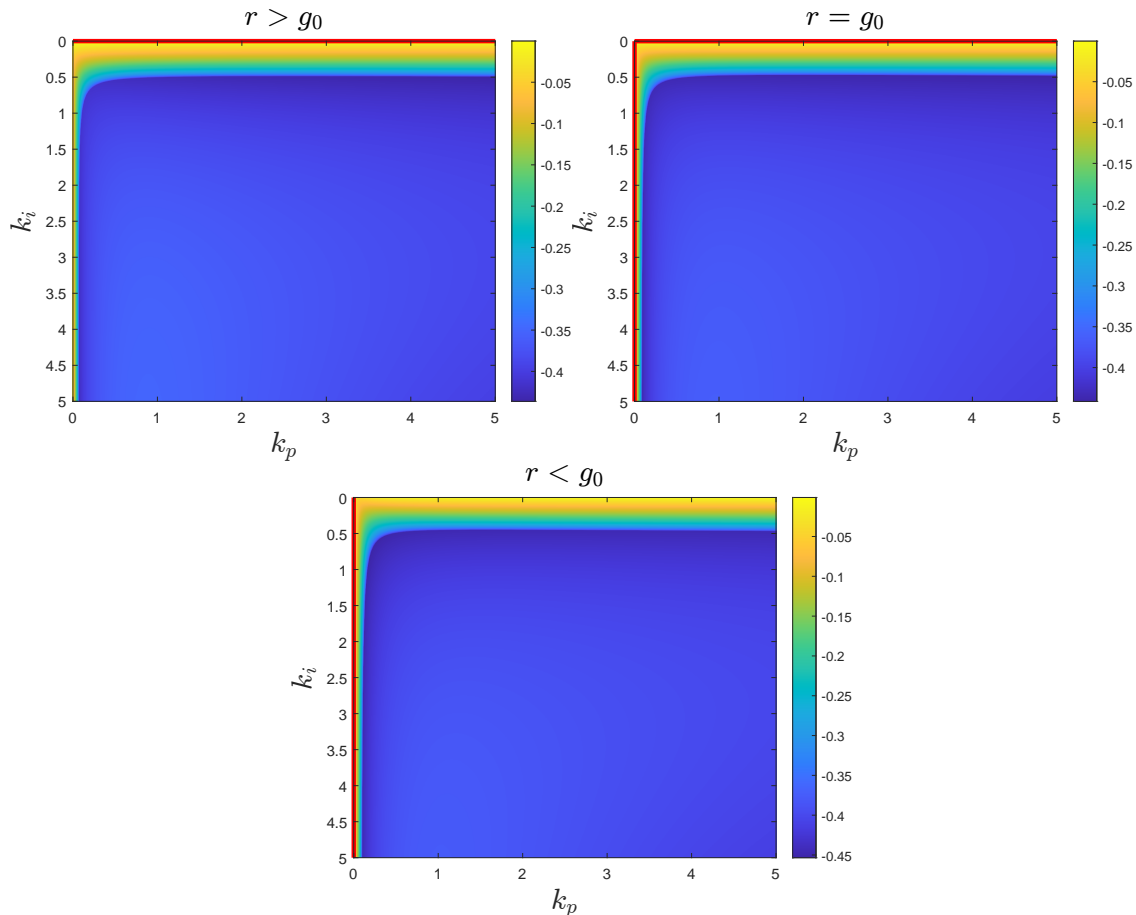


Figure 5: Stability regions in the (k_p, k_i) -plane for the unique equilibrium point of system (2.2), associated with the gene expression network with protein maturation (2.10) controlled by the aiAIRC with output inhibition (2.1). Common parameters for all simulation panels are: $\gamma_1 = 1$; $\gamma_2 = \gamma_3 = 2$; $k_{21} = 1$; $k_{32} = 1$; $k_{13} = 0$; $\nu = 0$; $\eta = 100$; $\theta = 1$; and $\mu = 2.5$. In the first panel, $k_0 = 5$ (which gives $g_0 = 1.25$), so $r > g_0$; in the second panel, $k_0 = 10$ (yielding $g_0 = 2.5$), so $r = g_0$; and in the third panel, $k_0 = 15$ (resulting in $g_0 = 3.75$), so $r < g_0$. The red regions along the boundary of the nonnegative orthant represent areas where the system either lacks a nonnegative equilibrium point (i.e., the set-point is not admissible) or where the unique nonnegative equilibrium point exists but is unstable.

General networks

We consider now the general case consisting of the interconnection of the network (1.1) and the niAIC with output inhibition (2.6), which can be described by the dynamical model

$$\begin{aligned}\dot{x}(t) &= f(x(t)) - e_n k_p z_2(t) x_n(t) + b_0 \\ \dot{z}_1(t) &= \mu - \eta k_p z_1(t) z_2(t) \\ \dot{z}_2(t) &= \theta e_n^T x - \eta k_p z_1(t) z_2(t),\end{aligned}\tag{2.19}$$

where the function $f(x)$ is sufficiently regular so that solutions to this model exist. In the current setting, this function will contain mass-action, Hill, or Michaelis-Menten terms.

Due to the nonlinear nature of the network, there are a number of additional difficulties over the unimolecular/linear case that need to be addressed. We briefly explain them here and refer the readers to the SI for more details. The first difficulty concerns the analytical calculation of the admissibility set and, while it may still be possible to characterize it analytically, numerical methods will be needed to compute the equilibrium solutions to the above system in most cases. So, one cannot expect to have a general, clean expression for the admissibility set in this case. The second difficulty is that there may be multiple equilibrium points $(x^*(r), z_1^*(r), z_2^*(r))$ associated with a given admissible set-point value r . To avoid complications, we assume here that this is not the case and that the set-point r uniquely defines the equilibrium point $(x^*(r), z_1^*(r), z_2^*(r))$. The third difficulty lies at the level of the static input-output function $F : u \mapsto y$, which maps input values to equilibrium output values. This function is much more difficult to explicitly characterize than in the unimolecular/linear case and one has to rely on its implicit definition given by the set of algebraic equations $f(x) - e_n u y + b_0 = 0$, $y = x_n$, and $y = F(u)$. In fact, a solution to this system is not even guaranteed to exist and additional conditions on the function f are required to ensure that this is the case. Finally, the last difficulty is that the function F needs to be locally decreasing at the equilibrium points of interests for them to be potentially stable. This corresponds to having a "negative gain", meaning that increasing the input decreases the output of the system.

Assuming that the above considerations have been adequately addressed and that the corresponding conditions/assumptions are satisfied, the stability of the equilibrium point associated with the set-point r can then be established through the analysis of the linearized dynamics

$$\begin{bmatrix} \dot{\tilde{x}}(t) \\ \dot{\tilde{z}}_1(t) \\ \dot{\tilde{z}}_2(t) \end{bmatrix} = \begin{bmatrix} J^*(r) - e_n e_n^T u_*(r) & 0 & -e_n k_p r \\ 0 & -\eta u_*(r) & -k_p \mu / u_*(r) \\ \theta e_n^T & -\eta u_*(r) & -k_p \mu / u_*(r) \end{bmatrix} \begin{bmatrix} \tilde{x}(t) \\ \tilde{z}_1(t) \\ \tilde{z}_2(t) \end{bmatrix}\tag{2.20}$$

where $J^*(r)$ is the Jacobian matrix of the system, defined as $J^*(r) := \left. \frac{\partial f(x)}{\partial x} \right|_{x=x^*(r)}$, and $u_*(r)$ is such that $r = F(u_*(r))$. The matrix $J^*(r)$ is the nonlinear analogue of the A matrix in (2.2) and (2.8), with the striking difference that the local dynamics is now influenced by the set-point. In this regard, different properties for the system are expected depending on our choice for the set-point value r . From the linear dynamics (2.20), we can define the local transfer function for the nonlinear network

$$H_n(s, r) = e_n^T (sI - (J^*(r) - u_*(r) e_n e_n^T))^{-1} e_n,\tag{2.21}$$

which plays an analogous role as in the linear/unimolecular case, with the difference now that the transfer function is set-point-dependent. This transfer function describes the behavior of the system about the corresponding equilibrium point. Interestingly, the DC-gain $H(0, r)$ is related to the static-output map F as $H(0, r) = - \left. \frac{dF(u)}{du} \right|_{u=u_*(r)}$ meaning that the DC-gain is positive if and only if the input-output map F is decreasing at $u_*(r)$.

With the above discussion in mind, we are now in position to state the main result of this section on general nonlinear networks:

Theorem 2.8 *Suppose that the assumptions and conditions discussed above and in the SI are satisfied, and assume further that*

- (a) *the set-point r is admissible,*
- (b) *the equilibrium $(x^*(r), u_*(r))$ is uniquely defined by the set-point r ,*
- (c) *$H_n(0, r) > 0$, and*
- (d) *one of the following equivalent statements holds:*

(d1) *There exist a symmetric positive definite matrix $P_1(r)$ and a scalar $\varepsilon > 0$ such that*

$$(J^*(r) - F^{-1}(r)e_n e_n^T)^T P(r) + P(r)(J^*(r) - F^{-1}(r)e_n e_n^T) + 2\varepsilon e_n e_n^T \quad (2.22)$$

is negative definite where

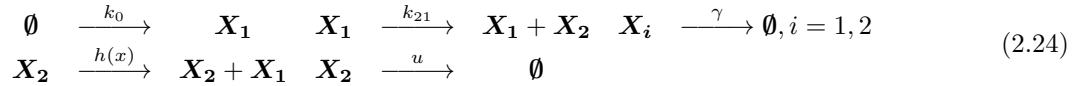
$$P(r) = \begin{bmatrix} P_1(r) & 0 \\ 0 & 1 \end{bmatrix}. \quad (2.23)$$

(d2) *There exists a scalar $\varepsilon > 0$ such that the system $(J_{11}^*(r), J_{12}^*(r), -J_{21}^*(r), u_*(r) - J_{22}^*(r) - \varepsilon)$ is strictly positive real.*

Then, the unique equilibrium point $(x^(r), z_1^*(r), z_2^*(r))$ of the system (2.19) is locally exponentially stable for all $\eta, k_p > 0$.*

Due to the generality of the problem, it is difficult to provide more explicit conditions than those ones and we provide below a computational procedure to verify them. The admissibility of a set-point (i.e. condition (a)) as well as the uniqueness of the associated equilibrium point (i.e. condition (b)) can be both established by numerically solving the expressions $f(x) - e_n k_p r z_2 + b_0 = 0$ and $x_n = r$ for (x, z_2) . If there is no nonnegative solution, then the set-point is not admissible, and if there are multiple nonnegative solutions, then the uniqueness of the equilibrium point does not hold. This provides a way to check the two first conditions. The Jacobian matrix $J(x)$ can be computed using symbolic calculations, from which a simple evaluation at $x = x^*(r)$ would yield $J^*(r)$. The transfer function $H(s, r)$ can be easily evaluated once $J^*(r)$ and $u_*(r)$ are known in order to check condition (c). Finally, condition (d1) is a so-called Linear Matrix Inequality (LMI) problem, a convex decision problem, which can be solved using freely available solvers [67, 69]. The condition (d2) can be numerically verified by computing the poles and the zeros of the associated transfer function and checking whether the Nyquist diagram remains in the open right half-plane according to the definitions and results stated in Box 2.

We illustrate the above result by considering the network



where the last reaction is here to represent the actuation reaction with input u . All reactions are mass-action with positive rates except for the catalytic reaction $\mathbf{X}_2 \xrightarrow{h(x)} \mathbf{X}_2 + \mathbf{X}_1$ which has a propensity function given by $h(x) = k_{12}/(1 + x_2)$. Those parameters are all in the set of fixed parameters \mathcal{P}_f . The goal here is to control the second species, that is, $\mathbf{Y} = \mathbf{X}_2$. As a result, the model of this system is given by

$$\begin{aligned} \dot{x}_1 &= -\gamma x_1 + \frac{k_{12}}{1 + x_2} + k_0, \\ \dot{x}_2 &= k_{21} x_1 - \gamma x_2 - u x_2 \end{aligned} \quad (2.25)$$

where x_1 and x_2 denote the mRNA and protein concentrations, respectively. It turns out that the admissibility set can be explicitly computed and is given by $(0, r_{\min})$ where r_{\min} is the unique positive root of the polynomial

$$\gamma^2 r^2 + r(\gamma^2 - k_{21} k_0) - k_{21}(k_{12} + k_0). \quad (2.26)$$

This also shows that the equilibrium point is unique. The Jacobian of this system is given by

$$J(x) = \begin{bmatrix} -\gamma & -\frac{k_{12}}{(1+x_2)^2} \\ k_{21} & -\gamma \end{bmatrix} \quad (2.27)$$

and is invertible for all $x_2 \geq 0$, and so is $J(x) - ue_n e_n^T$ for all $x \geq 0$ and $u \geq 0$. It can be shown that the function F is monotonically decreasing, hence invertible. Therefore, we have that $F(0) = r_{\min}$ and $\lim_{u \rightarrow \infty} F(u) = 0$. More details can be found in the SI.

The Jacobian evaluated at the equilibrium point corresponding to $x_2^* = r$ is given by

$$J^*(r) = \begin{bmatrix} -\gamma & -\frac{k_{12}}{(1+r)^2} \\ k_{21} & -\gamma \end{bmatrix}$$

and the associated transfer function is

$$H_n(s, r) = \frac{s + \gamma}{s^2 + (2\gamma + u_*(r))s + \gamma(\gamma + u_*(r)) + k_{21}k_{12}/(1+r)^2}.$$

From the Routh-Hurwitz criterion, the transfer function $H_n(s, r)$ is stable, has stable zeros and verifies $H(0, r) > 0$. Therefore, we just need to show the existence of a matrix $P(r)$ as defined in Theorem 2.8 such that

$$\begin{bmatrix} -2\gamma P(r) & -\frac{k_{12}}{(1+r)^2} P(r) + k_{21} \\ -\frac{k_{12}}{(1+r)^2} P(r) + k_{21} & -2(\gamma + u_*(r)) \end{bmatrix}$$

is negative definite. Alternatively, we may check whether the transfer function associated with the system

$$\begin{aligned} \dot{v} &= -\gamma v - \frac{k_{12}}{(1+r)^2} w \\ z &= -k_{21} v + (\gamma + u_*(r)) w \end{aligned} \quad (2.28)$$

is strictly positive real. It can be seen that this is the case since it is a first order stable transfer function of relative degree 0 with stable zeros, with positive gain and positive feedthrough. Therefore, the closed-loop system consisting of (2.24) and the niAIC with output inhibition (2.6) is stable for all $k_p, \eta > 0$ and $r > r_{\min}$.

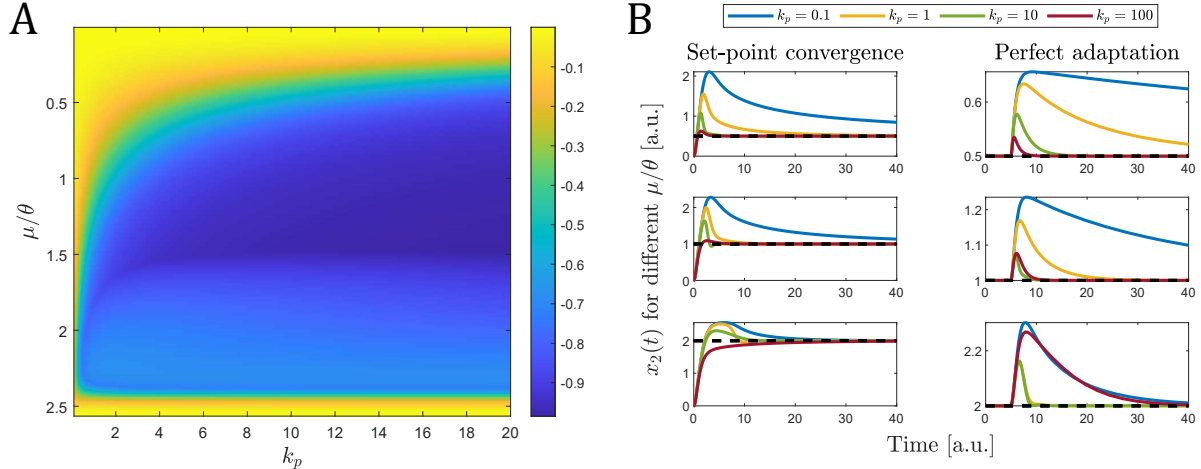


Figure 6: **A.** Spectral abscissa (i.e. real-part of the rightmost eigenvalue) of the system associated with the network (2.10)-(2.6) with the parameters $\gamma_1 = 1$, $k_{12} = 1$, $k_0 = 1$, $k_{21} = 2$, $\eta = 100/k_p$, and $\theta = 1$ and for various values for μ and k_p . We have that $r_{\min} = 2.5616$. **B.** Time domain evolution of the concentrations of \mathbf{X}_2 for various values for the set-point μ/θ and controller gains k_p . The left column depicts simulation results for zero initial conditions (convergence properties) whereas the right column depicts the response of the closed-loop network when the parameter k_{12} changes from 1 to 2 at $t = 5$ (perfect adaptation property).

This simple example shows how the conditions of Theorem 2.8 can be checked and emphasizes how difficult this verification could get when the dimension of the problem grows. However, some of those conditions dramatically simplify when considering specific subclasses of networks. This is discussed in the following sections.

The niAIC with output inhibition structurally stabilizes stable cooperative networks under some set-point admissibility condition

The class of cooperative networks is a class of networks for which the Jacobian matrix $J^*(r)$ is Metzler for some admissible set-points r , which means that the network locally behaves like a unimolecular network at that point. For all those points r where this is the case, we say that the system is cooperative at $x^*(r)$. This leads us to the following result

Proposition 2.9 *Let r be admissible and assume that the system (2.19) is cooperative at the equilibrium value $x^*(r)$, assumed to be unique, and that the matrix $J^*(r)$ is Hurwitz stable. Then, the unique equilibrium point $(x^*(r), z_1^*(r), z_2^*(r))$ of the cooperative system (2.19) is locally exponentially stable for all $\eta, k_p > 0$.*

As the class of cooperative networks is very similar to unimolecular ones, which are cooperative by construction, extensions to the case of output-unstable systems are rather immediate at the expense of additional notational burden stemming from the nonlinear nature of the network. For this reason, those results are omitted here. Another possible extension of the above result relies in the fact that it can be adapted to systems which are cooperative with respect to a different cone than the nonnegative orthant. Indeed, if one can find a diagonal matrix $S(r)$ with diagonal entries in $\{-1, 1\}$ such that $S(r)J^*(r)S(r)$ is Metzler, then the above result also applies to that system.

The niAIC with output inhibition structurally stabilizes Michaelis-Menten networks under some set-point admissibility condition

Another important class of nonlinear networks benefiting from a complexity reduction is the class of linear mass-action and Michaelis-Menten networks [2]. Such networks (2.19) are described by a function f of the

form

$$f(x) = Ax + N(x) \tag{2.29}$$

where $N_i(x) = \sum_j \alpha_{ij} \frac{1}{1 + x_j/\beta_{ij}} + \sum_j \gamma_{ij} \frac{x_j/\delta_{ij}}{1 + x_j/\delta_{ij}}$, where $\alpha_{ij}, \beta_{ij}, \delta_{ij}, \gamma_{ij}, > 0$ and $i = 1, \dots, n$ are all fixed parameters; i.e. they are all in \mathcal{P}_f .

This leads us to the following result:

Theorem 2.10 *Let r be admissible and assume that the controlled Michaelis-Menten network (2.19)-(2.29) has a unique equilibrium point $(x^*(r), z_1^*(r), z_2^*(r))$. Assume further that the graph of the network is strongly connected, that $b_0 \neq 0$, and that $H_n(0, r) > 0$. Then, the unique equilibrium point $(x^*(r), z_1^*(r), z_2^*(r))$ of the Michaelis-Menten system (2.19)-(2.29) is locally exponentially stable for all $\eta, k_p > 0$.*

Getting back to the network (2.25) considered previously, we can observe that it falls into the category considered here. As a result, we can quite readily conclude on its stability properties right after having checked the set-point admissibility and the condition that $H(0, r) > 0$ without the need for all the subsequent calculations.

Intein-based implementation

We provide here a possible implementation of the niAIRC with output inhibition based on inteins [51, 73]. Such molecules have been to be an effective tool in the design of synthetic circuits by allowing to implement synthetic networks capable of performing computations. Even though various AIC structures have already been discussed in [3], it seems that an intein-based implementation of the niAIC with output inhibition has not been addressed so far. The overall implementation, relying on a split protease connected with a linker containing an N-Intein, is depicted in Figure 7. Interestingly, our results demonstrate that the controller structure is intrinsically very robust and will function over a broad range of its implementation parameters – if not all values. This makes its implementation much easier and reduces the importance of precisely identifying its parameters, unlike other types of controllers that lack structural stability properties. However, fine-tuning may still be necessary to adjust certain quantitative properties of the controlled network, such as its settling time or other time-domain features. This tuning must be done on a case-by-case basis, as these properties depend heavily on the characteristics of the network being controlled. In this regard, formulating general guidelines is difficult and are not considered here.

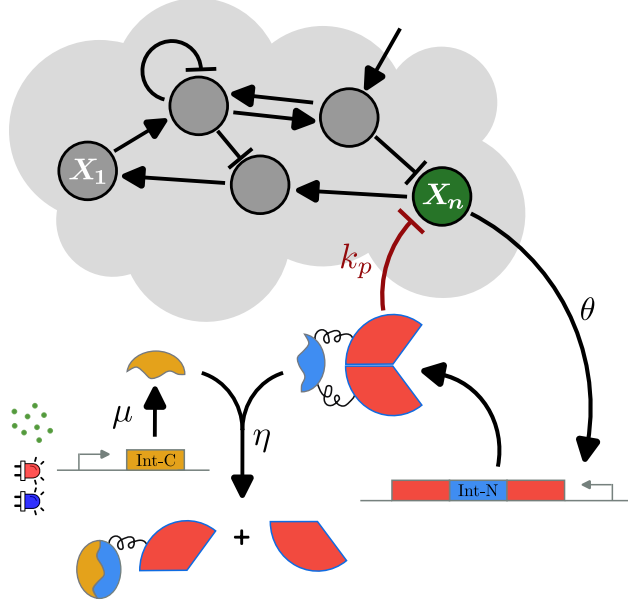


Figure 7: In-tein-based implementation of the niAIC with output inhibition: the species Z_2 is a split protease connected with a linker containing an N-Intein whereas the species Z_1 is a C-Intein, which is constitutively produced. When the two inteins bind, the protease is split in two inactive part. The output species X_n acts here as a transcription factor for the split protease-intein compound.

3 Discussion

This paper reports practical results regarding the use of niAICs with output inhibition and the consideration of networks for which the output can be directly actuated. Those practical results are implications of novel, more fundamental, and more general results which are all proven and discussed in the SI. Due to their high level of technicality, it seemed impractical to present them in the main text. Those results, which are based on ideas from dynamical systems theory, and systems and control theory, have intrinsic value on their own and are sufficiently general to be applicable to other, similar problems. For instance, they directly apply to other types of integral controllers such that as exponential integral controllers [65, 19, 13] and logistic integral controllers [13]. Those results are all reported in the SI where very similar conclusions as for the niAIC are also drawn.

The entire set-up is based on the assumption that the output can be actively degraded. It is, therefore, natural to ask the question whether the same results hold true whenever an intermediary molecule is degraded instead. The general answer is "no": one cannot guarantee that the closed-loop network is stable independently of the gains of the controller since the associated linearized system will not satisfy the required positive realness properties. This fact proves that it is essential that the output species be directly inhibited for the structural stability results to hold. The paper assumes that the control paths from X_1 to X_n and X_m to X_n have fixed activating or inhibiting roles that do not change over time. While this assumption is reasonable in the context of unimolecular mass-action systems, it may become restrictive in more complex, nonlinear networks, where a path might be activating in one region of the state space and inhibiting in another. This scenario is not addressed in the current work for several reasons. First, the focus of this paper is on output inhibition, which is inherently inhibitory by design, precluding any activation through this actuation path. Such behavior could only arise if the actuated species were different from the controlled species X_n . Second, the theoretical tools developed in the SI are not applicable to this case, except under very restrictive conditions. This limitation arises for two main reasons. From a technical perspective, the tools fail to provide meaningful predictions

about the structural stability of the controlled network in some instances of this scenario. Furthermore, the current controller topology is not really suited to address such complexities, and alternative controller structures may be necessary. Identifying an appropriate topology for this situation is an open and intriguing problem, which we leave for future research.

While the results obtained in this paper shed some light on the structural stability properties of networks controlled with an niAIC with output inhibition, those results do not provide any insights regarding how to properly choose the controller parameters. Such parameters could be numerically optimized so that certain performance properties are satisfied such that having a small spectral abscissa (which governs the rate of convergence near the equilibrium point) or reducing oscillations/overshoot, etc. Those performance criteria are typically difficult to optimize manually but could be easily done computationally using iterative methods.

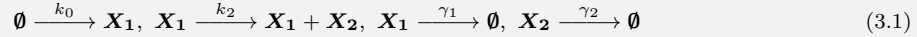
The obtained results rely on linearization, a procedure that makes the analysis simpler but with the additional caveat that the results will only hold locally: the convergence of the state trajectories to the equilibrium point is only guaranteed provided that the initial conditions are "close enough" to the equilibrium point. Analytically quantifying how close they need to be is a difficult task in general and this analysis should be performed on a case-by-case basis. An important question is whether the state trajectories will converge to the equilibrium point regardless the initial condition, a property called global asymptotic stability. This is a difficult problem and the obtained results can neither be used nor easily extended to assess this. A possible workaround consists of constructing a Lyapunov function which would prove the global asymptotic stability of the equilibrium point of the closed-loop network. Moreover, proving the structural stability of the closed-loop network with respect to (some of) the controller parameters requires an alternative route than through the consideration of transfer functions and their positive realness properties. Certainly the most natural way to resolve this problem would be to consider the time-domain analogue of positive realness properties called passivity properties. In this case, the main tools at our disposal are storage functions and supply-rates, that may allow us to prove the passivity properties of the controller and the network, and the structural stability properties for the closed-loop network [20, 70].

Some of the results obtained here for the niAIC with output inhibition have been also extended to the aiAIRC with output inhibition using a perturbation argument. This argument allows us to infer that the closed-loop network will maintain its structural stability property provided that the gain k_i is "small enough". However, the current methodology is not only unable to quantify how small this gain should be but also fails to prove or disprove the fact that the closed-loop network remains stable for all set-points and all controller parameters, as extensive simulations tend to suggest. The main bottleneck is that the current approach heavily relies on the fact that the linearized dynamics depends linearly on the gain of the controller and that the equilibrium point depends continuously on it. Those properties can be ensured by suitably modifying the initial problem, a procedure that was introduced in [14, 13] in the context of the naAIC. Unfortunately, this procedure does not work anymore for the aiAIRC for the simple reason that this controller involves two gains, k_p and k_i , which forbids the existence of a similar problem reformulation. Calculations notably show that the expressions for the equilibrium point and the linearized dynamics are discontinuous functions on the gains, which invalidates the entire approach and demonstrates the need for a radically different approach.

An important limitation of the niAIC with output inhibition that needs to be discussed lies at the level of the set-point admissibility set. It was shown that in the case of unimolecular networks, all the admissible set-points lie below the basal expression level. This can be seen as a serious issue whenever the basal expression levels are low. A first possible workaround would be to increase the basal expression levels through overexpression of the corresponding genes. This would allow for a wider range of values for the set-point but at the same time would create a futile cycle having a high metabolic burden, especially when the set-point is much lower than the basal level. A second, perhaps riskier, strategy consists of destabilizing the network, through the addition of a positive feedback loop or the addition of an autocatalytic reaction, which would place the network in a regime where all the set-points are admissible.

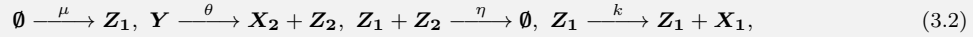
Box 1. The Perfect Adaptation Problem and (Antithetic) Integral Control

The objective of this separate section is to illustrate through simple examples the possibilities and limitations of two types of AICs, the naAIC and the niAIC with output inhibition, on the following simple gene expression network



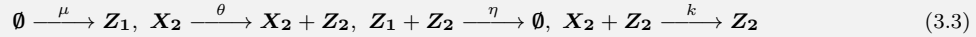
where \mathbf{X}_1 and \mathbf{X}_2 denote the mRNA and protein species, respectively. Above, the positive rate parameters k_0, k_2, γ_1 , and γ_2 of the mass-action reactions correspond to the basal transcription rate, the translation rate, the mRNA degradation rate, and the protein degradation rate, respectively. We consider here the problem of ensuring perfect adaptation for the protein concentration. Therefore, \mathbf{X}_2 is here both the controlled and the measured species. From the dynamical model associated with this network, the equilibrium basal level for the concentration of \mathbf{X}_2 is computed to be $g_0 := k_0 k_2 / (\gamma_1 \gamma_2)$.

The original version of the AIC, as introduced in [14], corresponds to the naAIC setup depicted in Figure 8. A possible reaction network representation for this controller is given by



where \mathbf{Z}_1 is both the actuating and set-point species, \mathbf{Z}_2 is the sensing species, and \mathbf{X}_1 is the actuated species. The parameters μ, θ, η, k are all positive rate parameters of the reactions, which are all assumed to be mass-action. We note that this controller activates the production of \mathbf{X}_1 , which means that it can only increase the level of the controlled species \mathbf{X}_2 over the basal level g_0 . Calculations accordingly show that the set-point $r = \mu/\theta$ must be such that $r > g_0$ for the controlled network to satisfy the perfect adaptation property stated in Definition 1.1. When this is not satisfied, one component of the state of the network grows without bound as depicted in Figure (9).B. However, when the stability conditions for the controlled network are met, we automatically have that $x_2(t) \rightarrow r$ as $t \rightarrow \infty$ demonstrating the perfect adaptation property for the controlled network; see Figure (9).A.

Consider now for the sake of comparison another type of AIC controller, the niAIC with output inhibition. A possible reaction network representation for this controller is given by



where now \mathbf{Z}_1 is the set-point species, \mathbf{Z}_2 is both the sensing and actuating species, and \mathbf{X}_2 is the measured/controlled/actuated species. We can observe in this case that the actuating species \mathbf{Z}_2 actively degrade the controlled species \mathbf{X}_2 , which indicates that this controller can only decrease the output with respect to the basal level g_0 . In fact, calculation show exactly that it is necessary that the set-point r be such that $r < g_0$ for the network to have stability and perfect adaptation properties. As for the naAIC, if this condition is not met, one component of the state of the network grows without bound as depicted in Figure (9).D. However, when the stability conditions for the controlled network are met, we automatically get that $x_2(t) \rightarrow r$ as $t \rightarrow \infty$ demonstrating the perfect adaptation property for the controlled network; see Figure (9).C.

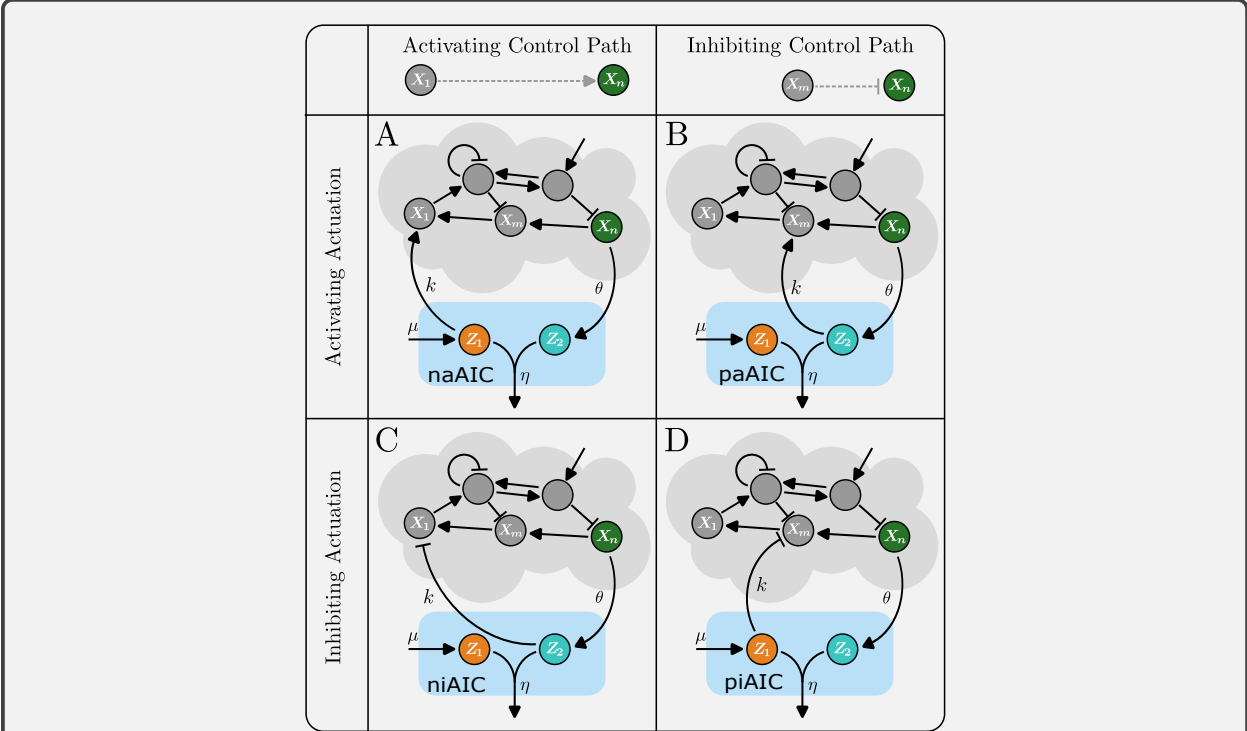


Figure 8: The main objective of Antithetic Integral Controllers is to interact with a network in a way that makes one of its species, here X_n , exhibit the robust perfect adaptation property. The core mechanism of the AIC is the sequestration reaction that allows to perform a comparison operation between the levels of the two controller species Z_1 and Z_2 . AICs admit different possible architectures depending on the role of its molecular species, which may act as activators or inhibitors. The naming convention for these controllers is as follows: "n" indicates that the loop is closed negatively by the controller (i.e., X_n inhibits X_1 or X_m), "p" signifies that the loop is closed positively (i.e., X_n activates X_1 or X_m), and "a" or "i" denotes whether the actuating species is an activator or a repressor. It is assumed that X_1 activates X_n in the networks of the first column, whereas X_m inhibits X_n in those in the second column. Based on this, the naAIC bears its name because it activates X_1 using Z_1 and closes the loop negatively, since $X_n \rightarrow Z_2 \dashv Z_1 \rightarrow X_1$, which can be reduced to $X_n \dashv X_1$. Similarly, the piAIC bears its name because it inhibits X_m using Z_1 and closes the loop positively, since $X_n \rightarrow Z_2 \dashv Z_1 \dashv X_m$, which can be reduced to $X_n \rightarrow X_m$.

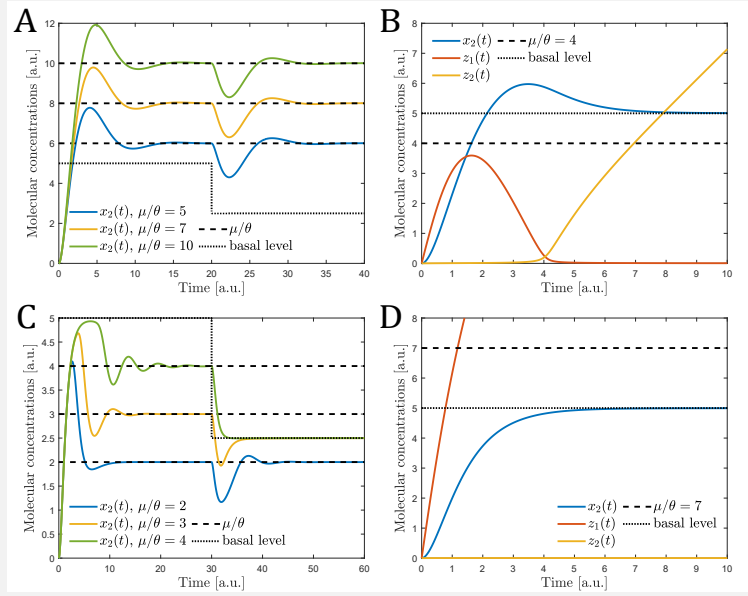


Figure 9: **A.** Simulation of the reaction network (3.1)-(3.2) with the parameters $\gamma_1 = 1, \gamma_2 = 2, k_2 = 1, k_0 = 10, k = 1, \eta = 100, \theta = 1$ and for various values for μ . At time $t = 20$, the value of k_0 is divided by 2. When the set point μ/θ is set above the basal level, the controlled species \mathbf{X}_2 exhibits the robust perfect adaptation property. **B.** When the set-point is set to a value lower than the basal level, the concentration of controller species \mathbf{Z}_2 grows without bound and perfect adaptation is not achieved for \mathbf{X}_2 . **C.** Simulation of the reaction network (3.1)-(3.3) with the parameters $\gamma_1 = 1, \gamma_2 = 2, k_2 = 1, k_0 = 10, k = 0.5, \eta = 100, \theta = 1$ and for various values for μ . At time $t = 30$, the value of k_0 is divided by 2. When the set point μ/θ is set below the basal level, the controlled species \mathbf{X}_2 exhibits the robust perfect adaptation property. **D.** When the set-point is set to a value higher than the basal expression level, the concentration of the controller species \mathbf{Z}_1 grows without bound and perfect adaptation is not achieved for \mathbf{X}_2 , which can only converge to its basal level.

Box 2. Passivity analysis and the analysis of interconnections

A very powerful tool for the analysis of feedback linear systems is called the Nyquist criterion, which is a frequency domain graphical criterion. Consider a linear system with transfer function $H_1(s)$ with poles with negative real part and such that $H_1(0) > 0$. Consider further the transfer function $H_2(s) = k/s$ where $k > 0$. We are now interested in studying the stability of the interconnection depicted in Figure 10.B. The Nyquist criterion for stable systems provide a way to answer to this question:

Theorem 3.1 (Nyquist stability criterion for stable systems) *The feedback interconnection depicted in Figure 10.B with the previously defined transfer functions is stable if and only if $kH(j\omega)/j\omega$ does not encircle the point -1 in the complex plane as ω sweeps from $-\infty$ to ∞ .*

This criterion is very simple to use as one just needs to plot the Nyquist diagram using off-the-shelf computational tools and verify whether it encircles the critical point -1 or not. This can also be checked analytically by verifying that for all critical frequencies ω_c defined as $\arg(kH(j\omega_c)/j\omega_c) = -\pi$, the condition $|kH(j\omega_c)/j\omega_c| < 1$ holds.

We now consider the question of establishing whether the interconnection is stable for all positive k 's. To this aim, first observe that if there exists a critical frequency ω_c as defined above, then one can select $k > k_c := -(H(j\omega_c)/j\omega_c)^{-1} > 0$ such that $kH(j\omega)/j\omega$ will encircle the point -1. Therefore, one can conclude that the stability of the interconnection holds for all $k > 0$ if and only if there is no such critical frequency ω_c . Noting that

$$\arg(kH(j\omega)/j\omega) = \arg(H(j\omega)) - \arg(j\omega) = \arg(H(j\omega)) - \pi/2, \quad (3.4)$$

we can conclude that there are no critical frequencies if and only if

$$\arg(H(j\omega)) \in (-\pi/2, \pi/2) \quad (3.5)$$

for all $\omega \in \mathbb{R}$. This is equivalent to saying that $\Re[H(j\omega)] > 0$ for all $\omega \in \mathbb{R}$ or that the Nyquist diagram is strictly included in the open right half-plane as illustrated in Figure 10.A. Interestingly, we can connect this property to the positive realness properties of transfer functions given below:

Definition 3.2 *The rational, proper function $H : \mathbb{C} \mapsto \mathbb{C}$ is said to be*

(1) *Weakly Strictly Positive Real (WSPR) if*

- (1a) *all the poles of $H(s)$ are in the open left half-plane, and*
- (1b) *$\Re[H(j\omega)] > 0$ for all $\omega \in [0, \infty)$.*

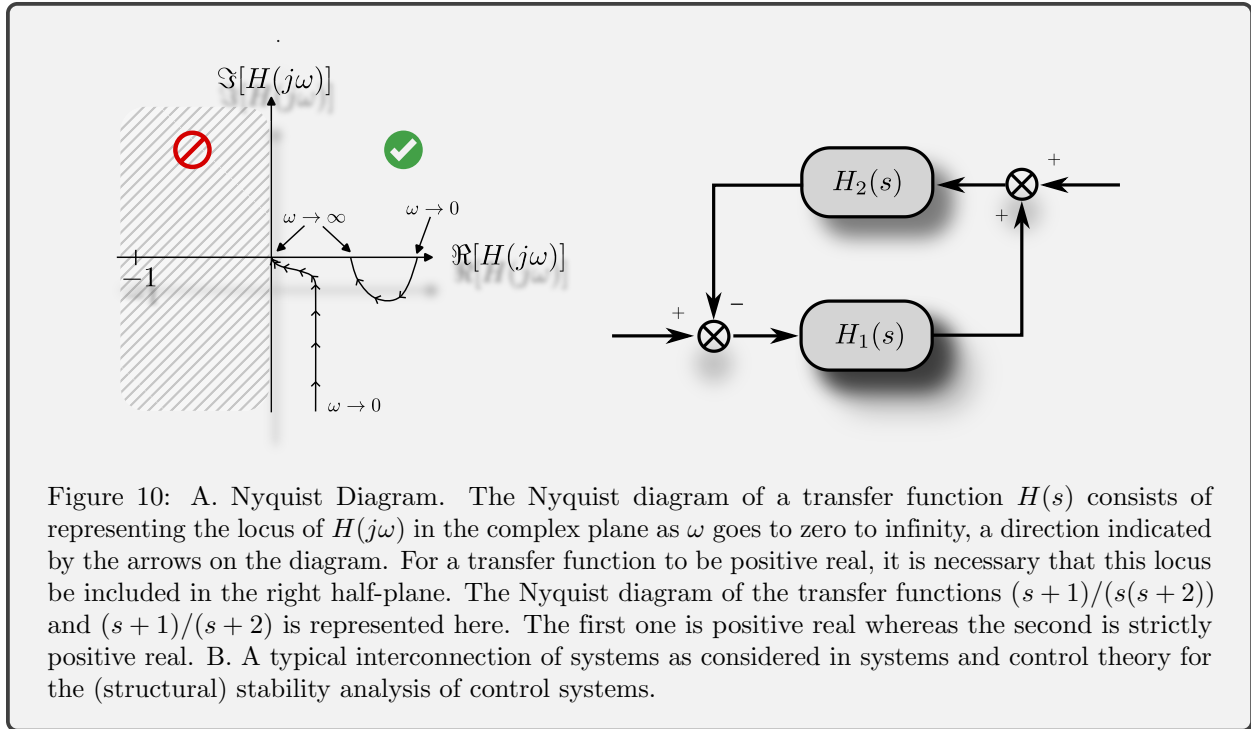
(2) *Strictly Positive Real (SPR) if*

- (2a) *it is weakly strictly positive real, and*
- (2b) *$H(\infty) > 0$ or $\lim_{\omega \rightarrow \infty} \omega^2 \Re[H(j\omega)] > 0$.*

As previously said, checking those properties can be done computationally and graphically. Computing the poles of the transfer function as well as plotting the Nyquist diagram can be easily performed using off-the-shelf software. A difficulty is the possible existence of values for ω for which the diagram come very close to the imaginary axis, making it difficult to establish whether they intersect. To palliate this, the existence of intersections can be assessed by finding real solutions ω to the equation $\Re[H(j\omega)] = 0$, which amounts to numerically solving a polynomial for real solutions. Finally, the additional condition in the SPR property can be easily checked using the expression

$$\lim_{\omega \rightarrow \infty} \omega^2 \Re[H(j\omega)] = \sum_{i=1}^{n_z} z_i - \sum_{i=1}^{n_p} p_j, \text{ whenever } n_p = n_z + 1, \quad (3.6)$$

and where the z_i 's and p_j 's are the zeros and the poles of the transfer function $H(s)$, respectively.



Author contributions

M.K. and C.B. conceived the study, C.B. performed the research, C.B. performed the numerical simulations, M.K. supervised the research and secured the funding, C.B. and M.K. wrote the paper.

Declaration of interests

The authors declare no competing interests.

Declaration of generative AI and AI-assisted technologies in the writing process

During the preparation of this work the authors used ChatGPT in order to improve the readability and language of the manuscript. After using this tool/service, the authors reviewed and edited the content as needed and take full responsibility for the content of the published article.

Acknowledgments

The authors gratefully thank Christian Cuba Samaniego, Maurice Filo, Jean-Baptiste Lugagne, Noah Olsman, and Yili Qian for fruitful discussions.

Supplementary Information

Contents

S1 Preliminary definitions and results	29
S1.1 Results on (positive) linear systems	30
S1.2 Positive real transfer functions and associated results	32
S2 Reaction networks and robust perfect adaptation	34
S2.1 Reaction Networks	34
S2.2 Perfect Adaptation Problem and Integral Control	35
S2.3 Antithetic Integral Controllers	36
S2.3.1 naAIC	37
S2.3.2 niAIC	38
S2.4 Antithetic Integral Rein Controllers	40
S2.4.1 Generalities	40
S2.4.2 Output Rein Control	41
S3 Unimolecular mass-action networks	42
S3.1 The general problem and its properties	42
S3.2 Reduced problem - The niAIC with output inhibition	46
S3.3 Existence results for the niAIC with output inhibition	47
S3.4 Structural stability analysis for the niAIC with output inhibition - Stable case	49
S3.5 Structural stability analysis for the niAIC with output inhibition - Unstable case	52
S3.5.1 Preliminaries	52
S3.5.2 Persistent external excitation	54
S3.6 Partial structural stability analysis of the network controlled with an AIRC with output inhibition	55
S4 Structural stability of the niAIC - Nonlinear case	57
S4.1 Definitions, assumptions, and preliminary results	57
S4.2 General results	60
S4.3 Cooperative and Michaelis-Menten networks	64
S5 Extension to other types of integral controllers	66
S5.1 Exponential integral controllers	66
S5.2 Logistic integral controllers	67

Notations. The cone of symmetric positive (semi)definite matrices of dimension n is denoted by $(\mathbb{S}_{\succeq 0}^n \ \mathbb{S}_{> 0}^n)$. For two symmetric matrices A, B with same dimension, $A \succ B$ ($A \succeq B$) means that $A - B \succ 0$ ($A - B \succeq 0$); i.e. $A - B$ is positive (semi)definite. The natural basis for \mathbb{R}^n is denoted by $\{e_1, \dots, e_n\}$.

S1 Preliminary definitions and results

This section is devoted to introducing the main definitions and results that will prove instrumental in proving the main results of the paper.

S1.1 Results on (positive) linear systems

Let us introduce the following Linear Time-Invariant (LTI) system

$$\begin{aligned} \dot{x}(t) &= Ax(t) + Bu(t), t \geq 0 \\ y(t) &= Cx(t) + Du(t) \\ x(0) &= x_0 \end{aligned} \tag{S1.1}$$

where $A \in \mathbb{R}^{n \times n}$, $B \in \mathbb{R}^{n \times m}$, $C \in \mathbb{R}^{p \times n}$, and $D \in \mathbb{R}^{p \times m}$. The following definition introduces the concept of spectral abscissa:

Definition S1.1 *The spectral abscissa $\alpha(A)$ of a matrix $A \in \mathbb{R}^{n \times n}$ is defined as*

$$\alpha(A) := \max \{ \Re(\lambda) : \det(\lambda I - A) = 0 \}. \tag{S1.2}$$

This concept is essential in the analysis of linear dynamical systems of the form (S1.1) since it is immediate to see that this the 0-equilibrium point of that system is asymptotically stable if and only $\alpha(A) < 0$, which is equivalent to saying that the spectrum of A is included in the open left half-plane of the complex plane. The next result states conditions under which the system (S1.1) is internally positive:

Proposition S1.2 ([29]) *The following statements are equivalent:*

- (a) *The linear dynamical system (S1.1) is internally positive; i.e. for all $x_0 \geq 0$ and all $u(t) \geq 0$, $t \geq 0$, we have that $x(t) \geq 0$, $y(t) \geq 0$, for all $t \geq 0$.*
- (b) *The matrix A is Metzler (i.e. all the off-diagonal entries are nonnegative) and the matrices B, C, D are nonnegative (i.e. all the entries are nonnegative).*

Proposition S1.3 ([9, 29, 44, 47]) *Let $A \in \mathbb{R}^{n \times n}$ be Metzler. Then, the following statements are equivalent:*

- (a) *A is Hurwitz stable (i.e. all its eigenvalues have negative real part or, equivalently, $\alpha(A) < 0$),*
- (b) *For all $q \in \mathbb{R}_{>0}^n$, there exists a vector $v \in \mathbb{R}_{>0}^n$ such that $v^T A = -q^T$, and*
- (c) *There exists a diagonal matrix D with positive diagonal such that $A^T D + DA \prec 0$ (i.e. $A^T D + DA$ is negative definite).*
- (d) *A is invertible and $-A^{-1}$ is nonnegative.*

Lemma S1.4 ([14]) *Assume that A is Metzler and Hurwitz stable, then the system (A, e_i, e_j^T) , $i, j \in \{1, \dots, n\}$, with transfer function $H_{ij}(s) = e_j^T (sI - A)^{-1} e_i$, is output controllable if and only if one of the following statements holds:*

1. *The impulse response $h_{ij}(t) = e_j^T e^{At} e_i$ is not identically zero.*
2. *The DC-gain $H_{ij}(0) = -e_j^T A^{-1} e_i$ is positive.*
3. *The rank condition $\text{rank} \begin{bmatrix} e_j^T e_i & e_j^T A e_i & e_j^T A^2 e_i \\ \vdots & \vdots & \vdots \\ e_j^T A^{n-1} e_i \end{bmatrix} = 1$ is satisfied.*

Proposition S1.5 ([9]) *Assume that the matrix $M \in \mathbb{R}^{n \times n}$ is Metzler. Then, the following statements hold:*

- (a) *There exists an eigenvalue $\lambda_{\text{PF}}(A)$ of A that is equal to $\alpha(A)$, which is referred to as the Perron-Frobenius eigenvalue. Moreover, if the matrix A is irreducible, then this eigenvalue is unique.*

(b) Let \tilde{M} be a Metzler matrix such that $M \leq \tilde{M}$ (where the inequality is component-wise), then $\alpha(M) \leq \alpha(\tilde{M})$.

Finally, the following result will be crucial for proving the main results of the paper:

Lemma S1.6 Consider the linear system

$$\begin{aligned} \dot{x} &= Mx + e_n w \\ z &= e_n^T x \end{aligned} \quad (\text{S1.3})$$

where $M \in \mathbb{R}^{n \times n}$. Then, we have that

$$e_n^T \text{Adj}(sI - M)e_n = \det(sI - M_{11}), \quad (\text{S1.4})$$

where M_{11} is $(n-1) \times (n-1)$ upper left block of M and $\text{Adj}(\cdot)$ denotes the adjugate matrix. Moreover,

(a) if the pairs (M, e_n) and (M, e_n^T) are controllable and observable, respectively, then

$$H(s) := e_n^T (sI - M)^{-1} e_n = \frac{\det(sI - M_{11})}{\det(sI - M)}. \quad (\text{S1.5})$$

(b) if M is a Metzler, Hurwitz stable matrix, then the solutions of $\det(sI - M_{11}) = 0$ are all located in the open left half-plane of the complex plane.

Proof : First note that

$$e_n^T \text{Adj}(sI - M)e_n = \det \begin{bmatrix} sI - M_n & -e_n \\ e_n^T & 0 \end{bmatrix}. \quad (\text{S1.6})$$

If we decompose M as

$$M =: \begin{bmatrix} M_{11} & M_{12} \\ M_{21} & M_{22} \end{bmatrix}, \quad (\text{S1.7})$$

where $M_{11} \in \mathbb{R}^{(n-1) \times (n-1)}$, $M_{12} \in \mathbb{R}^{(n-1) \times 1}$, $M_{21} \in \mathbb{R}^{1 \times (n-1)}$, and $M_{22} \in \mathbb{R}$, then the expression (S1.6) becomes

$$\begin{bmatrix} sI - M_n & -e_n \\ e_n^T & 0 \end{bmatrix} = \begin{bmatrix} sI - M_{11} & -M_{12} & 0 \\ -M_{21} & s - M_{22} & -1 \\ 0 & 1 & 0 \end{bmatrix}. \quad (\text{S1.8})$$

Using now the properties of the determinant on the last row, we get that

$$\det \begin{bmatrix} sI - M_{11} & -M_{12} & 0 \\ -M_{21} & s - M_{22} & -1 \\ 0 & 1 & 0 \end{bmatrix} = -\det \begin{bmatrix} M_{11} - sI_n & 0 \\ M_{21} & -1 \end{bmatrix} = \det(sI - M_{11}), \quad (\text{S1.9})$$

which proves the first statement of the result.

Assuming now that the pairs (M, e_n) and (M, e_n^T) are controllable and observable, respectively, then there is no pole/zero cancellations in the transfer function $H(s) = \frac{e_n^T \text{Adj}(sI - M)e_n}{\det(sI - M)}$ and the result follows.

Finally, assuming that the matrix M is Metzler and Hurwitz stable, then it is immediate to see that

$$M_d := \begin{bmatrix} M_{11} & 0 \\ 0 & M_{22} \end{bmatrix} \leq M \quad (\text{S1.10})$$

where the inequality is entry-wise. From Perron-Frobenius theory (or Proposition S1.5), $M_d \leq M$ implies that $\lambda_{\text{PF}}(M_d) \leq \lambda_{\text{PF}}(M)$. Since M is Hurwitz stable, then $\lambda_{\text{PF}}(M) < 0$, which implies that M_d , M_{11} and M_{22} are all Hurwitz stable matrices. This proves the third statement of the result and completes the proof. \diamond

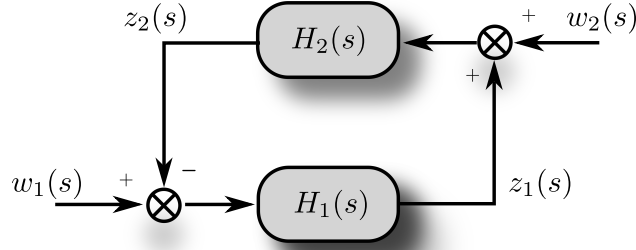


Figure S11: Negative interconnection

S1.2 Positive real transfer functions and associated results

We consider the following definitions which can be found in [20]:

Definition S1.7 *The function $H : \mathbb{C} \mapsto \mathbb{C}$ is said to be*

(1) *Positive Real (PR) if*

- (1a) *all the poles of $H(s)$ are in the closed left half-plane,*
- (1b) *$\Re[H(j\omega)] \geq 0$ for all $\omega \in [0, \infty)$, and*
- (1c) *any pure imaginary pole $j\omega$ is simple and $\lim_{s \rightarrow j\omega} (s - j\omega)H(s) \geq 0$.*

(2) *Weakly Strictly Positive Real (WSPR) if*

- (2a) *all the poles of $H(s)$ are in the open left half-plane, and*
- (2b) *$\Re[H(j\omega)] > 0$ for all $\omega \in [0, \infty)$.*

(3) *Strictly Positive Real (SPR) if*

- (3a) *it is weakly strictly positive real, and*
- (3b) *$H(\infty) > 0$ or $\lim_{\omega \rightarrow \infty} \omega^2 \Re[H(j\omega)] > 0$.*

(4) *Strong Strictly Positive Real (Strong SPR) if*

- (4a) *it is weakly strictly positive real, and*
- (4b) *there exists a $\delta > 0$ such that $\Re[H(j\omega)] \geq \delta$ for all $\omega \in [0, \infty]$.*

The following result pertaining to the stability of the interconnection depicted in Figure S11 will be instrumental in proving the main results of the paper:

Theorem S1.8 ([20, Lemma 3.37]) *Let $H_1, H_2 : \mathbb{C} \mapsto \mathbb{C}$ be two transfer functions. Assume further that*

1. *H_1 is strictly or weakly positive real, and*
2. *H_2 is positive real.*

Then, the negative feedback interconnection defined as $z_1 = H_1(w_1 - z_2)$ and $z_2 = H_2(w_2 + z_1)$, depicted in Figure S11, is internally stable, this is, the transfer $w \mapsto z$ given by

$$\frac{1}{1 + H_1 H_2} \begin{bmatrix} H_1 & -H_1 H_2 \\ H_1 H_2 & H_2 \end{bmatrix} \quad (\text{S1.11})$$

is stable.

The following result provides sufficient conditions under which a rational, strictly proper transfer function is WSPR:

Proposition S1.9 *Let us consider the matrices $A \in \mathbb{R}^{n \times n}$, $B \in \mathbb{R}^{n \times m}$, and $C \in \mathbb{R}^{m \times n}$, and define the function $H(s) := C(sI - A)^{-1}B$. Assume further that*

- (1) $H(s)$ has no zero on the imaginary axis, and
- (2) there exist a matrix $P \in \mathbb{S}_{>0}^n$ and an $\varepsilon > 0$ such that $PB - C^T = 0$ and $A^T P + PA + 2\varepsilon C^T C \prec 0$.

Then, $H(s)$ is weakly strictly positive real.

Proof : Note that $A^T P + PA + 2\varepsilon C^T C \prec 0$ for some $P \succ 0$ and $\varepsilon > 0$ implies that A is Hurwitz stable, meaning that all the poles of $H(s)$ have negative real part. This proves that condition (2a) of Definition S1.7 holds.

To show that the condition (2b) of Definition S1.7 holds, first note that under the conditions of the result, the following matrix

$$\begin{bmatrix} A^T P + PA + 2\varepsilon C^T C & PB - C^T \\ B^T P - C & 0 \end{bmatrix} = \begin{bmatrix} A^T P + PA & PB \\ B^T P & 0 \end{bmatrix} + \begin{bmatrix} C & 0 \\ 0 & I \end{bmatrix}^T \begin{bmatrix} 2\varepsilon I & -I \\ -I & 0 \end{bmatrix} \begin{bmatrix} C & 0 \\ 0 & I \end{bmatrix} \quad (\text{S1.12})$$

is negative semidefinite. From the Kalman-Yakubovich-Popov Lemma [75,59], this is equivalent to saying that

$$\begin{bmatrix} H(j\omega) \\ I \end{bmatrix}^* \begin{bmatrix} 2\varepsilon I & -I \\ -I & 0 \end{bmatrix} \begin{bmatrix} H(j\omega) \\ I \end{bmatrix} \leq 0, \text{ for all } \omega \in [0, \infty). \quad (\text{S1.13})$$

Note that $H(j\omega)$ is well-defined since A has no eigenvalues on the imaginary axis. Expanding the left-hand side yields

$$2\varepsilon |H(j\omega)|^2 - 2\Re[H(j\omega)] \leq 0, \text{ for all } \omega \in [0, \infty), \quad (\text{S1.14})$$

which implies that $\Re[H(j\omega)] \geq \varepsilon |H(j\omega)|^2$ for $\omega \in [0, \infty)$. Since $H(s) \neq 0$ on the imaginary axis, this implies that the statement (2b) in Definition S1.7 holds, and proves the desired result. \diamond

The following technical result will also prove to be very useful for proving the main results of the paper.

Lemma S1.10 *Let $H : \mathbb{C} \mapsto \mathbb{C}$ be a strictly proper, rational transfer function and decompose it $H(s) =: kN(s)/D(s)$ where $k \in \mathbb{R}$, and $N(s), D(s)$ are coprime, monic polynomials such that $\deg(D) = n$ and $\deg(N) = n - 1$. Then, we have that*

$$\lim_{\omega \rightarrow \infty} \omega^2 k \Re[H(j\omega)] = k \left(\sum_{i=1}^{n-1} z_i - \sum_{i=1}^n p_i \right) \quad (\text{S1.15})$$

where the p_i 's are the poles and the z_i 's are the zeros of the transfer function $H(s)$; i.e. $N(z_i) = 0$, $i = 1, \dots, n-1$, and $D(p_i) = 0$, $i = 1, \dots, n$.

Proof : We have that

$$\Re \left[\frac{N(j\omega)}{D(j\omega)} \right] = \frac{\Re [N(j\omega)D(j\omega)^*]}{|D(j\omega)|^2} = \frac{\Re [N(j\omega)D(-j\omega)]}{|D(j\omega)|^2}. \quad (\text{S1.16})$$

Since the degree of $N(j\omega)D(-j\omega)$ in ω is $2n - 1$ and the degree of $|D(j\omega)|^2$ is $2n$, to properly evaluate the limit of $\omega^2 \Re[H(j\omega)]$, we need to find the coefficient of the term in ω^{2n-2} of $N(j\omega)D(-j\omega)$.

To figure this out, let $N(s) = \sum_{i=0}^{n-1} N_i s^i$ and $D(s) = \sum_{i=0}^n D_i s^i$, which yields

$$\begin{aligned} \Re[N(j\omega)D(-j\omega)] &= \Re \left[\left(\sum_{i=0}^{n-1} N_i (j\omega)^i \right) \left(\sum_{i=0}^n D_i (-j\omega)^i \right) \right] \\ &= N_{n-1} (j\omega)^{n-1} D_{n-1} (-j\omega)^{n-1} + N_{n-2} (j\omega)^{n-2} D_n (-j\omega)^n + R_N(\omega) \\ &= (N_{n-1} D_{n-1} - N_{n-2} D_n) \omega^{2n-2} + R_N(\omega), \end{aligned} \quad (\text{S1.17})$$

where $R_N(\omega)$ is the remainder containing even powers of ω less than $2n - 2$. Define also $R_D(\omega)$ to be a polynomial of even powers less than $2n$ such that $|D(j\omega)|^2 = \omega^{2n} + R_D(\omega)$. This yields

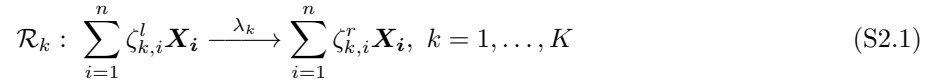
$$\begin{aligned} \lim_{\omega \rightarrow \infty} \omega^2 k \Re[H(j\omega)] &= \lim_{\omega \rightarrow \infty} \omega^2 k \frac{(N_{n-1} D_{n-1} - N_{n-2} D_n) \omega^{2n-2} + R_N(\omega)}{\omega^{2n} + R_D(\omega)} \\ &= k (N_{n-1} D_{n-1} - N_{n-2} D_n). \end{aligned} \quad (\text{S1.18})$$

As $N(s)$ and $D(s)$ are both monic polynomials, we have that $D_n = N_{n-1} = 1$, and this, together with the fact that $-D_{n-1}$ coincides with the sum of the poles and $-N_{n-2}$ coincides with the sum of the zeros, prove the desired result. \diamond

S2 Reaction networks and robust perfect adaptation

S2.1 Reaction Networks

Reaction networks are a very powerful modeling paradigm that can be used to represent any population system, such as those arising in ecology, epidemiology, opinion dynamics, multi-agent systems, etc.[37]. A reaction network $(\mathbf{X}, \mathcal{R})$ consists of a set of n molecular species $\mathbf{X} = \{\mathbf{X}_1, \dots, \mathbf{X}_n\}$ that interacts through K reaction channels $\mathcal{R} = \{\mathcal{R}_1, \dots, \mathcal{R}_K\}$ denoted as



where $\zeta_{k,i}^l, \zeta_{k,i}^r \in \mathbb{Z}_{\geq 0}^n$ are the left and right stoichiometric vectors. The stoichiometric vector of reaction \mathcal{R}_k is given by $\zeta_k := \zeta_k^r - \zeta_k^l \in \mathbb{Z}^n$ where $\zeta_k^r = \text{col}(\zeta_{k,1}^r, \dots, \zeta_{k,n}^r)$ and $\zeta_k^l = \text{col}(\zeta_{k,1}^l, \dots, \zeta_{k,n}^l)$. Each reaction \mathcal{R}_k is also described by its propensity function λ_k that describes the conditions under which this reaction occurs. Such functions may take various forms depending on the context and the type of kinetics, such as mass-action, Hill, Michaelis-Menten, etc.; see [71, 2]. In particular, when the network only has mass-action kinetics, only the reaction rates are indicated in (S2.1). This will be explicitly mentioned when this is the case. In all those cases, we define \mathcal{P} to be the set of the network parameters.

In the deterministic setting, reaction networks are quantitatively described in terms of a vector of concentrations, denoted here by $x(t)$, which evolves on the state-space $\mathcal{S} \subseteq \mathbb{R}_{\geq 0}^n$. In that case, the propensity functions $\lambda_k : \mathcal{S} \mapsto \mathbb{R}_{\geq 0}$ are defined in such a way that \mathcal{S} is forward invariant; i.e. for all $x_0 \in \mathcal{S}$, we have that $x(t) \in \mathcal{S}$ for all $t \geq 0$. This will be tacitly assumed to be the case in the rest of the paper. The dynamical model

representing the deterministic reaction network (S2.1) is therefore given by the Reaction Rate Equation (RRE)

$$\begin{aligned} \dot{x}(t) &= \sum_{k=1}^K \zeta_k \lambda_k(x(t)), \quad t \geq 0 \\ x(0) &= x_0 \end{aligned} \tag{S2.2}$$

which takes the form of a system of differential equations, emphasizing that reactions are considered as continuous processes which all push the state in the direction given by their associated stoichiometric vector.

S2.2 Perfect Adaptation Problem and Integral Control

The perfect adaptation property [2] is the property of a reaction network that certain molecular counts will return to the equilibrium levels they had before some environmental changes and network perturbations. This is one of the many types of homeostatic behaviors that can be found in living organisms [21] or that can be theoretically constructed [2, 48, 14, 36, 45, 39]. The version we consider in this paper is formally defined below:

Definition S2.1 (Perfect Adaptation) *Consider a reaction network $(\mathbf{X}, \mathcal{R})$ and a species $\mathbf{Y} \in \mathbf{X}$. The species \mathbf{Y} is said to exhibit the perfect adaptation property in the network $(\mathbf{X}, \mathcal{R})$ if*

1. *the equilibrium point x^* is (locally) asymptotically stable for the dynamics of the network (S2.2), and*
2. *the equilibrium value of the concentrations of the species \mathbf{Y} , denoted by y^* , is independent of all the parameters in a subset of \mathcal{P} .*

Perfect adaptation is a very strong property. Indeed, almost all networks will not exhibit it and a natural problem that comes to mind is: given a network that does not show any adaptation property, how can we modify it in an appropriate way so that it exhibits this property? This can either be done by suitably modifying the current network, or through the introduction of new molecular species and reactions. The latter approach is formalized below:

Definition S2.2 (Perfect Adaptation Problem) *Consider a reaction network $(\mathbf{X}, \mathcal{R})$ and a species $\mathbf{Y} \in \mathbf{X}$. The robust perfect adaptation problem consists of finding a controller network $(\mathbf{Z}, \mathcal{R}^c)$ such that*

1. *\mathbf{Y} exhibits the perfect adaptation property in the network $(\mathbf{X} \cup \mathbf{Z}, \mathcal{R} \cup \mathcal{R}^c)$, and*
2. *y^* is equal to a tunable set-point which is a known function of the controller parameters only (i.e. it is independent of the parameters of the network $(\mathbf{X}, \mathcal{R})$).*

This problem is an instance of the regulation problem in control theory – an ubiquitous problem in science and engineering– which consists of finding a controller that makes a controlled system not only stable but also such that its output converges to a desired set-point. Many relevant control problems fall into this category such as temperature control, cruise control, auto-pilot design, etc. [7] Different controller structures need to be considered depending on the class of perturbations/stimuli sought to be compensated for. This structure is dictated by the so-called Internal Model Principle [34, 66], which stipulates that controllers need to embed a model of the perturbations they aim at rejecting. This internal model principle is a fundamental result which goes beyond the realm of control theory and is also central in other fields such as neuroscience, cognition, etc. [10]. When the perturbations/stimuli are assumed to be (locally) constant, this principle states that controllers that solves the regulation problem necessarily incorporate an integral action, whence the name of integral controllers. It has also been recently shown that reaction networks exhibiting robust perfect adaptation properties necessarily involved a hidden integral action [39, 5, 41] implemented in terms of molecular reactions.

A necessary condition for perfect adaptation is that the set-point be a valid value for the species \mathbf{Y} . This leads us to the concept of set-point admissibility:

Definition S2.3 (Set-point admissibility) Consider a reaction network $(\mathbf{X}, \mathcal{R})$ and a species $\mathbf{Y} \in \mathbf{X}$. Moreover, decompose \mathcal{P} as $\mathcal{P}_f \cup \mathcal{P}_t$ where \mathcal{P}_f is a set of fixed network parameters and \mathcal{P}_t is a set of tunable network parameters.

We say that a set-point r is admissible for the species \mathbf{Y} if, given the values for the parameters in \mathcal{P}_f , we can select values for the parameters in \mathcal{P}_t such that $x^* \geq 0$ and $y^* = r$ where x^* is an equilibrium point for the dynamics (S2.2).

S2.3 Antithetic Integral Controllers

The Antithetic Integral Controller (AIC), introduced in [14] and further discussed in [13, 54, 55], is one of the few, structurally simple, integral controllers that can be implemented in terms of chemical reactions. Other ones include zeroth-order integral controllers [52] and autocatalytic integral controllers [25, 19, 76, 13]. This controller relies on molecular sequestration as core mechanism, which consists of two complementary molecular species strongly binding with each other. Sequestration is a well-known mechanism that has been widely selected to achieve certain pivotal functions within living organisms, such as bacterial stress response through the use of sigma-factors [68]. More theoretically, it has also been shown that such a sequestration reaction is essential in the realization problem [53, 28] and that it can be interpreted as a molecular implementation of a subtraction operator [24, 30], as also emphasized in [14, 13]. The internal complementarity structure of the AIC makes it a very flexible controller that can easily implement negative and positive feedback loops using both activation or inhibition interactions, as illustrated in Table 1. More advanced controller structures than those depicted in Table 1 exist and can be cleverly generated through the addition of controller reactions/species to achieve more complex regulatory behaviors [33]. The common denominator to all those designs is that the set-point should activate the controlled species, which should in turn repress itself, both possibly through a sequence of reactions.

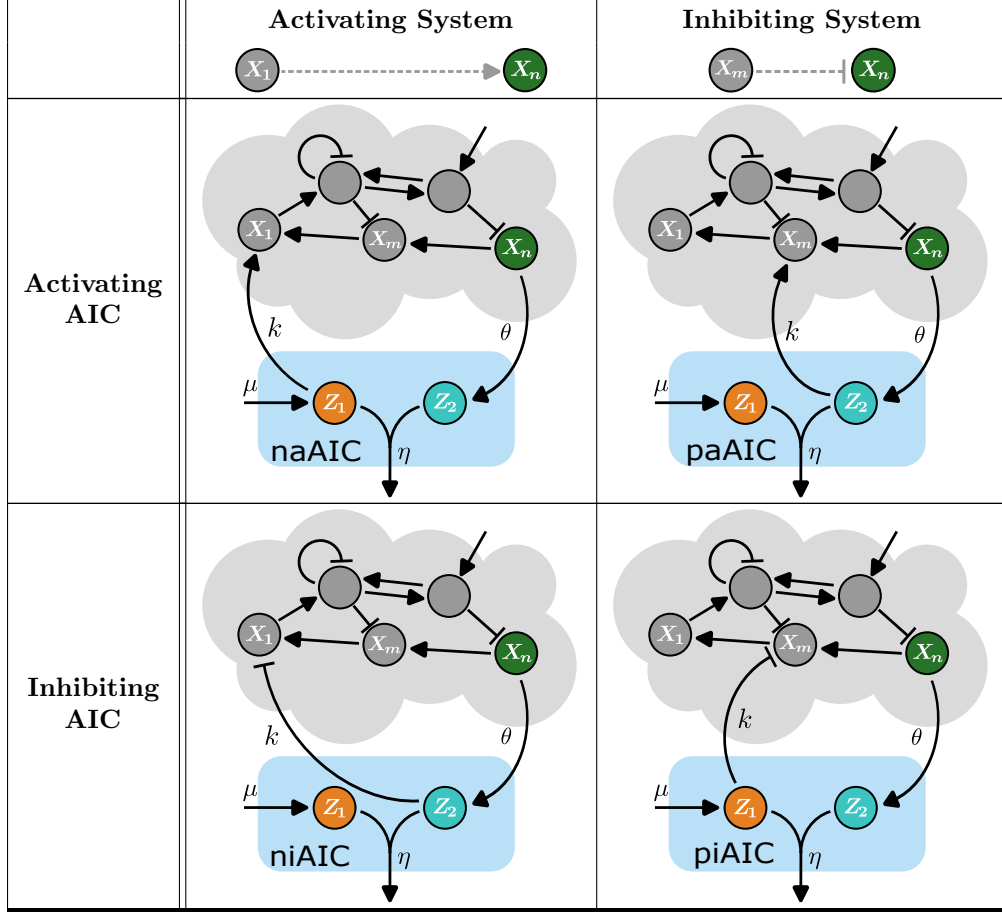
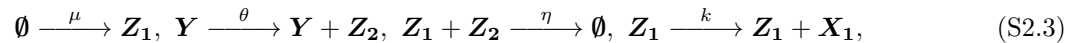


Table 1: Four different flavors of the Antithetic Integral Controller depending on whether it activates an activating system (naAIC), inhibits an activating system (niAIC), activates an inhibiting system (paAIC), and inhibits an inhibiting system (piAIC). This controller involves two additional molecular species, Z_1 and Z_2 , and four additional reactions. The controllers have information about the level of the controlled species $Y = X_n$ through the sensing reaction and act back onto the system through the reaction. The set-point is (partially) set by the set-point μ and, finally, the essential sequestration reaction $Z_1 + Z_2 \longrightarrow \emptyset$ plays the role of a comparator between the levels of the controlled species. In all those designs, we can observe that μ promotes the expression of X_n , which in turn represses itself through a sequence of reactions. It can be shown that all those controllers solve the perfect adaptation problem described in Definition S2.2 in the sense that $y = x_n^* = \mu/\theta$ independently of the values of the parameters of the networks, provided those verify various technical assumptions.

S2.3.1 naAIC

The original version of the AIC, as introduced in [14], corresponds to the naAIC setup depicted in Table 1. A possible reaction network representation for this controller is given by

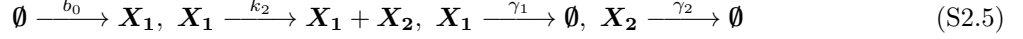


where Z_1 is both the actuating and reference species, Z_2 is the sensing species, Y is the measured/controlled species, and X_1 is the actuated species. The parameters μ, θ, η, k are all positive rate parameters of the reactions, which are all assumed to be mass-action. In compliance with the naAIC structure, it is assumed

here that \mathbf{X}_1 activates \mathbf{Y} , possibly through a sequence of reactions. The deterministic model of this controller is given by

$$\dot{z}_1(t) = \mu - \eta z_1(t) z_2(t) \quad \text{and} \quad \dot{z}_2(t) = \theta y(t) - \eta z_1(t) z_2(t). \quad (\text{S2.4})$$

To avoid entering too technical discussions, we simply illustrate that this controller indeed solves the perfect adaptation problem stated in Definition S2.2 for the gene expression network



where \mathbf{X}_1 and \mathbf{X}_2 denote the mRNA and protein species, respectively. Above, the positive rate parameters b_0, k_2, γ_1 , and γ_2 of the mass-action reactions correspond to the basal transcription rate, the translation rate, the mRNA degradation rate, and the protein degradation rate, respectively. We consider here the problem of ensuring perfect adaptation for the protein concentration, that is, we set $\mathbf{Y} = \mathbf{X}_2$. It can be shown that the basal equilibrium level

$$(x_1^*, x_2^*) = \left(\frac{b_0}{\gamma_1}, \frac{b_0 k_2}{\gamma_1 \gamma_2} \right)$$

is asymptotically stable for the system

$$\begin{aligned} \dot{x}_1(t) &= -\gamma_1 x_1(t) + b_0 \\ \dot{x}_2(t) &= k_2 x_1(t) - \gamma_2 x_2(t) \end{aligned} \quad (\text{S2.6})$$

describing the network (S2.5). Adding now the input u so as to act on the transcription rate, we obtain the following system describing

$$\begin{aligned} \dot{x}_1(t) &= -\gamma_1 x_1(t) + b_0 + u(t) \\ \dot{x}_2(t) &= k_2 x_1(t) - \gamma_2 x_2(t) \\ y(t) &= x_2(t) \end{aligned} \quad (\text{S2.7})$$

from which we can observe that $y^* = \frac{(b_0 + u^*)k_2}{\gamma_1 \gamma_2} > \frac{b_0 k_2}{\gamma_1 \gamma_2}$. This means that one can only increase the output from its basal expression level and this will be so regardless the type of controllers that is considered.

When the set-point $r = \mu/\theta$ is admissible (i.e. $r > \frac{b_0 k_2}{\gamma_1 \gamma_2}$) and certain conditions are met for the closed-loop network consisting of the interconnection of (S2.5)-(S2.3)

$$\begin{aligned} \dot{x}_1(t) &= -\gamma_1 x_1(t) + b_0 + k z_1(t) \\ \dot{x}_2(t) &= k_2 x_1(t) - \gamma_2 x_2(t) \\ \dot{z}_1(t) &= \mu - \eta z_1(t) z_2(t) \\ \dot{z}_2(t) &= \theta y(t) - \eta z_1(t) z_2(t), \end{aligned} \quad (\text{S2.8})$$

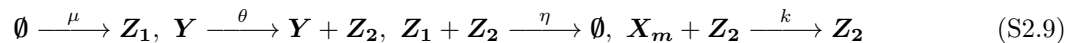
then this network exhibits perfect adaptation properties and

$$\lim_{t \rightarrow \infty} x_2(t) = \frac{\mu}{\theta}.$$

When the admissibility condition is not met, however, there is no equilibrium point in the positive orthant, which implies it cannot include any compact forward invariant set, which is equivalent to saying that the solution must grow without bound [60,61]. Those facts are illustrated in Figure S12.

S2.3.2 niAIC

The niAIC shown in Table 1 is another important class of AICs, which will turn out to be an essential part of this paper. This structure was briefly mentioned in [14] without entering into technical details. A possible reaction network representation for this controller is given by



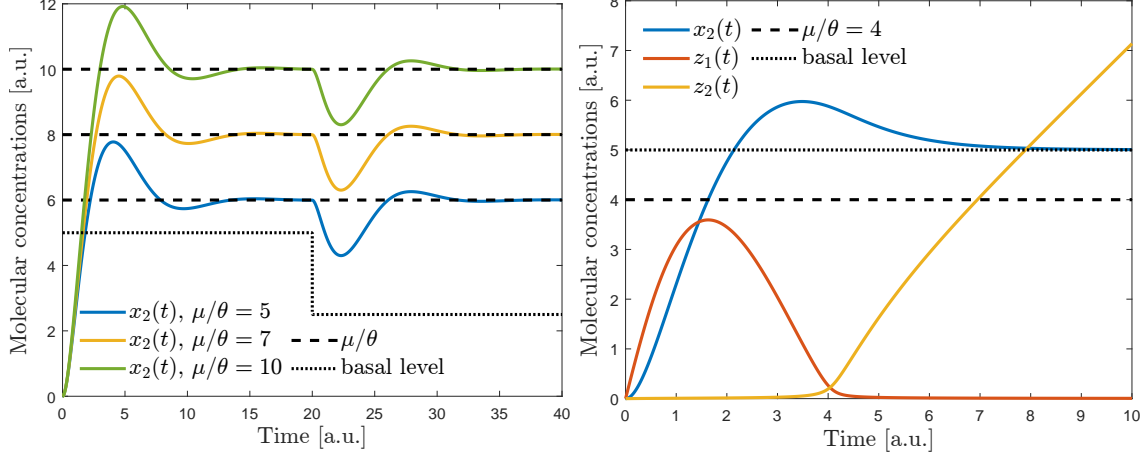


Figure S12: Simulation of the reaction network (S2.5)-(S2.3) with the parameters $\gamma_1 = 1$, $\gamma_2 = 2$, $k_2 = 1$, $b_0 = 10$, $k = 1$, $\eta = 100$, $\theta = 1$ and for various values for μ . At time $t = 20$, the value of b_0 is divided by 2. When the set point μ/θ is set above the basal level, the controlled species \mathbf{X}_2 exhibits the robust perfect adaptation property. When the set-point is set to a value lower than the basal level, the concentration of controller species \mathbf{Z}_2 grows without bound and perfect adaptation is not achieved for \mathbf{X}_2 .

where \mathbf{Z}_1 is the reference species, \mathbf{Z}_2 is both the sensing and actuating species, \mathbf{Y} is the measured/controlled species, and \mathbf{X}_m is the actuated species. The parameters μ, θ, η, k are all positive rate parameters of the reactions, which are all assumed to be mass-action. In compliance with the niAIC structure, it is assumed here that \mathbf{X}_m represses \mathbf{Y} , possibly through a sequence of reactions. The deterministic model of this controller is also given by (S2.4).

As in the previous section, we illustrate the controller properties on the gene expression network (S2.5) to which we add the control input according to the structure of the controller (S2.9) as follows

$$\begin{aligned}\dot{x}_1(t) &= -\gamma_1 x_1(t) + b_0 \\ \dot{x}_2(t) &= k_2 x_1(t) - \gamma_2 x_2(t) - u(t)x_2(t) \\ y(t) &= x_2(t).\end{aligned}\tag{S2.10}$$

From this expression we can observe that $y^* = \frac{b_0 k_2}{\gamma_1(\gamma_2 + u^*)} < \frac{b_0 k_2}{\gamma_1 \gamma_2}$. This means that one can only decrease the output from its basal expression level and this will be so regardless the type of controllers that is considered.

When the set-point $r = \mu/\theta$ is admissible (i.e. $r < \frac{b_0 k_2}{\gamma_1 \gamma_2}$) and certain conditions are met for the closed-loop network consisting of the interconnection of (S2.5)-(S2.9)

$$\begin{aligned}\dot{x}_1(t) &= -\gamma_1 x_1(t) + b_0 \\ \dot{x}_2(t) &= k_2 x_1(t) - \gamma_2 x_2(t) - k z_2(t) x_2(t) \\ \dot{z}_1(t) &= \mu - \eta z_1(t) z_2(t) \\ \dot{z}_2(t) &= \theta y(t) - \eta z_1(t) z_2(t),\end{aligned}\tag{S2.11}$$

then this network exhibits perfect adaptation properties and

$$\lim_{t \rightarrow \infty} x_2(t) = \frac{\mu}{\theta}.$$

As for the naAIC, the solution of this system must grow without bound whenever this admissibility condition is not met, as illustrated in Figure S13.

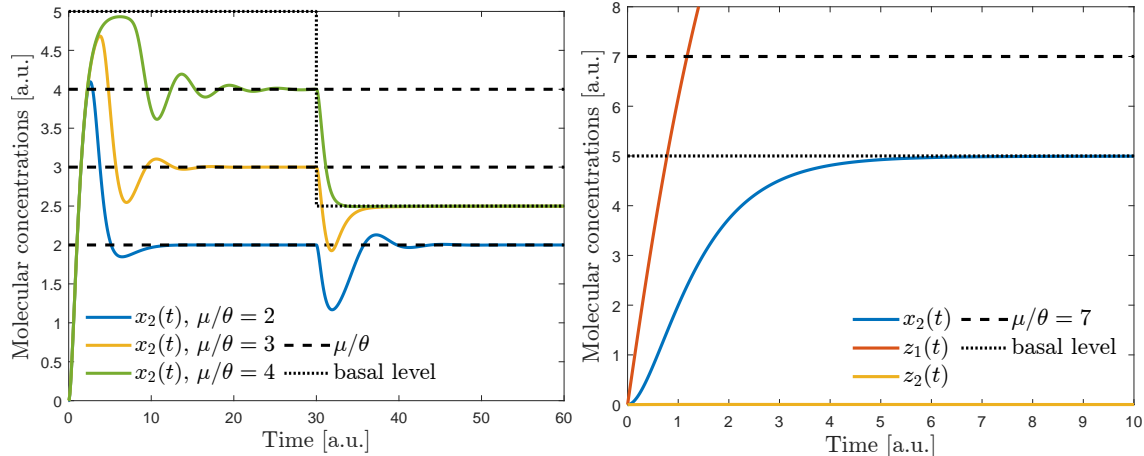


Figure S13: Simulation of the reaction network (S2.5)-(S2.9) with the parameters $\gamma_1 = 1$, $\gamma_2 = 2$, $k_2 = 1$, $b_0 = 10$, $k = 0.5$, $\eta = 100$, $\theta = 1$ and for various values for μ . At time $t = 30$, the value of b_0 is divided by 2. When the set point μ/θ is set below the basal level, the controlled species \mathbf{X}_2 exhibits the robust perfect adaptation property. When the set-point is set to a value higher than the basal expression level, the concentration of the controller species \mathbf{Z}_1 grows without bound and perfect adaptation is not achieved for \mathbf{X}_2 , which can only converge to its basal level.

S2.4 Antithetic Integral Rein Controllers

S2.4.1 Generalities

In light of the previous discussion, it seems interesting to combine both strategies in order to eliminate the limitations on the set of admissible set-points. This may be achieved through the consideration of Antithetic Integral Rein Controllers (AIRCs) that make use of both controller species in order to actuate the system where one would activate the output while the other one would inhibit it. Different versions for the AIRC are depicted in Table 2. The use of both species has been considered in the past in the context of Brink controllers [23] where both positive and negative actuation were performed to modulate a phosphorylation cycle. It is also expected that a two-way actuation would greatly improve the temporal behavior of the closed-loop network as we would not be relying anymore on the natural convergence properties of the system, which may be slow. Indeed, inhibition is expected to improve decreasing properties of the output while activation should improve the increasing properties.

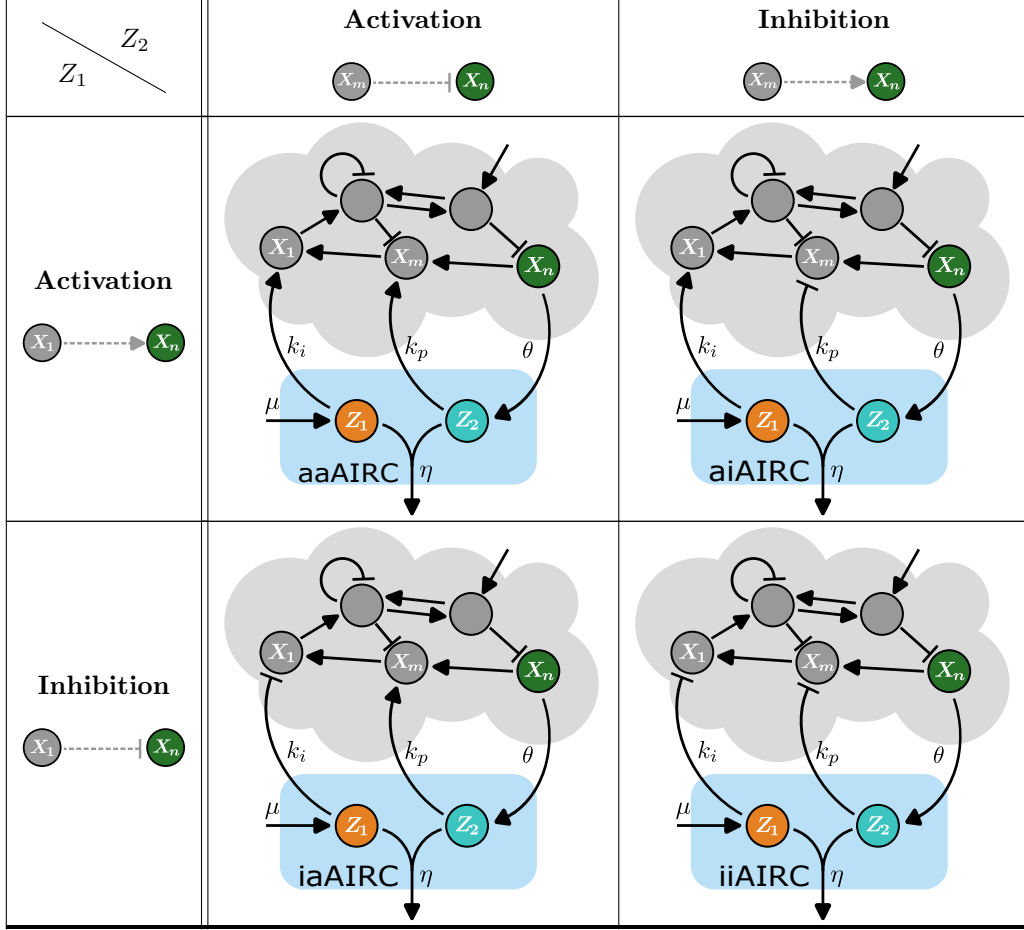
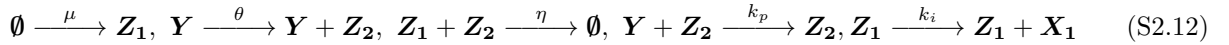


Table 2: Different structures of the Antithetic Integral Rein Controller depending on whether Z_1 and Z_2 activate or repress their respective actuated species. Once again, the key idea is that μ must activate X_n , which should in turn repress itself.

S2.4.2 Output Rein Control

A particular instance of the AIRC, depicted in Figure S14, is when the output is directly repressed by the sensing species while the reference species indirectly activate the output through X_1 . This specific instance, first considered in [38] and also discussed in [56], has been shown to ensure better convergence properties in the case of a simple gene expression network. A reaction network implementation of the output aiAIRC is given by



where Z_1 is both the reference and the activating species, Z_2 is both the sensing and inhibiting species, Y is the measured/controlled species, and both X_1 and X_m are actuated species. The parameters $\mu, \theta, \eta, k_p, k_i$ are all positive rate parameters of the reactions, which are all assumed to be mass-action. In compliance with the aiAIRC structure, it is assumed here that X_1 activates Y , possibly through a sequence of reactions. The deterministic model of this controller is also given by (S2.4).

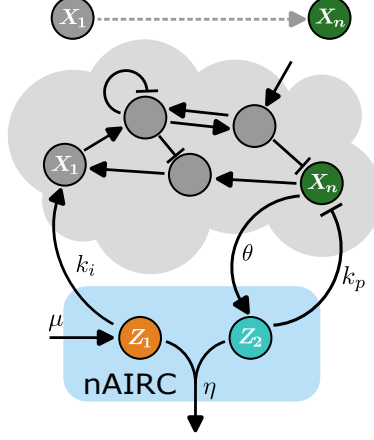


Figure S14: Output aiAIRC: The sensing species Z_2 directly represses the output $Y = X_n$ whereas the reference species Z_1 indirectly activate it by activating X_1 .

We again illustrate the benefits of this controller structure on the previously introduced gene expression network to which we add now two control inputs u_1 and u_2 as

$$\begin{aligned}
 \dot{x}_1(t) &= -\gamma_1 x_1(t) + b_0 + u_1(t) \\
 \dot{x}_2(t) &= k_2 x_1(t) - \gamma_2 x_2(t) - u_2(t) x_2(t) \\
 y(t) &= x_2(t).
 \end{aligned} \tag{S2.13}$$

It can be shown that at stationarity we have that

$$y^* = \frac{k_2(b_0 + u_1^*)}{\gamma_1(\gamma_2 + u_2^*)},$$

which implies that for all $r > 0$, there will exist $u_1^*, u_2^* \geq 0$ such that $y^* = r$. This demonstrates that this specific controller structure enables a broader class of admissible set-point values than the naAIC and niAIC admissible set-points by combining them. The dynamical model of the interconnection of that controller and the gene expression network (S2.5) is now given by

$$\begin{aligned}
 \dot{x}_1(t) &= -\gamma_1 x_1(t) + b_0 + k_i z_1(t) \\
 \dot{x}_2(t) &= k_2 x_1(t) - \gamma_2 x_2 - k_p z_2(t) x_2(t) \\
 \dot{z}_1(t) &= \mu - \eta z_1(t) z_2(t) \\
 \dot{z}_2(t) &= \theta y(t) - \eta z_1(t) z_2(t).
 \end{aligned} \tag{S2.14}$$

Under some conditions, it is possible to show that $\lim_{t \rightarrow \infty} x_2(t) = \frac{\mu}{\theta}$ will hold under some stability conditions and with no restriction on the set-point (i.e. the admissible set is the set of nonnegative numbers). This is illustrated in Figure S15.

S3 Unimolecular mass-action networks

S3.1 The general problem and its properties

Let us consider a mass-action unimolecular reaction network (X, \mathcal{R}) described by the following dynamical system

$$\begin{aligned}
 \dot{x}(t) &= Ax(t) + b_0 \\
 x(0) &= x_0
 \end{aligned} \tag{S3.1}$$

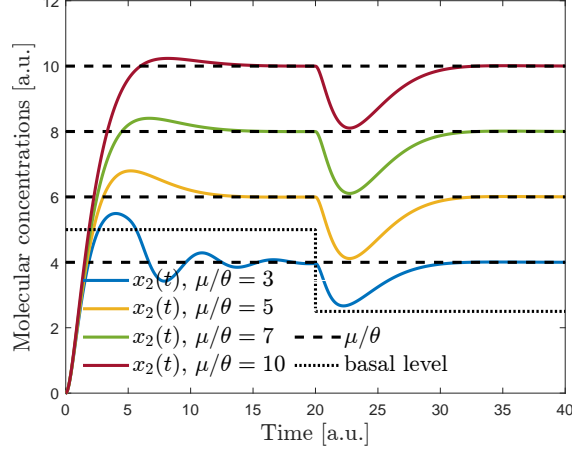


Figure S15: Simulation of the reaction network (S2.5)-(S2.12) with the parameters $\gamma_1 = 1$, $\gamma_2 = 2$, $k_2 = 1$, $b_0 = 10$, $k_p = k_i = 0.5$, $\eta = 100$, $\theta = 1$ and for various values for μ . At time $t = 30$, the value of b_0 is divided by 2. One can observe that the controlled species X_2 exhibits the robust perfect adaptation property for set-points that are both below and above the basal level, which illustrates the benefits of such a controller.

where $x, x_0 \in \mathbb{R}_{\geq 0}^n$ are the state of the system and the initial condition, respectively. The matrix A is Metzler (i.e. all its off-diagonal elements are nonnegative) while the vector b_0 is nonnegative. Connecting that network to the output aiAIRC network previously described yields the model

$$\begin{aligned} \dot{x}(t) &= Ax(t) + e_1 k_i z_1(t) - e_n x_n(t) k_p z_2(t) + b_0 \\ \dot{z}_1(t) &= \mu - \eta z_1(t) z_2(t) \\ \dot{z}_2(t) &= \theta x_n(t) - \eta z_1(t) z_2(t) \end{aligned} \quad (\text{S3.2})$$

where $z_1, z_2 \in \mathbb{R}_{\geq 0}$ are the states of the controller, and $\eta, k_p, k_i > 0$ are the parameters of the controller. Again, the set-point for the equilibrium output is given by $r = \mu/\theta$. This setup is a generalization of the one considered in [38] where a less general class of systems was considered.

The proposition below states that all positive set-points are admissible for the system (S3.2):

Proposition S3.1 *Assume that A is Hurwitz stable, that $r = \mu/\theta > 0$, and that $-e_n^T A^{-1} e_1 \neq 0$. Then, the equilibrium point (x^*, z_1^*, z_2^*) of the closed-loop system (S3.2) is unique and nonnegative. It is, moreover, given by*

$$\begin{aligned} x^* &= -A^{-1} \left(e_1 k_i z_1^* - \frac{e_n r k_p \mu}{\eta z_1^*} + b_0 \right) \\ z_2^* &= \frac{\mu}{\eta z_1^*} \end{aligned} \quad (\text{S3.3})$$

where z_1^* is the unique positive root to the polynomial

$$P_1(z_1) := \eta g_1 k_i z_1^2 + (g_0 - r) \eta z_1 - g_n k_p \mu r, \quad (\text{S3.4})$$

where $r := \mu/\theta$, $g_1 := -e_n^T A^{-1} e_1$, $g_n := -e_n^T A^{-1} e_n$, and $g_0 := -e_n^T A^{-1} b_0$.

Alternatively, the equilibrium point for the controller species can be characterized as $z_1^* = \mu/(\eta z_2^*)$ where z_2^* is the unique positive root of the polynomial

$$P_2(z_2) = -\eta g_n k_p r z_2^{*2} + (g_0 - r) \eta z_2^* + g_1 k_i \mu. \quad (\text{S3.5})$$

Proof : The equilibrium points solve the expressions

$$\begin{aligned} Ax^* + e_1 k_i z_1^* - e_n x_n^* k_p z_2^* + b_0 &= 0, \\ \mu - \eta z_1^* z_2^* &= 0, \\ \theta x_n^* - \eta z_1^* z_2^* &= 0 \end{aligned} \tag{S3.6}$$

which implies that $z_1^* z_2^* \neq 0$. Subtracting the two last rows in (S3.6) yields $x_n^* = r$ and

$$\begin{aligned} Ax^* + e_1 k_i z_1^* - e_n x_n^* k_p z_2^* + b_0 &= 0, \\ \mu - \eta z_1^* z_2^* &= 0. \end{aligned} \tag{S3.7}$$

This implies that x^* can be written as

$$x^* = -A^{-1} (e_1 k_i z_1^* - e_n k_p r z_2^* + b_0), \tag{S3.8}$$

which implies

$$\begin{aligned} r &= e_n^T x^* \\ &= -e_n^T A^{-1} (e_1 k_i z_1^* - e_n k_p r z_2^* + b_0) \\ &= g_1 k_i z_1^* - g_n k_p r z_2^* + g_0. \end{aligned} \tag{S3.9}$$

Substituting $z_2^* = \mu/(\eta z_1^*)$ and multiplying the resulting expression by ηz_1^* yields

$$\eta g_1 k_i z_1^{*2} + (g_0 - r) \eta z_1^* - g_n k_p \mu r = 0 \text{ and } z_2^* = \mu/(\eta z_1^*). \tag{S3.10}$$

Using the fact that $g_1, g_n, r > 0$ (see Lemma S1.4), one can see that there is exactly one change of sign in the coefficients of the polynomial. From Descartes' rule of sign [40], this implies that there exists one positive root to this polynomial. The alternative statement with z_2^* is proven analogously.

We need to prove now that the equilibrium point is nonnegative. First of all, z_1^* is positive, which implies that z_2^* is positive as well. Noting now that the equilibrium state value x^* can be written as

$$x^* = -(A - k_p e_n e_n^T z_2^*)^{-1} (e_1 k_i z_1^* + b_0) \tag{S3.11}$$

where $z_1^*, z_2^* > 0$. Using now the fact that A is Hurwitz stable, then so is $A - k_p e_n e_n^T z_2^*$ and, therefore, $(A - k_p e_n e_n^T z_2^*)^{-1} \leq 0$ (see Proposition S1.3). This implies that $x^* \geq 0$ since $e_1 k_i z_1^* + b_0 \geq 0$, which proves that the equilibrium point is nonnegative. Since there are no assumptions on the value for the set-point r besides its positivity, we can conclude that all positive set-points are admissible. \diamond

The closed-loop network exhibits an interesting switching behavior in the large η limit as stated in the following result:

Proposition S3.2 *The following statements hold:*

1. If $r > g_0$, then we have that $(z_1^*, z_2^*) \xrightarrow{\eta \rightarrow \infty} (u_1^*/k_i, 0)$ where $u_1^* = (r - g_0)/g_1$.
2. If $r < g_0$, then we have that $(z_1^*, z_2^*) \xrightarrow{\eta \rightarrow \infty} (0, u_2^*/k_p)$ where $u_2^* = (g_0 - r)/(g_n r)$.
3. If $r = g_0$, then

$$z_1^* = \sqrt{\frac{g_n k_p \mu r}{\eta g_1 k_i}} \text{ and } z_2^* = \sqrt{\frac{\theta g_1 k_i}{\eta g_n k_p}} \tag{S3.12}$$

and they both tend to 0 when $\eta \rightarrow \infty$ while keeping the product $\eta z_1^* z_2^*$ constant and equal to μ .

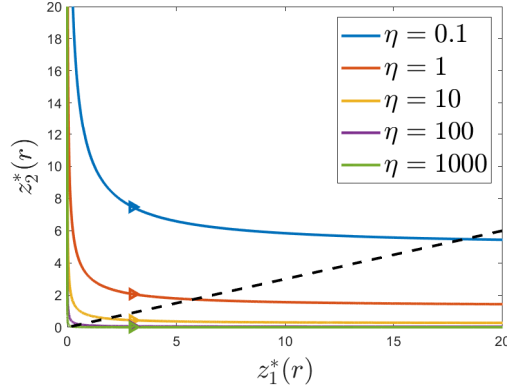


Figure S16: Illustration of the switching behavior described in Proposition S3.2. The curves describe the equilibrium values $(z_1^*(r), z_2^*(r))$ of the controller species parameterized in terms of the set-point r . Each curve corresponds to a specific value for η . The dashed line corresponds to the values of $(z_1^*(g_0), z_2^*(g_0))$. The values above that line corresponds to the case $r < g_0$ whereas the values below to the case $r > g_0$. One can observe that as η increase we converge to a switching behavior where one of the equilibrium concentrations is zero, except in the particular case $r = g_0$ (not visible).

Proof : Assuming that $r > g_0$ and letting $\eta \rightarrow \infty$ in (S3.4) make its positive root go to $z_1^* = u_1^*/k_i$. The other statements are proven analogously. \diamond

This result can be interpreted as follows: when the set-point r is set beyond the basal level g_0 and η is large enough, the naAIC part of the controller dominates its niAIC part whereas the opposite holds whenever the set-point is set below the basal level g_0 . When the set-point is exactly equal to the basal level – a rather pathological case – both components act simultaneously in a rather fragile and unstable manner. This switching behavior is illustrated in Figure S16 where one can observe the evolution of the equilibrium values of the states of the controller for different values for η as the set-point r increases.

Interestingly this result can be connected to an optimization problem at steady-state. To show this, consider the following adaptation of the system (S3.13) to which we add two control inputs u_1, u_2 to mimic how the rein controller acts on the system in (S3.2):

$$\begin{aligned} \dot{x}(t) &= Ax(t) + b_0 + e_1 u_1(t) - e_n x_n u_2(t) \\ x(0) &= x_0. \end{aligned} \quad (\text{S3.13})$$

Assuming that A is Hurwitz stable, the steady-state relationship between the inputs and the output is given by

$$y^* = g_0 + g_1 u_1 - g_n y^* u_2, \quad (\text{S3.14})$$

from which is immediate to see that for any given $y^* > 0$, there is an infinite number of pairs $(u_1, u_2) \in \mathbb{R}_{\geq 0}^2$ that satisfy this equation. Therefore, it is natural to seek to find a pair that minimize the overall control effort that leads to that output y^* . This problem can be formulated as the following linear programming problem

$$\begin{aligned} \min_{(u_1, u_2) \in \mathbb{R}^2} \quad & u_1 + u_2 \\ \text{s.t.} \quad & y^* = g_0 + g_1 u_1 - g_n y^* u_2 \\ & u_1, u_2 \geq 0. \end{aligned} \quad (\text{S3.15})$$

The unique solution to that problem is given by

$$(u_1^*, u_2^*) = \begin{cases} \left(\frac{y^* - g_0}{g_1}, 0 \right), & \text{if } y^* > g_0 \\ \left(0, \frac{g_0 - y^*}{g_1 y^*} \right), & \text{if } y^* < g_0 \\ (0, 0), & \text{if } y^* = g_0 \end{cases} \quad (\text{S3.16})$$

and coincides with the conclusions of Proposition S3.2. Interestingly, the output rein controller can be shown to solve a relaxed version of the above problem by restricting the solution to lie on a surface of the form $u_1 u_2 = c$, where $c \geq 0$. To show this, consider the feasibility problem

$$\begin{aligned} \text{find } & (u_1, u_2) \in \mathbb{R}^2 \\ \text{s.t. } & y^* = g_0 + g_1 u_1 - g_n y^* u_2, \\ & u_1 u_2 = c, \\ & u_1, u_2 \geq 0. \end{aligned} \quad (\text{S3.17})$$

which has the unique solution

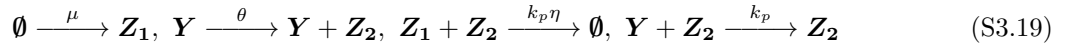
$$u_1^* = \frac{g_0 - y^* + \sqrt{(y^* - g_0)^2 + 4g_1 g_n y^* c}}{2g_1}, \quad u_2^* = \frac{c}{u_1^*}. \quad (\text{S3.18})$$

When $c \rightarrow 0$, which is analogous to $\eta \rightarrow \infty$, the solution of the above problem converges to (S3.16). In this case, the parameter c (or η , equivalently) allows one to tune the optimality of the choice for the input.

The discussions above show that in the case of large sequestration parameter, the output rein controller either behaves like an naAIC or an niAIC depending on the value of the set-point. The class of naAIC's has been extensively studied since its introduction [14, 57, 13, 54, 55] and there is no reason to analyze it further here. On the other hand, the output niAIC is a structure that has not been thoroughly analyzed so far.

S3.2 Reduced problem - The niAIC with output inhibition

The objective of this section is to provide a thorough analysis of the output niAIC part of the considered rein controller with output inhibition



where \mathbf{Z}_1 is the reference species, \mathbf{Z}_2 is both the sensing and actuating species, \mathbf{Y} is the measured, controlled and actuated species. The parameters μ, θ, η, k_p are all positive rate parameters of the reactions, which are all assumed to be mass-action. The interconnection of this network with the (unimolecular) network to be controlled (S2.1) yields the dynamical model

$$\begin{aligned} \dot{x}(t) &= Ax(t) - e_n x_n(t) k_p z_2(t) + b_0 \\ \dot{z}_1(t) &= \mu - k_p \eta z_1(t) z_2(t) \\ \dot{z}_2(t) &= \theta x_n(t) - k_p \eta z_1(t) z_2(t) \end{aligned} \quad (\text{S3.20})$$

where we have slightly changed the structure of the AIC by letting $\eta \leftarrow \eta k_p$. This modification does not change the nature of the results while simplifying their derivation; see e.g. [13]. The following result states under what condition the set-point is admissible:

Proposition S3.3 *Assume that A is Hurwitz stable. Then, the equilibrium point (x^*, z_1^*, z_2^*) of the closed-loop system (S3.20) given by*

$$(x^*, z_1^*, z_2^*) = \left(-A^{-1}(-e_n r u_* + b_0), \quad \frac{\mu}{\eta u_*}, \quad \frac{u_*}{k_p} \right), \quad u_* = \frac{g_0 - r}{g_n r} \quad (\text{S3.21})$$

is unique and positive if and only if $r < g_0$.

Proof : The equilibrium points solve the following system of equations

$$\begin{aligned} 0 &= Ax^* - e_n x_n x^* k_p z_2 x^* + b_0 \\ 0 &= \mu - k_p \eta z_1 x^* z_2 x^* \\ 0 &= \theta x_n^* - k_p \eta z_1 x^* z_2 x^*. \end{aligned} \quad (\text{S3.22})$$

From the two last rows, we obtain that $x_n^* = r$, $z_1^* = \mu/(k_p \eta z_2^*)$, and hence

$$Ax^* - e_n r k_p z_2^* + b_0 = 0. \quad (\text{S3.23})$$

Therefore, we get

$$x^* = -A^{-1}(-e_n r k_p z_2^* + b_0) \quad (\text{S3.24})$$

which implies that $r = -g_n r k_p z_2^* + g_0$ and

$$z_2^* = \frac{g_0 - r}{r k_p g_n} = \frac{u_*}{k_p}. \quad (\text{S3.25})$$

Substituting this into the expression $z_1^* = \mu/(k_p \eta z_2^*)$ and (S3.24) yields $z_1^* = \mu/(\eta u_*)$ and the final expression for the unique equilibrium point.

For z_2^* to be positive, it is necessary and sufficient to have $g_0 - r > 0$, which then implies that z_1^* is also positive. The first row of (S3.22) can be written as $(A - u^* e_n e_n^T)x^* + b_0 = 0$, which implies that $x^* = -(A - u^* e_n e_n^T)^{-1} b_0$ which implies that $x^* \geq 0$ since $b_0 \geq 0$ and $A - u^* e_n e_n^T$ is Metzler and Hurwitz stable, as A is Hurwitz stable by assumption. The proof is completed. \diamond

S3.3 Existence results for the niAIC with output inhibition

The following result states that the equilibrium point of the closed-loop network (S3.20) is locally exponentially stable for any sufficiently small $k_p > 0$.

Proposition S3.4 *Assume that $\bar{A} = A - e_n e_n^T u_*$ is Metzler and Hurwitz stable, and let $\eta, \mu, \theta > 0$ be given and such that $r < g_0$. Then, the equilibrium point of the closed-loop network (S3.20) is locally exponentially stable for any sufficiently small $k_p > 0$.*

Proof : The linearized dynamics of the system about that equilibrium point is given by

$$\begin{bmatrix} \dot{\tilde{x}}(t) \\ \dot{\tilde{z}}_1(t) \\ \dot{\tilde{z}}_2(t) \end{bmatrix} = \begin{bmatrix} \bar{A} & 0 & -e_n k_p r \\ 0 & -\eta u_* & -\mu k_p / u_* \\ \theta e_n^T & -\eta u_* & -\mu k_p / u_* \end{bmatrix} \begin{bmatrix} \tilde{x}(t) \\ \tilde{z}_1(t) \\ \tilde{z}_2(t) \end{bmatrix} \quad (\text{S3.26})$$

where $\bar{A} := A - e_n e_n^T u_*$. The matrix of the linearized dynamics can be decomposed as

$$\begin{bmatrix} \bar{A} & 0 & 0 \\ 0 & -\eta u_* & 0 \\ \theta e_n^T & -\eta u_* & 0 \end{bmatrix} + k_p \begin{bmatrix} 0 & 0 & -e_n r \\ 0 & 0 & -\mu / u_* \\ 0 & 0 & -\mu / u_* \end{bmatrix}. \quad (\text{S3.27})$$

The matrix to the left is marginally stable with one eigenvalue at 0. To show the existence of a k_p that makes the matrix in (S3.26) Hurwitz stable, we use a perturbation argument [64] and check at what happens when we slightly increases k_p from 0 to (small) positive values. The normalized left- and right-eigenvectors associated with the zero eigenvalue are given by

$$u = [-\theta e_n^T \bar{A}^{-1} \quad -1 \quad 1]^T \quad \text{and} \quad v = [0 \quad 0 \quad 1]^T. \quad (\text{S3.28})$$

Therefore, the zero eigenvalue bifurcates according to the expression [64]

$$\lambda_0(k_p) = 0 + k_p u^T \begin{bmatrix} 0 & 0 & -e_n r \\ 0 & 0 & -\mu/u_* \\ 0 & 0 & -\mu/u_* \end{bmatrix} v + o(k_p) = k_p \mu e_n^T \bar{A}^{-1} e_n + o(k_p). \quad (\text{S3.29})$$

Since \bar{A} is Metzler and Hurwitz stable, then $\bar{A}^{-1} \leq 0$ with negative diagonal entries, and we have that $e_n^T \bar{A}^{-1} e_n < 0$. Therefore, the zero eigenvalue moves inside the open left half-plane when positively perturbing k_p from the 0 value, which implies that for any sufficiently small $k_p > 0$ the matrix in (S3.26) is Hurwitz stable. \diamond

Similarly, the following result states that the equilibrium point of the closed-loop network (S3.20) is locally exponentially stable for any sufficiently small $\eta > 0$.

Proposition S3.5 *Assume that $\bar{A} = A - e_n e_n^T u_*$ is Metzler and Hurwitz stable, and let $\eta, \mu, \theta > 0$ be given and such that $r < g_0$. Then, the equilibrium point of the closed-loop network (S3.20) is locally exponentially stable for any sufficiently small $\eta > 0$.*

Proof : Similarly, one can rewrite the matrix in (S3.26) as

$$\begin{bmatrix} \bar{A} & 0 & -e_n k_p r \\ 0 & 0 & -\mu k_p / u_* \\ \theta e_n^T & 0 & -\mu k_p / u_* \end{bmatrix} + \eta \begin{bmatrix} 0 & 0 & 0 \\ 0 & -u_* & 0 \\ 0 & -u_* & 0 \end{bmatrix}. \quad (\text{S3.30})$$

Again the matrix on the left is marginally stable with one eigenvalue at zero. The normalized left- and right-eigenvectors associated with the zero eigenvalue are given by

$$u = [* \quad 1 \quad *]^T \quad \text{and} \quad v = [0 \quad 1 \quad 0]^T \quad (\text{S3.31})$$

where $*$ means that the entries are unimportant here. The zero eigenvalue bifurcates according to the expression [64]

$$\lambda_0(\eta) = 0 + \eta u^T \begin{bmatrix} 0 & 0 & 0 \\ 0 & -u_* & 0 \\ 0 & -u_* & 0 \end{bmatrix} v + o(\eta) = -u_* \eta + o(\eta). \quad (\text{S3.32})$$

Since $r < g_0$, then we have that $u^* > 0$ and, as a result, the matrix in (S3.26) is Hurwitz stable for any sufficiently small $\eta > 0$. \diamond

Conversely, the following result states that the equilibrium point of the closed-loop network (S3.20) is locally exponentially stable for any sufficiently large $\eta > 0$ provided that an extra condition is met.

Proposition S3.6 *Assume that $\bar{A} = A - e_n e_n^T u_*$ is Metzler and Hurwitz stable, and let $\eta, \mu, \theta > 0$ be given and such that $r < g_0$. Assume further that the matrix*

$$\begin{bmatrix} \bar{A} & -e_n k_p \mu \\ e_n^T & 0 \end{bmatrix} \quad (\text{S3.33})$$

is Hurwitz stable. Then, the equilibrium point of the closed-loop network (S3.20) is locally exponentially stable for any sufficiently large $\eta > 0$.

Proof : The matrix in (S3.26) can be rewritten as

$$\frac{1}{\varepsilon} \left(\begin{bmatrix} 0 & 0 & 0 \\ 0 & -u_* & 0 \\ 0 & -u_* & 0 \end{bmatrix} + \varepsilon \begin{bmatrix} \bar{A} & 0 & -e_n k_p r \\ 0 & 0 & -\mu k_p / u_* \\ \theta e_n^T & 0 & -\mu k_p / u_* \end{bmatrix} \right) \quad (\text{S3.34})$$

where $\varepsilon := 1/\eta$. Therefore, one can study the stability of the above matrix in brackets for small positive values which are close to $\varepsilon = 0$. The matrix on the left is marginally stable with a semisimple eigenvalue at 0 of multiplicity $n + 1$. The normalized left- and right-eigenvectors associated with the zero eigenvalue are given by

$$u = \begin{bmatrix} I & 0 & 0 \\ 0 & -1 & 1 \end{bmatrix}^T \quad \text{and} \quad v = \begin{bmatrix} I & 0 & 0 \\ 0 & 0 & 1 \end{bmatrix}^T. \quad (\text{S3.35})$$

Therefore, the zero eigenvalues bifurcate according to the expression [64]

$$\begin{aligned} \lambda_0(\eta) &= 0 + \varepsilon \lambda_i \left(u^T \begin{bmatrix} \bar{A} & 0 & -e_n k_p r \\ 0 & 0 & -\mu k_p / u_* \\ \theta e_n^T & 0 & -\mu k_p / u_* \end{bmatrix} v \right) + o(\varepsilon) \\ &= \varepsilon \lambda_i \left(\begin{bmatrix} \bar{A} & -e_n k_p r \\ \theta e_n^T & 0 \end{bmatrix} \right) + o(\varepsilon) \\ &= \varepsilon \lambda_i \left(\begin{bmatrix} \bar{A} & -e_n k_p \mu \\ e_n^T & 0 \end{bmatrix} \right) + o(\varepsilon) \end{aligned} \quad (\text{S3.36})$$

where $\lambda_i(\cdot)$ denotes the i -th eigenvalue of the matrix and where the last matrix has been obtained by pre- and post-multiplying the previous matrix by $\text{diag}(\theta I, 1)$ and $\text{diag}(\theta^{-1} I, 1)$, respectively. Therefore, under the condition of the result, the real part of the eigenvalues of the matrix are negative and all the zero eigenvalues bifurcate inside the open left half-plane when increasing ε from 0 to small positive values. As this corresponds to moving η from infinity to large positive values, the result is proven. \diamond

S3.4 Structural stability analysis for the niAIC with output inhibition - Stable case

This result is instrumental in proving the main result of the section:

Theorem S3.7 *Assume that M is Metzler and Hurwitz stable. Then, the transfer function $H(s) := e_n^T (sI - M)^{-1} e_n$ is strictly positive real.*

Proof: Since M is Hurwitz stable, then the poles of $H(s)$ have all negative real part, and the condition (2a) of Definition S1.7 is met.

Using now Lemma S1.6, the zeros are given by the eigenvalues of M_{11} which have all negative real part, and we have $H(s) = N(s)/D(s)$ with $D(s) = \det(sI - M)$ and $N(s) = \det(sI - M_{11})$ together with $\deg(D) = n$ and $\deg(N) = s$. As a result, we have that $H(0) > 0$ and $H(\infty) = 0$. So, we need to check the second property of the statement (3b) of Definition S1.7. To this aim, we use Lemma S1.10 and note that all the assumptions of this result are verified with $K = 1$. Therefore, we get that

$$\lim_{\omega \rightarrow \infty} \omega^2 \Re[H(j\omega)] = \text{trace}(M_{11}) - \text{trace}(M) = -e_n^T M e_n. \quad (\text{S3.37})$$

Since M is Metzler and Hurwitz stable, then $-e_n^T M e_n > 0$ and the conclusion follows; i.e. the condition (3b) of Definition S1.7 is verified.

We now check the condition (2b) of Definition S1.7. To this aim, we consider Proposition S1.9. Adapted to our problem, we need to find a matrix $P \in \mathbb{S}_{>0}^d$ such that $M^T P + PM + 2\varepsilon e_n e_n^T \prec 0$ and $P e_n - e_n = 0$. The equality constraint imposes that $P = \text{diag}(P_1, 1)$ where $P_1 \in \mathbb{S}_{>0}^{n-1}$. Clearly, we have that if $M^T P + PM \prec 0$ holds, then $M^T P + PM + 2\varepsilon e_n e_n^T \prec 0$ holds for any sufficiently small $\varepsilon > 0$. Using now the fact that M is Hurwitz stable and Metzler, then this is equivalent [29] to say that there exists a diagonal matrix D with positive diagonal entries such that $M^T D + DM \prec 0$. Dividing this inequality by $e_n^T D e_n > 0$ and letting

$P_s := D/e_n^T D e_n$, we get that $M^T P_s + P_s M < 0$. Observing that this P_s satisfies the conditions of the result shows that the condition (2b) of Definition S1.7 is met. Therefore, the transfer function $H(s)$ is SPR. \diamond

We can now state the main result of the section:

Theorem S3.8 *Let $\mu, \theta > 0$ be given and such that $r < g_0$ and assume that A is Metzler and Hurwitz stable. Then, the unique equilibrium point of the system (S3.20) is locally exponentially stable for all $\eta, k_p > 0$.*

Proof : To analyze the stability of the system in (S3.26) for all $k_p > 0$, we can reformulate the problem as the stability analysis of a negative feedback interconnection of two systems. To see this, we can consider the following equivalent reformulation of (S3.26)

$$\begin{aligned} \begin{bmatrix} \dot{x}(t) \\ \dot{z}_1(t) \end{bmatrix} &= \begin{bmatrix} \bar{A} & 0 \\ 0 & -\eta u_* \end{bmatrix} \begin{bmatrix} x(t) \\ z_1(t) \end{bmatrix} + \begin{bmatrix} e_n r \\ \mu \\ u_* \end{bmatrix} w(t) \\ v(t) &= \begin{bmatrix} \theta e_n^T & -\eta u_* \end{bmatrix} \begin{bmatrix} x(t) \\ z_1(t) \end{bmatrix} + \frac{\mu}{u_*} w(t) \\ w(t) &= k_p \int_0^t v(s) ds. \end{aligned} \quad (\text{S3.38})$$

The transfer from v to w is simply given by k_p/s whereas the transfer function from w to v is given by

$$\begin{aligned} G_\eta(s) &:= \begin{bmatrix} \theta e_n^T & -\eta u_* \end{bmatrix} \begin{bmatrix} sI - \bar{A} & 0 \\ 0 & s + \eta u_* \end{bmatrix}^{-1} \begin{bmatrix} e_n r \\ \mu/u_* \end{bmatrix} + \mu/u_* \\ &= H_n(s)\mu + \frac{-\eta\mu}{s + \eta u_*} + \frac{\mu}{u_*} \\ &= H_n(s)\mu + G(s) \end{aligned} \quad (\text{S3.39})$$

where

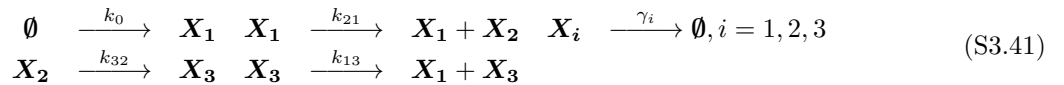
$$\begin{aligned} G(s) &:= \frac{\mu s}{u_*(s + \eta u_*)} \\ H_n(s) &:= e_n^T (sI - \bar{A})^{-1} e_n, \end{aligned} \quad (\text{S3.40})$$

which results in the interconnection is depicted in Figure S17. Since, k_p/s is positive real for all $k_p > 0$, if we can prove that $G_\eta(s)$ is (weakly) strictly positive real, then from Theorem S1.8, the feedback interconnection will be stable for all $k_p > 0$. From Theorem S3.7, the transfer function $H_n(s)$ is SPR. One can also observe that $G(s)$ is stable for all $\eta > 0$, positive real since $\Re[G(j\omega)] = \omega^2/(\omega^2 + \eta^2 u_*^2) \geq 0$ for all $\omega \geq 0$, and such that $G(\infty) = \mu/u_* > 0$. As a result, the sum of those transfer functions is SPR for all $\eta > 0$ and, therefore, the feedback interconnection is stable for all $k_p, \eta > 0$. This proves the result. \diamond

This result is quite powerful in the sense that the only assumption we have on the system is its stability and the only one on the controller is that the set-point is admissible. Interestingly, this result readily generalizes to uncertain systems using the same ideas as in [17].

We illustrate Theorem S3.8 through the following simple example:

Example S3.9 - *Let us consider the following mass-action gene expression network with protein maturation and positive feedback:*



where $\mathbf{X}_1, \mathbf{X}_2$, and \mathbf{X}_3 are the mRNA, protein, and matured protein species, respectively, and where the parameters of the reactions of positive real numbers. We assume here that we would like to control the

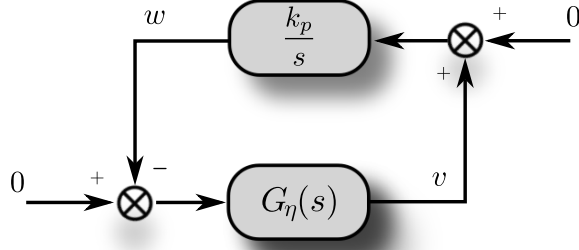


Figure S17: Equivalent negative interconnection

matured species, that is, $\mathbf{Y} = \mathbf{X}_3$. The model of the system is given by

$$\begin{bmatrix} \dot{x}_1 \\ \dot{x}_2 \\ \dot{x}_3 \end{bmatrix} = \begin{bmatrix} -\gamma_1 & 0 & k_{13} \\ k_{21} & -\gamma_2 & 0 \\ 0 & k_{32} & -\gamma_3 \end{bmatrix} \begin{bmatrix} x_1 \\ x_2 \\ x_3 \end{bmatrix} + \begin{bmatrix} k_0 \\ 0 \\ 0 \end{bmatrix} \quad (\text{S3.42})$$

where x_1, x_2, x_3 are the mRNA, protein, and matured protein concentrations, respectively. The matrix describing the dynamics of the network is Metzler, by construction, and is Hurwitz stable provided that $\gamma_1\gamma_2\gamma_3 - k_{13}k_{32}k_{21} > 0$ (Routh-Hurwitz criterion). This yields the following result which is immediate application of Theorem S3.8

Theorem S3.10 Assume that the matrix describing the dynamics of the network is Hurwitz stable, then the closed-loop network (S3.41), (S3.19) is locally exponentially stable for all $0 < \mu/\theta < g_0$ and all $k_p > 0, \eta > 0$ where

$$g_0 = \frac{k_0 k_{21} k_{32}}{\gamma_1 \gamma_2 \gamma_3 - k_{21} k_{32} k_{13}} > 0. \quad (\text{S3.43})$$

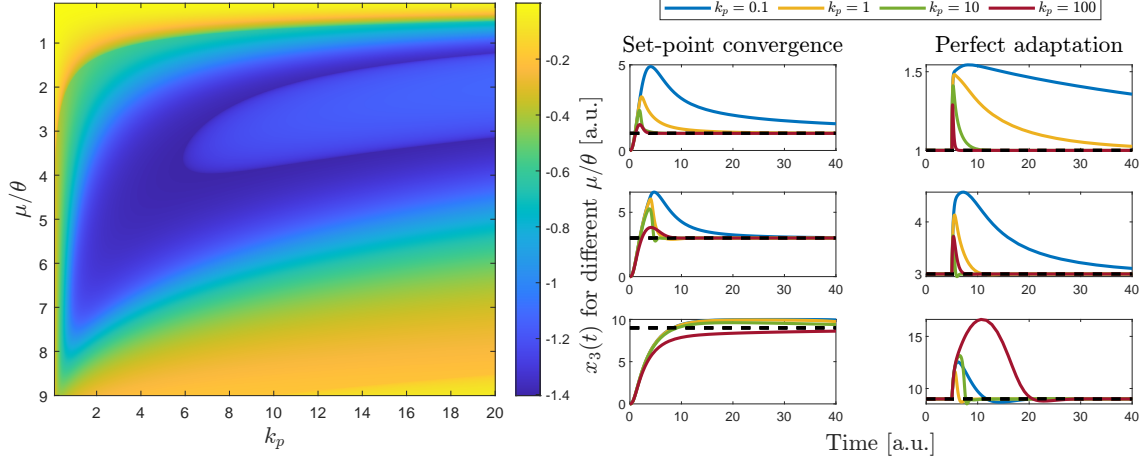


Figure S18: **Left.** Spectral abscissa of the system associated with the (S3.41), (S3.19) with the parameters $\gamma_1 = 1$, $\gamma_2 = \gamma_3 = 2$, $k_{21} = 1$, $k_{32} = 2$, $b_0 = 10$, $k_{13} = 1$, $\eta = 100/k_p$, and $\theta = 1$ and for various values for μ and k_p . In this case, we have that $g_0 = 10$. Simple calculations show that the spectral abscissa of A , is $\alpha(A) = -0.3044$ while the spectral abscissa of the closed-loop system may reach smaller values, which indicates that this controller is able to improve the convergence properties of the system near the equilibrium point. **Right.** Time domain evolution of the concentrations of \mathbf{X}_3 various values for the set-point μ/θ and controller gains k_p . The left column depicts simulation results under zero initial conditions whereas the right column depicts the response of the closed-loop network when the parameter k_{32} changes from 2 to 3 at $t = 5$.

S3.5 Structural stability analysis for the niAIC with output inhibition - Unstable case

We relax in this section the condition that A is Hurwitz stable and derive a sequence of results to address the more general case where A is allowed to be unstable.

S3.5.1 Preliminaries

The results obtained in the previous section relies on the assumption that A is Hurwitz stable. However, this assumption appears to be too strict since only the matrix $\bar{A} = A - e_n e_n^T u_*$ would need to be Hurwitz stable. As it will be shown later, the class of matrices A that can actually be considered is that of *output-unstable matrices*, which is defined below:

Definition S3.11 We say that a matrix $M \in \mathbb{R}^{n \times n}$ partitioned as

$$M =: \begin{bmatrix} M_{11} & M_{12} \\ M_{21} & M_{22} \end{bmatrix} \quad (\text{S3.44})$$

where $M_{11} \in \mathbb{R}^{(n-1) \times (n-1)}$, $M_{12} \in \mathbb{R}^{n-1}$, $M_{21}^T \in \mathbb{R}^{n-1}$, and $M_{22} \in \mathbb{R}$ is output unstable if

- (a) M_{11} is Hurwitz stable, and
- (b) $M_{22} - M_{21} M_{11}^{-1} M_{12} > 0$.

The following result characterizes the sign pattern of the inverse matrix M^{-1} as well as the sign of the gains g_n and g_0 defined in Proposition S3.3:

Lemma S3.12 Assume that the matrix M is Metzler, output unstable, and nonsingular. Then, the following statements hold:

(a) The inverse matrix exhibits the sign-pattern $S^T M^{-1} e_n \geq 0$, $e_n^T M^{-1} S \geq 0$, and $e_n^T M^{-1} e_n > 0$ where $S := \begin{bmatrix} I_{n-1} \\ 0 \end{bmatrix}$; and

(b) The gains g_0 and g_n are such that $g_0 := -e_n^T M^{-1} b_0 \leq 0$ and $g_n := -e_n^T M^{-1} e_n < 0$.

Proof : From the block matrix inversion formula, we have that

$$M^{-1} = \begin{bmatrix} \star & -M_{11}^{-1} M_{12} (M_{22} - M_{21} M_{11}^{-1} M_{12})^{-1} \\ -(M_{22} - M_{21} M_{11}^{-1} M_{12})^{-1} M_{21} M_{11}^{-1} & (M_{22} - M_{21} M_{11}^{-1} M_{12})^{-1} \end{bmatrix}. \quad (\text{S3.45})$$

Since M is Metzler, output unstable, and nonsingular, then we have both $M_{11}^{-1} \leq 0$ and $M_{22} - M_{21} M_{11}^{-1} M_{12} > 0$. This implies that $S^T M^{-1} e_n \geq 0$, $e_n^T M^{-1} S \geq 0$, and $e_n^T M^{-1} e_n > 0$. Since $e_n^T M^{-1} \geq 0$, then we have that $e_n^T M^{-1} b_0 \geq 0$, and the result follows. \diamond

The following result provides a condition for which the matrix $\bar{A} = A - e_n e_n^T u_*$ to be Hurwitz stable.

Lemma S3.13 *Assume that the matrix A is Metzler and output unstable and that $r > 0$. Then, $\bar{A} = A - e_n e_n^T u_*$ is Hurwitz stable if and only if $g_0 < 0$.*

Proof : The control law is stabilizing if and only if there exist a vector $v_1 \in \mathbb{R}_{>0}^{n-1}$ and scalar $v_2 > 0$ such that

$$\begin{bmatrix} A_{11} & A_{12} \\ A_{21} & A_{22} - u_* \end{bmatrix} \begin{bmatrix} v_1 \\ v_2 \end{bmatrix} = - \begin{bmatrix} w_1 \\ w_2 \end{bmatrix}, \quad (\text{S3.46})$$

for some $w_1 \in \mathbb{R}_{>0}^{n-1}$ and $w_2 > 0$. Solving for the first row yields

$$v_1 = -A_{11}^{-1} (w_1 + A_{12} v_2) \quad (\text{S3.47})$$

where $v_1 > 0$ since A_{11} is Metzler and Hurwitz stable (so its inverse is a nonpositive matrix). Substituting the value for v_1 in the second row yields

$$(A_{22} - A_{21} A_{11}^{-1} A_{12} - u_*) v_2 = A_{21} A_{11}^{-1} w_1 - w_2 \leq -w_2 < 0 \quad (\text{S3.48})$$

where we have used the fact that $A_{11}^{-1} \leq 0$. The above inequality can only hold if $A_{22} - A_{21} A_{11}^{-1} A_{12} - u_* < 0$.

Noting that $A_{22} - A_{21} A_{11}^{-1} A_{12} = -1/g_n$ the stability condition can be rewritten as $-1/g_n - u_* < 0$ or, equivalently,

$$\frac{-1}{g_n} - \frac{g_0 - r}{g_n r} = \frac{-g_0}{g_n r} < 0 \quad (\text{S3.49})$$

where the inequality holds provided that $g_0 < 0$ since $g_n < 0$. This proves the result. \diamond

The following result states under what conditions the network has a unique, nonnegative equilibrium point:

Theorem S3.14 *Assume that the matrix A is Metzler, output unstable, and nonsingular, and that $g_0 < 0$, then $u^* > 0$, any set-point $r > 0$ is admissible for the system (S3.20), and the associated equilibrium point is nonnegative and unique.*

Proof : The equilibrium point satisfies the expressions

$$-(A - e_n e_n^T k_p z_2^*) x^* + b_0 = 0, \quad x_n^* = \mu/\theta, \quad z_2^* = u_*/k_p, \quad \text{and} \quad z_1^* = \frac{\mu}{\eta u_*} \quad (\text{S3.50})$$

Under the assumptions of the result, the matrix $A - e_n e_n^T u_*$ is Metzler and Hurwitz stable, which shows the existence and uniqueness of a nonnegative equilibrium point for all $r > 0$. The positivity of u^* follows from the expression $u^* = (g_0 - r)/(g_n r)$. \diamond

S3.5.2 Persistent external excitation

Based on the results of the previous section, we can state the main stability result in the case where $g_0 < 0$:

Theorem S3.15 *Assume that A is Metzler, output unstable, and nonsingular and that $g_0 \neq 0$. Then, the unique equilibrium point of the system (S3.20) is locally exponentially stable for all $\eta, k_p, \mu, \theta > 0$.*

Proof: Under the condition that $r > 0$ then the equilibrium point is positive by virtue of Lemma S3.14. Under the extra condition that $g_0 \neq 0$, we have that $g_0 < 0$ (see Lemma S3.12), then the matrix $\bar{A} = A - e_n e_n^T u_*$ is Metzler and Hurwitz stable from Lemma S3.13. The rest of the proof is then identical to that of Theorem S3.8 as we are now in exactly the same setting. \diamond

The underlying assumption that A_{11} be Hurwitz stable is not restrictive in this case since this is a necessary condition for the matrix $A - e_n e_n^T u_*$ to be Hurwitz stable. Additionally, the strict positive realness property of the transfer function $H_n(s)$ also requires the zeros to be stable, which is equivalent to saying that A_{11} be Hurwitz stable. Interestingly, the set of admissible set-points is much larger in the unstable case than in the stable case. This phenomenon can be easily explained by the fact that in the unstable case, the controller can always let the output increase until it exceeds the set-point before starting repressing it to stabilize it around the desired set-point. For this to happen, the system needs to be persistently excited, which is the meaning of the condition that $g_0 \neq 0$. The case where $g_0 = 0$ will be treated in the next section.

We consider now the following illustrative example:

Example S3.16 *Consider the following gene expression network with maturation, positive feedback (k_{13}) and autocatalytic reaction (ν)*

$$\begin{bmatrix} \dot{x}_1 \\ \dot{x}_2 \\ \dot{x}_3 \end{bmatrix} = \begin{bmatrix} -\gamma_1 & 0 & k_{13} \\ k_{21} & -\gamma_2 & 0 \\ 0 & k_{32} & \nu - \gamma_3 \end{bmatrix} \begin{bmatrix} x_1 \\ x_2 \\ x_3 \end{bmatrix} + \begin{bmatrix} k_0 \\ 0 \\ 0 \end{bmatrix} \quad (\text{S3.51})$$

where x_1, x_2, x_3 are the mRNA, protein, and matured protein concentrations, respectively. All the model parameters are positive except, possibly, k_{13} and ν . This matrix is output unstable if and only if

$$\gamma_1 \gamma_2 (\nu - \gamma_3) + k_{21} k_{32} k_{13} > 0, \quad (\text{S3.52})$$

which yields the following result

Theorem S3.17 *Assume that $\gamma_1, \gamma_2 > 0$ that*

$$\gamma_1 \gamma_2 (\nu - \gamma_3) + k_{21} k_{32} k_{13} > 0 \quad (\text{S3.53})$$

and

$$g_0 = \frac{-k_0 k_{21} k_{32}}{\gamma_1 \gamma_2 (\nu - \gamma_3) + k_{21} k_{32} k_{13}} < 0. \quad (\text{S3.54})$$

then the closed-loop network (S3.51), (S2.9) is locally exponentially stable for all $\mu, \theta, k_p > 0, \eta > 0$.

Proof: In particular, the autocatalytic parameter is supposed to exceed the degradation rate of the matured protein; i.e. $\nu - \gamma_3 > 0$. We have that A_{11} is Metzler and Hurwitz stable and that $\nu - \gamma_3 > 0$. Therefore, the matrix is Metzler and output unstable. Computing g_0 yields

$$g_0 = -\frac{b k_2 k_3}{k_2 k_3 \alpha + \gamma_1 \gamma_2 (\nu - \gamma_3)} < 0. \quad (\text{S3.55})$$

Therefore, from Theorem S3.15, the equilibrium point of the closed-loop system is structurally stable provided that $r > 0$. \diamond

This result is illustrated by simulation in Figure S19 and Figure S20 where we can observe the predictions of the above theorem.

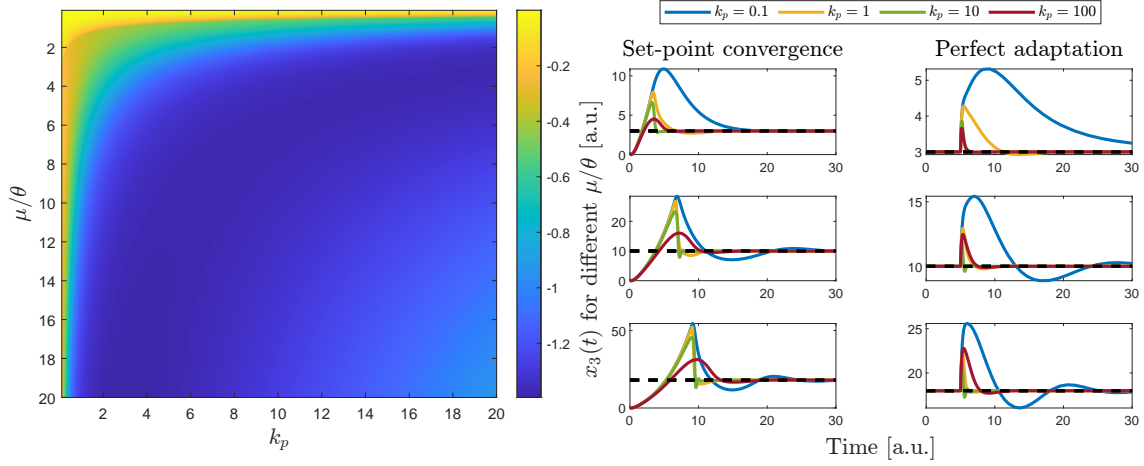


Figure S19: **Left panel.** Spectral abscissa of the system associated with the (S3.51), (S2.9) with the parameters $\gamma_1 = 1$, $\gamma_2 = \gamma_3 = 2$, $k_{21} = 1$, $b_0 = 10$, $k_{13} = 3$, $\nu = 0$, $\theta = 1$, $\eta = 100/k_p$ and for various values for μ and k_p . We have that which corresponds to $g_0 = -10$, $g_n = -1$ and a spectral abscissa of A given by $\alpha(A) = 0.2188$. **Right panel.** State response from a zero initial condition (first column) and as a response to a change of k_{21} from 2 to 3.

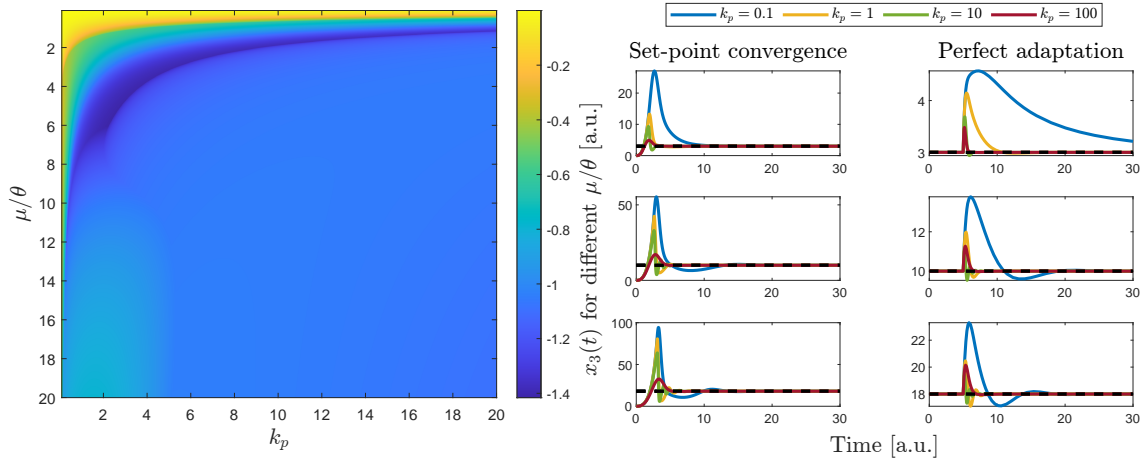


Figure S20: **Left panel.** Spectral abscissa of the system associated with the (S3.51), (S2.9) with the parameters $\gamma_1 = 1$, $\gamma_2 = \gamma_3 = 2$, $k_{21} = 1$, $b_0 = 10$, $k_{13} = 1$, $\nu = 3$, $\theta = 1$, $\eta = 100/k_p$ and for various values for μ and k_p . We have that which corresponds to $g_0 = -5$, $g_n = -1/2$, and a spectral abscissa of A given by $\alpha(A) = 1.2695$ while the spectral abscissa of the closed-loop system reach smaller, negative values, which indicates that this controller is able to stabilize and improve the convergence properties of the system near the equilibrium point. **Right panel.** State response from a zero initial condition (first column) and as a response to a change of k_{21} from 2 to 3.

S3.6 Partial structural stability analysis of the network controlled with an AIRC with output inhibition

Up to now all the results pertained to structural stability analysis of unimolecular networks controlled with an output-niAIC. We now connect the above results to the initial rein controller with output inhibition (S3.2) for which we have now the following result:

Theorem S3.18 *Assume that A is Metzler, output unstable, and nonsingular and that $g_0 \neq 0$. Then, the unique equilibrium point of the system (S3.2) is locally exponentially stable for all $\eta, k_p, \mu, \theta > 0$ and all $k_i \in [0, \bar{k}_i]$.*

Proof : Consider the general system (S3.2) recalled below for simplicity:

$$\begin{bmatrix} \dot{x}(t) \\ \dot{z}_1(t) \\ \dot{z}_2(t) \end{bmatrix} = F(x(t), z_1(t), z_2(t)) + \begin{bmatrix} e_1 \\ 0 \\ 0 \end{bmatrix} k_i z_1(t) \quad (\text{S3.56})$$

where $k_i > 0$ and

$$F(x, z_1, z_2) := \begin{bmatrix} Ax + b_0 - e_n e_n^T k_p z_2 \\ \mu - \eta z_1 z_2 \\ \theta x_n - \eta z_1 z_2 \end{bmatrix}. \quad (\text{S3.57})$$

From Theorem S3.15, the unique equilibrium point of the above system for $k_i = 0$ is structurally locally exponentially stable. We shall prove now that this is also the case for any sufficiently small $k_i > 0$. Let $\bar{x}^*(k_i) := (x^*(k_i), z_1^*(k_i), z_2^*(k_i))$ be the equilibrium point of (S3.56)-(S3.57). Since the system is polynomial, this implies that the equilibrium point $\bar{x}^*(k_i)$ is a continuous function of k_i . In fact, by virtue of the implicit function theorem, we have that

$$\frac{d}{dk_i} \begin{bmatrix} x^*(k_i) \\ z_1^*(k_i) \\ z_2^*(k_i) \end{bmatrix} = \tilde{J}(k_i)^{-1} \begin{bmatrix} e_1 z_1^*(k_i) \\ 0 \\ 0 \end{bmatrix} \quad (\text{S3.58})$$

where

$$\tilde{J}(k_i) = \begin{bmatrix} A - e_n e_n^T k_p z_2^*(k_i) & e_1 k_i & -e_n k_p r \\ 0 & -\eta z_2^*(k_i) & -\eta z_1^*(k_i) \\ \theta e_n^T & -\eta z_2^*(k_i) & -\eta z_1^*(k_i) \end{bmatrix}, \quad (\text{S3.59})$$

for all the k_i 's for which is it invertible. In fact, we proved that for $k_i = 0$, the matrix $\tilde{J}(0)$ is Hurwitz stable for all $k_p, \eta > 0$ provided that some conditions on $\mu, \theta > 0$ and A are satisfied. This implies that the equilibrium point $\bar{x}^*(k_i)$ is locally differentiable in k_i around $k_i = 0$. Now decompose $\tilde{J}(k_i)$ as

$$J(k_i) = J_0 + k_i J_1 + (z_1^*(k_i) - z_1^*(0)) J_2 + (z_2^*(k_i) - z_2^*(0)) J_3 \quad (\text{S3.60})$$

where

$$\begin{aligned} J_0 &= \begin{bmatrix} A - e_n e_n^T k_p z_2^*(0) & 0 & -e_n k_p \mu / \theta \\ 0 & -\eta z_2^*(0) & -\eta z_1^*(0) \\ \theta e_n^T & -\eta z_2^*(0) & -\eta z_1^*(0) \end{bmatrix}, \quad J_1 = \begin{bmatrix} 0 & e_1 & 0 \\ 0 & 0 & 0 \\ 0 & 0 & 0 \end{bmatrix} \\ J_2 &= \begin{bmatrix} 0 & 0 & 0 \\ 0 & 0 & -\eta \\ 0 & 0 & -\eta \end{bmatrix}, \quad J_3 = \begin{bmatrix} -e_n e_n^T k_p & 0 & 0 \\ 0 & -\eta & 0 \\ 0 & -\eta & 0 \end{bmatrix}. \end{aligned} \quad (\text{S3.61})$$

Therefore, we have that

$$J(k_i) = J_0 + k_i \left(J_1 + J_2 \left. \frac{dz_1^*(k_i)}{dk_i} \right|_{k_i=0} + J_3 \left. \frac{dz_2^*(k_i)}{dk_i} \right|_{k_i=0} \right) + o(k_i) \quad (\text{S3.62})$$

which shows that the eigenvalues are also locally continuous in k_i at $k_i = 0$. This implies that given all the other parameters of the system and the controller, there exists a $\bar{k}_i > 0$ such that $\tilde{J}(k_i)$ is Hurwitz stable for all $k_i \in [0, \bar{k}_i]$. \diamond

S4 Structural stability of the niAIC - Nonlinear case

We provide immediate extensions of the results to other types of integral controllers that have been reported in the literature.

S4.1 Definitions, assumptions, and preliminary results

We now address the more general case where the network (S2.1) is neither restricted to be unimolecular nor mass-action. The network is now described by the following model

$$\begin{aligned}\dot{x}(t) &= f(x(t)) + b_0 \\ x(0) &= x_0\end{aligned}\tag{S4.1}$$

where $x(t), x_0 \in \mathbb{R}^n$ are the state of the system and the initial condition, respectively. We assume here that the function f is such that there exists a unique solution to that system which is defined for all times $t \geq 0$. Additionally, since this model describes the evolution of the state of a reaction network, then the function f_a is such that the solution $x(t)$ is nonnegative for all $t \geq 0$ provided that $x(0), b_0$ are also nonnegative. Anticipating the interconnection of that network with an niAIC controller with output inhibition, we define the following extension

$$\begin{aligned}\dot{x}(t) &= f(x(t)) - e_n x_n(t) u(t) + b_0 \\ y(t) &= x_n(t) \\ x(0) &= x_0\end{aligned}\tag{S4.2}$$

where $u(t) \geq 0$ is the input and $y(t)$ is the output of the system. It is immediate to see that this system is internally positive (i.e. for all $x(0), u(t), b_0 \geq 0$ we have that $x(t), y(t) \geq 0$ for all $t \geq 0$) since the solution to (S4.1) is nonnegative.

Definition S4.1 *The geometry of equilibrium states and inputs is more complicated than in the unimolecular mass-action case and is described by the following sets:*

- the set of all possible equilibrium output values for a given input

$$\mathcal{Y}(u) := \{e_n^T x : \exists x \in \mathbb{R}_{\geq 0}^n \text{ s.t. } f(x) - e_n e_n^T u + b_0 = 0\}, \quad u > 0\tag{S4.3}$$

- the set of all possible equilibrium output values across all possible input values

$$\mathcal{Y} := \{e_n^T x : \exists (x, u) \in \mathbb{R}_{\geq 0}^n \times \mathbb{R}_{> 0} \text{ s.t. } f(x) - e_n e_n^T u + b_0 = 0\} = \bigcup_{u > 0} \mathcal{Y}(u),\tag{S4.4}$$

- the set of equilibrium behaviors for a given equilibrium output

$$\mathcal{B}(y^\circ) := \{(x, u) \in \mathbb{R}_{\geq 0}^n \times \mathbb{R}_{> 0} : f(x) - e_n e_n^T u + b_0 = 0, e_n^T x = y^\circ\}, \quad y^\circ \in \mathcal{Y}\tag{S4.5}$$

- the set of equilibrium inputs achieving a given value for the equilibrium output

$$\begin{aligned}\mathcal{U}(y^\circ) &:= \{u \in \mathbb{R}_{> 0} : \exists x \in \mathbb{R}_{\geq 0}^n \text{ s.t. } f(x) - e_n e_n^T u + b_0 = 0, e_n^T x = y^\circ\}, \quad y^\circ \in \mathcal{Y} \\ &:= \{u \in \mathbb{R}_{> 0} : \exists x \in \mathbb{R}_{\geq 0}^n \text{ s.t. } (x, u) \in \mathcal{B}(y^\circ)\}, \quad y^\circ \in \mathcal{Y},\end{aligned}\tag{S4.6}$$

- the set of equilibrium states corresponding to a given equilibrium output

$$\begin{aligned}\mathcal{X}(y^\circ) &:= \{x \in \mathbb{R}_{\geq 0}^n : \exists u \in \mathbb{R}_{> 0} \text{ s.t. } f(x) - e_n e_n^T u + b_0 = 0, e_n^T x = y^\circ\}, \quad y^\circ \in \mathcal{Y} \\ &:= \{x \in \mathbb{R}_{\geq 0}^n : \exists u \in \mathbb{R}_{> 0} \text{ s.t. } (x, u) \in \mathcal{B}(y^\circ)\}, \quad y^\circ \in \mathcal{Y}.\end{aligned}\tag{S4.7}$$

We also define the global sets

$$\mathcal{B} := \bigcup_{y^\circ \in \mathcal{Y}} \mathcal{B}(y^\circ), \quad \mathcal{U} := \bigcup_{y^\circ \in \mathcal{Y}} \mathcal{U}(y^\circ), \quad \text{and} \quad \mathcal{X} := \bigcup_{y^\circ \in \mathcal{Y}} \mathcal{X}(y^\circ). \quad (\text{S4.8})$$

We make now the following assumption:

Assumption S4.2 *The set \mathcal{Y} is non-empty and connected, and for all $y^\circ \in \mathcal{Y}$, the sets $\mathcal{U}(y^\circ)$ and $\mathcal{X}(y^\circ)$ are singletons.*

This assumption means that for any equilibrium value for the output, there exists a unique associated equilibrium state and constant input. Note that this does not imply that the system necessarily has a unique equilibrium point and the system is still allowed to have multiple equilibrium points. However, only one of them will be associated with the specified value for the output. A simple example is the system $\dot{x} = x(x - u)$, $y = x$. This assumption is not required but dramatically simplifies the exposition of the results.

Nevertheless, this is not enough for our results which also require the existence of a function that maps elements of \mathcal{U} to elements of \mathcal{X} . The (local) existence of such a function is guaranteed by the following assumption

Assumption S4.3 *The matrices*

$$J(x) \text{ and } J(x) - ue_n e_n^T \quad (\text{S4.9})$$

are invertible for all $(x, u) \in \mathcal{E}$ where $J(x) := \partial f(x)/\partial x$.

This assumption can be relaxed to consider a subset \mathcal{R} of \mathcal{E} on which those matrices are invertible. As for the previous assumption, this is not considered so as to simplify the exposition of the results but all the subsequent results can be adapted to this case at the expense of a higher notational cost. This leads to the following result:

Proposition S4.4 *Assume that the conditions in Assumption S4.2 and S4.3 hold. Then, there exists (at least locally) a function $\sigma : \mathcal{U} \mapsto \mathcal{X}$ such that $f(\sigma(u)) - e_n e_n^T \sigma(u)u + b_0 = 0$. Moreover, we have that*

$$\frac{dF(u)}{du} = \frac{-g_n(u)}{1 + g_n(u)u} F(u) \quad (\text{S4.10})$$

where $g_n(u) := -e_n^T J(\sigma(u))^{-1} e_n$ and $F := \pi_n \circ \sigma$ where π_n denotes the projection operator on the n -th component; observe that $y_n^*(u) = e_n^T x^*(u) = e_n^T \sigma(u) = F(u)$, locally on $u \in \mathcal{U}$.

Moreover, if there exists an $c > 0$ such that

$$\sup_{u \in \mathcal{U}} \left| \frac{-g_n(u)y^*(u)}{1 + g_n(u)u} \right| \leq c,$$

then the function $F(u)$ is globally defined on $u \in \mathcal{U}$.

Proof : The existence of the function σ is a consequence of Assumption S4.3 and the implicit function theorem. The same theorem also yields the expression

$$\frac{d\sigma(u)}{du} = (J(\sigma(u)) - e_n e_n^T u)^{-1} e_n e_n^T \sigma(u) \quad (\text{S4.11})$$

at all the points where it is defined. In particular, this implies that

$$\frac{dy^*(u)}{du} = e_n^T (J(\sigma(u)) - e_n e_n^T u)^{-1} e_n y^*(u). \quad (\text{S4.12})$$

Using Sherman-Morrison formula, we get that

$$\begin{aligned} (J(\sigma(u)) - e_n e_n^T u)^{-1} &= J(\sigma(u))^{-1} - \frac{(-1)J(\sigma(u))^{-1}e_n e_n^T J(\sigma(u))^{-1}u}{1 + (-1)e_n^T J(\sigma(u))^{-1}e_n u} \\ &= J(\sigma(u))^{-1} + \frac{J(\sigma(u))^{-1}e_n e_n^T J(\sigma(u))^{-1}u}{1 + g(u)u} \end{aligned} \quad (\text{S4.13})$$

where $g_n(u) = -e_n^T J(\sigma(u))^{-1}e_n$. Therefore,

$$\begin{aligned} e_n^T (J(\sigma(u)) - e_n e_n^T u)^{-1} e_n &= e_n^T \left(J(\sigma(u))^{-1} + \frac{J(\sigma(u))^{-1}e_n e_n^T J(\sigma(u))^{-1}u}{1 + g(u)u} \right) e_n \\ &= -g_n(u) + \frac{g_n(u)^2 u}{1 + g_n(u)u} \\ &= \frac{g_n(u)}{1 + g_n(u)u}, \end{aligned} \quad (\text{S4.14})$$

from which the first result follows. Finally, the global existence of F on \mathcal{U} comes from the linear growth of the right hand side of the differential equation and the boundedness of the Lipschitz constant on \mathcal{U} . \diamond

Unlike in the unimolecular mass-action case, the "gain" $g_n(u)$ now depends on the value of the control input, which may lead to more complex behaviors than in the unimolecular mass-action case. Yet, it still exhibits useful regularity properties, as stated in the result below:

Proposition S4.5 *Assume that the conditions in Assumption S4.2 and S4.3 hold, and that $J(x) - u e_n e_n^T$ is Hurwitz stable for all $(x, u) \in \mathcal{B}$. Then, we have that*

(a) $\text{sign}(1 + g_n(u)u) = \text{sign}(\det(-J(\sigma(u))))$, and

(b) $\text{sign}(g_n(u)) = \text{sign}\left(\frac{\det(-J_{11}(\sigma(u)))}{\det(-J(\sigma(u)))}\right)$.

Moreover, if $J(x)$ is Hurwitz stable for all $x \in \mathcal{X}$, we have that

(c) $1 + g_n(u)u > 0$ holds for all $u \in \mathcal{U}$, and

(d) $g_n(u) > 0$ if and only if $\det(-J_{11}(\sigma(u))) > 0$.

Proof : Since $J(x) - u e_n e_n^T$ is Hurwitz stable on \mathcal{B} and $J(x)$ invertible on \mathcal{X} , then we have that $0 < \det(-J(x) + e_n e_n^T u) = \det(-J(x))(1 + g_n(u)u)$. Therefore $1 + g_n(u)u$ has the same sign as $\det(-J(x))$ on \mathcal{B} . Similarly,

$$g_n(u) = -e_n^T J(\sigma(u))^{-1}e_n = \frac{\det(-J_{11}(\sigma(u)))}{\det(-J(\sigma(u)))}, \quad (\text{S4.15})$$

which proves the second statement. Assuming that $J(\sigma(u))$ is Hurwitz stable on \mathcal{U} implies that $\det(-J(\sigma(u))) > 0$ on \mathcal{U} , from which the two last statements follow. \diamond

Assumption S4.6 *The nonlinear gain function $F = \pi_n \circ \sigma : \mathcal{U} \mapsto \mathcal{Y}$, defined in Proposition S4.4, is bijective.*

This leads us to the following result:

Proposition S4.7 *Consider the system (S4.2) which is assumed to satisfy Assumption S4.2, S4.3, and S4.6. Then, the equilibrium point $(x^*(r), u_*(r))$ associated with the steady-state output $y^* = r \in \mathcal{Y}$ for the system (S4.2) is given by*

$$u_*(r) = F^{-1}(r), \text{ and } x^*(r) = \sigma(F^{-1}(r)). \quad (\text{S4.16})$$

Proof : This follows from Proposition S4.4 and Assumption S4.6. \diamond

S4.2 General results

We now move on with the main results of the section. The closed-loop network consisting of the interconnection of the network (S2.1) described by (S4.1) and the niAIC (S3.19) is represented by the following system

$$\begin{aligned}\dot{x}(t) &= f(x(t)) - e_n z_\iota(t) x_n(t) + b_0 \\ \dot{z}_1(t) &= \mu - \eta k_p z_1(t) z_2(t) \\ \dot{z}_2(t) &= \theta e_n^T x - \eta k_p z_1(t) z_2(t),\end{aligned}\tag{S4.17}$$

where $(x(0), z_1(0), z_2(0)) = (x_0, z_{1,0}, z_{2,0})$. Note that we have left free the choice of the actuating species which can either be z_1 or z_2 depending on whether $\iota = 1$ or $\iota = 2$, respectively. This leads to the following result:

Proposition S4.8 *Assume that Assumption S4.2, S4.3, and S4.6 are satisfied for the systems (S4.1) and (S4.2). Then, the unique equilibrium point of the closed-loop system (S4.17) is given by*

$$x^*(r) = g(F^{-1}(r)), \quad z_\iota^*(r) = \frac{\mu}{\eta F^{-1}(r)} \quad \text{and} \quad z_{3-\iota}^*(r) = \frac{F^{-1}(r)}{k_p}.\tag{S4.18}$$

Moreover, defining $J^*(r) := J(x^*(r))$, we define the transfer function

$$H_n(s, r) = e_n^T (sI - (J^*(r) - F^{-1}(r) e_n e_n^T))^{-1} e_n.\tag{S4.19}$$

Finally, the linearized dynamics of the system (S4.17) about the equilibrium point (S4.18) when $\iota = 1$ is governed by the matrix

$$M_1(r) := \begin{bmatrix} J^*(r) - F^{-1}(r) e_n e_n^T & -k_p e_n r & 0 \\ 0 & -\mu k_p / F^{-1}(r) & -\eta F^{-1}(r) \\ \theta e_n^T & -\mu k_p / F^{-1}(r) & -\eta F^{-1}(r) \end{bmatrix}\tag{S4.20}$$

whereas it is given by

$$M_2(r) := \begin{bmatrix} J^*(r) - F^{-1}(r) e_n e_n^T & 0 & -k_p e_n r \\ 0 & -\eta F^{-1}(r) & -\mu k_p / F^{-1}(r) \\ \theta e_n^T & -\eta F^{-1}(r) & -\mu k_p / F^{-1}(r) \end{bmatrix}\tag{S4.21}$$

when $\iota = 2$.

Proof : The proof follows from the previous results and assumptions and the standard linearization procedure. \diamond

It is important to clarify under what conditions there exists a $k_p > 0$ such that the equilibrium point (S4.18) is locally asymptotically stable for the dynamics (S4.17). This is stated in the result below:

Proposition S4.9 *Assume that Assumption S4.2, S4.3, and S4.6 are satisfied for the systems (S4.1) and (S4.2). Assume further that r is admissible (i.e. $r \in \mathcal{D}$), that $J^*(r) - F^{-1}(r) e_n e_n^T$ is Hurwitz stable, and let $\iota \in \{1, 2\}$. Then, the following statements hold:*

- (a) *If $(-1)^\iota H_n(0, r) > 0$, then there exists a sufficiently small $k_p > 0$ such that the equilibrium point (S4.18) is locally exponentially stable for the dynamics (S4.17)*
- (b) *If $(-1)^\iota H_n(0, r) < 0$, then, for all $k_p > 0$, the equilibrium point (S4.18) is unstable for the dynamics (S4.17).*

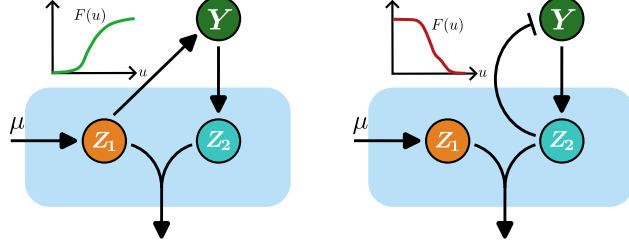


Figure S21: Valid control topologies. **Left.** Case $\iota = 1$ where Z_1 is the actuating species. In that case, the map F needs to be increasing for the map $\mu \mapsto z_1^*$ to be increasing and the feedback loop from Y to Y to be negative. **Right.** Case $\iota = 2$ where Z_2 is the actuating species. In that case, the map F needs to be decreasing for the map $\mu \mapsto z_1^*$ to be increasing and the feedback loop from Y to Y to be negative.

Proof : The proof follows from the same arguments as the proof of Proposition S3.4 and relies on proving that there exists a $k_p > 0$ such that the matrix (S4.21) or (S4.21) is Hurwitz stable. In the current case, the zero-eigenvalue locally obeys the expression

$$\begin{aligned}
\lambda(k_p) &= (-1)^\iota \mu e_n^T (J^*(r) - F^{-1}(r) e_n e_n^T)^{-1} e_n k_p + o(k_p) \\
&= (-1)^{\iota-1} \mu H_n(0, r) k_p + o(k_p) \\
&= (-1)^\iota \theta \left. \frac{dF(u)}{du} \right|_{u=F^{-1}(r)} k_p + o(k_p) \\
&= (-1)^{\iota-1} \theta \frac{g_n(F^{-1}(r))}{1 + g_n(F^{-1}(r)) F^{-1}(r)} k_p + o(k_p).
\end{aligned} \tag{S4.22}$$

One can observe that stabilization is only possible if $(-1)^\iota H_n(0, r) > 0$, which proves the first statement of the result.

Now assume that $(-1)^\iota H_n(0, r) < 0$. Then, using the Schur complement and the properties of the determinant, we have that

$$\det(-M_\iota(r)) = \xi(r) (-1)^\iota H_n(0, r), \quad \iota = 1, 2, \tag{S4.23}$$

where $\xi(r) := \eta F^{-1}(r) k_p \mu \det(-J^*(r) + F^{-1}(r) e_n e_n^T)$. Since $J^*(r) - F^{-1}(r) e_n e_n^T$ is Hurwitz stable, then $\det(-J^*(r) + F^{-1}(r) e_n e_n^T) > 0$ and, therefore, $\xi(r) > 0$, which implies that $\det(-M_\iota(r)) < 0$ since $(-1)^\iota H_n(0, r) < 0$, implying, in turn, that $M_\iota(r)$ has at least one eigenvalue with positive real part, implying that the equilibrium point is unstable. This proves the second statement. \diamond

It seems important to discuss the meaning of that result. It was previously explained that it is necessary that the feedback loop from Y to Y be negative and the map from μ to Y be increasing for the equilibrium point to be locally exponentially stable as illustrated in Figure S21. For those properties to be satisfied, the function F needs to be increasing (i.e. activating) whenever $\iota = 1$ and decreasing (i.e. inhibiting) whenever $\iota = 2$.

We are now ready to state the main result of this section:

Theorem S4.10 *Assume that Assumption S4.2, S4.3, and S4.6 are satisfied for the systems (S4.1) and (S4.2). Assume further that r is admissible (i.e. $r \in \mathcal{Y}$), that $H_n(0, r) > 0$, and that one of the following equivalent statements holds:*

(a) *There exist a matrix $P_1(r) = P_1(r)^T \succ 0$ and an $\varepsilon > 0$ such that*

$$(J^*(r) - F^{-1}(r) e_n e_n^T)^T P(r) + P(r) (J^*(r) - F^{-1}(r) e_n e_n^T) + 2\varepsilon e_n e_n^T \prec 0 \tag{S4.24}$$

where

$$P(r) = \begin{bmatrix} P_1(r) & 0 \\ 0 & 1 \end{bmatrix}. \quad (\text{S4.25})$$

(b) There exists an $\varepsilon > 0$ such that the system $(J_{11}^*(r), J_{12}^*(r), -J_{21}^*(r), u_*(r) - J_{22}^*(r) - \varepsilon)$ is SPR.

Then, the equilibrium point (S4.18) of the system (S4.17) is locally exponentially stable for all $\eta, k_p > 0$. If it holds for all $r \in \mathcal{Y}$, then the closed-loop system is also structurally stable for all admissible set-point.

Proof : The equivalence between the statements follows from the fact that the condition (S4.24) in the first statement can be written as

$$\begin{bmatrix} P_1 J_{11}^*(r) + J_{11}^*(r)^T P_1(r) & P_1(r) J_{12}^*(r) + J_{21}^*(r)^T \\ \star & 2(J_{22}^*(r) - u_* + \varepsilon) \end{bmatrix} \prec 0 \quad (\text{S4.26})$$

which is a time-domain characterization of the SPR condition; i.e. input strict passivity or strong strict positive realness. Now, let us prove that all the conditions for SPR are met. First of all, the condition (S4.24) implies that $J^*(r) - F^{-1}(r)e_n e_n^T$ is Hurwitz stable (stable poles). Moreover, the condition (S4.26) implies that $J_{22}^*(r) - u_* < 0$ and that $J_{11}^*(r)$ is Hurwitz stable (stable zeros). Those two properties all together implies that the condition at infinity holds. Finally, from the Kalman-Yakubovich-Popov Lemma we have that $\Re[H_n(j\omega, r)] \geq \varepsilon |H_n(j\omega, r)|^2$. Since the zeros of the transfer function $H_n(s, r)$ are stable, then $|H_n(j\omega, r)| \neq 0$ for all $\omega \in \mathbb{R}$ and from the assumption that $H_n(0, r) > 0$, we get that $\Re[H_n(j\omega, r)] > 0$ for all $\omega \in \mathbb{R}$. The conclusion then follows. \diamond

We have the immediate corollary:

Corollary S4.11 Assume that Assumption S4.2, S4.3, and S4.6 are satisfied for the systems (S4.1) and (S4.2). Assume further that r is admissible (i.e. $r \in \mathcal{Y}$), that $H_n(0, r) > 0$, and that one of the following statements holds:

(a) $J_{12}^*(r) = 0$ and $J^*(r)$ is Hurwitz stable;

(b) $J_{21}^*(r) = 0$ and $J^*(r)$ is Hurwitz stable;

Then, the equilibrium point (S4.18) of the system (S4.17) is locally exponentially stable for all $\eta, k_p > 0$.

Proof : From the conditions, we have that $J^*(r)$ is triangular with $J_{22}^*(r) < 0$, which implies that $J_{22}^*(r) - u_* < 0$. Therefore, the linear matrix inequality (S4.26) holds if and only if

$$P_1(r) J_{11}^*(r) + J_{11}^*(r)^T P_1(r) + \frac{1}{2(u_* - J_{22}^*(r))} (P_1(r) J_{12}^*(r) + J_{21}^*(r)^T) (J_{12}^*(r)^T P_1(r) + J_{21}^*(r)) \prec 0. \quad (\text{S4.27})$$

Case (a). Assume that $J_{12}^*(r) = 0$. Therefore, the inequality (S4.27) reduces to

$$P_1(r) J_{11}^*(r) + J_{11}^*(r)^T P_1(r) + \frac{1}{2(u_* - J_{22}^*(r))} J_{21}^*(r)^T J_{21}^*(r) \prec 0. \quad (\text{S4.28})$$

Since $J_{11}^*(r)$ is Hurwitz stable, then one can find a $P_1(r)$ such that the above inequality holds, which proves this case.

Case (b). Assume that $J_{21}^*(r) = 0$ and let $Q_1(r)$ be such that $Q_1(r) J_{11}^*(r) + J_{11}^*(r) Q_1(r) = -R_1(r)$ for some $R_1(r) \succ 0$. Such a $Q_1(r)$ exists as $J_{11}^*(r)$ is Hurwitz stable. Let $P_1(r) = \varepsilon(r) Q_1(r)$ for some $\varepsilon(r) > 0$. Then, the condition (S4.27) reduces to

$$-\varepsilon(r) R_1(r) + \frac{\varepsilon(r)^2}{2(u_* - J_{22}^*(r))} Q_1(r) J_{12}^*(r) J_{12}^*(r)^T Q_1(r) \prec 0. \quad (\text{S4.29})$$

Dividing by $\varepsilon(r) > 0$, this equivalent to say that

$$-R_1(r) + \frac{\varepsilon(r)}{2(u_* - J_{22}^*(r))} Q_1(r) J_{12}^*(r) J_{12}^*(r)^T Q_1(r) < 0. \quad (\text{S4.30})$$

This inequality is readily shown to be negative definite provided that $\varepsilon(r) > 0$ is small enough, which proves this case. \diamond

Let us illustrate Theorem S4.10 through this simple example

Example S4.12 Consider a gene expression network where the protein represses its own production described by

$$\begin{aligned} \dot{x}_1 &= -\gamma x_1 + \frac{k_{12}}{1+x_2} + b_0, \\ \dot{x}_2 &= k_{21} x_1 - \gamma x_2 - u x_2 \end{aligned} \quad (\text{S4.31})$$

where x_1 denotes the mRNA concentration and x_2 the protein concentration. The parameters $\gamma, k_{12}, k_{21}, b_0$ are all positive. The admissibility set for this system is given by

$$\mathcal{Y} := (0, r_{\min}) \quad (\text{S4.32})$$

where r_{\min} is the unique positive root of the polynomial

$$Y(r) := \gamma^2 r^2 + r(\gamma^2 - k_{21} b_0) - k_{21}(k_{12} + b_0). \quad (\text{S4.33})$$

Moreover, the sets

$$\mathcal{X}(y^\circ) = \left\{ \left(\frac{1}{\gamma} \left[\frac{k_{12}}{1+y^\circ} + b_0 \right], y^\circ \right) \right\} \quad (\text{S4.34})$$

and

$$\mathcal{U}(y^\circ) = \left\{ -\gamma + \frac{k_{21}}{\gamma y^\circ} \left[\frac{k_{12}}{1+y^\circ} + b_0 \right] \right\}, \quad (\text{S4.35})$$

both consist of singletons, as required by Assumption S4.2. The Jacobian of the system (S4.31) with $u = 0$ is given by

$$J(x) = \begin{bmatrix} -\gamma & -\frac{k_{12}}{(1+x_2)^2} \\ k_{21} & -\gamma \end{bmatrix} \quad (\text{S4.36})$$

and is invertible for all $x_2 \geq 0$, and so is $J(x) - u e_n e_n^T$ for all $x \geq 0$ and $u \geq 0$. Therefore, the conditions in Assumption S4.3 are satisfied. As a result, maps $\sigma : \mathcal{U} \mapsto \mathcal{X}$ and $F : \mathcal{U} \mapsto \mathcal{Y}$ exist. Furthermore, we have that $g_n(u) = \gamma(1 + x_2^*(u))^2 / (\gamma^2 + k_{12} k_{21}) > \gamma / (\gamma^2 + k_{12} k_{21})$, which implies, by virtue of Proposition S4.4, that the map F is monotonically decreasing. This shows that the condition in Assumption S4.6 is also satisfied.

The Jacobian evaluated at the equilibrium point corresponding to $x_2^* = r$ is given by

$$J^*(r) = \begin{bmatrix} -\gamma & -\frac{k_{12}}{(1+r)^2} \\ k_{21} & -\gamma \end{bmatrix}$$

and the associated transfer function is

$$H_n(s, r) = \frac{s + \gamma}{s^2 + (2\gamma + u_*(r))s + \gamma(\gamma + u_*(r)) + k_{21} k_{12} / (1+r)^2}.$$

From the Routh-Hurwitz criterion, the transfer function $H_n(s, r)$ is stable, has stable zeros and verifies $H(0, r) > 0$. Therefore, we just need to show the existence of a $P(r) \succ 0$ such that

$$\begin{bmatrix} -2\gamma P(r) & -\frac{k_{12}}{(1+r)^2}P(r) + k_{21} \\ -\frac{k_{12}}{(1+r)^2}P(r) + k_{21} & -2(\gamma + u_*(r)) \end{bmatrix} \prec 0.$$

Alternatively, we may check whether the transfer function associated with the system

$$\begin{aligned} \dot{v} &= -\gamma v - \frac{k_{12}}{(1+r)^2}w \\ z &= -k_{21}v + (\gamma + u_*(r))w \end{aligned} \quad (\text{S4.37})$$

is strictly positive real. It can be seen that this is the case since it is a first order stable transfer function of relative degree 0 with stable zeros, with positive gain and positive feedthrough. Therefore, the closed-loop system consisting of (S4.31) and the niAIC (S3.19) is structurally stable with respect to $k_p, \eta > 0$ and $r > r_{\min}$.

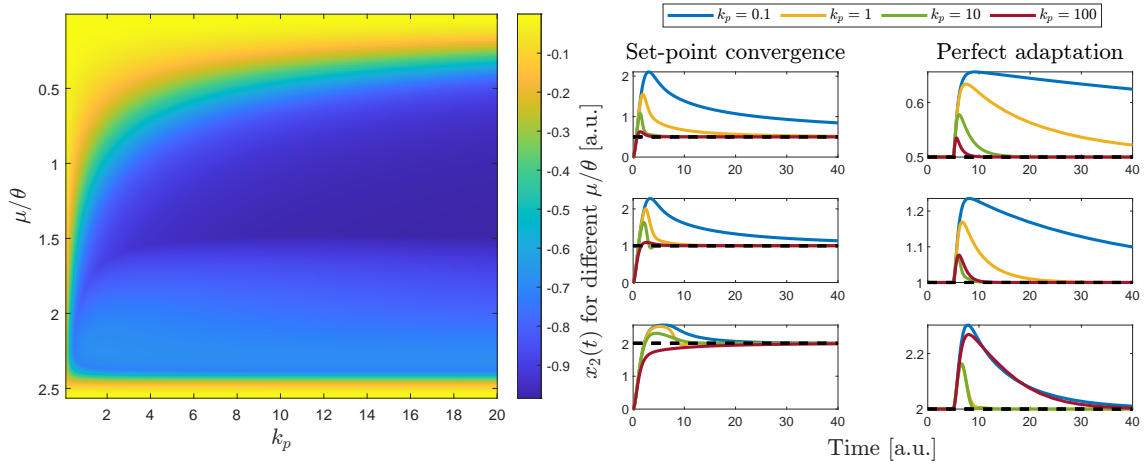


Figure S22: **Left panel.** Spectral abscissa of the system associated with the (S4.31), (S2.9) with the parameters $\gamma = 1$, $k_{21} = 2$, $b_0 = 1$, $k_{12} = 2$, $\theta = 1$, $\eta = 100/k_p$ and for various values for μ and k_p . We have that $r_{\min} = 2.5616$. **Right panel.** State response from a zero initial condition (first column) and as a response to a change of k_{12} from 1 to 2.

S4.3 Cooperative and Michaelis-Menten networks

In some cases, the conditions in Theorem S4.10 can be shown to be automatically satisfied (as in the unimolecular case) and the only conditions that will need to be checked are those stated in the various assumptions introduced in Section S4.1.

The class of cooperative systems benefits from such a simplified procedure, as stated in the result below:

Proposition S4.13 *Assume that the set of admissible set-point \mathcal{Y} is non-empty, that the function f is cooperative⁶ and such that $J^*(r)$ is Hurwitz stable for all $r \in \mathcal{Y}$. Then, the equilibrium point (S4.18) of the system (S4.17) is locally exponentially stable for all $\eta, k_p > 0$ and all $r \in \mathcal{Y}$.*

⁶A function $f : X \mapsto X$, $X \subset \mathbb{R}^n$, is cooperative if $\partial f / \partial x$ is Metzler for all $x \in X$.

Proof : Since f is cooperative, then $J(x)$ is Metzler. Moreover, if $J^*(r)$ is Hurwitz stable for all $r \in \mathcal{Y}$, then so is $J^*(r) - u_*(r)e_n e_n^T$, and this implies that both matrices are invertible, which shows that the conditions in Assumption S4.3 are satisfied. Since $J^*(r)$ is Metzler and Hurwitz stable, then we have that $g_n(u) > 0$ (see Lemma S1.4) for all $u \in \mathcal{U}$, which implies that $F(u)$ is monotonically decreasing on \mathcal{U} and shows that the condition in Assumption S4.6 is verified. From Lemma S1.4, we also have that $H_n(0, r) > 0$. Finally, using the fact that $J^*(r) - u_*(r)e_n e_n^T$ is Metzler and Hurwitz stable, Proposition S1.3 allows us to state that there exists a diagonal matrix $P_1(r) \succ 0$ that satisfies (S4.24). The result then follows from Theorem S4.10. \diamond

The class of cooperative networks is very similar to unimolecular ones, which are cooperative by construction. As a result, extensions to the case of output-unstable systems are rather immediate at the expense of additional notational burden stemming from the nonlinear nature of the network. For this reason, those results are omitted. Without entering into details, it is also possible to go beyond the class of cooperative systems by considering a more general class of systems which are cooperative with respect to a different cone than the nonnegative orthant; see e.g, [72]. Indeed, if one can find a diagonal matrix $S(r)$ with diagonal entries in $\{-1, 1\}$ such that $S(r)J^*(r)S(r)$ is Metzler, one can show that there also exists a diagonal matrix $P_1(r)$ such that the inequality (S4.24) holds. This implies that networks described by such matrices also exhibit the properties stated in Proposition S4.13.

Another important class of networks having beneficial properties is the class of networks governed by a combination of linear mass-action and Michaelis-Menten dynamics. The following lemma summarizes some important results proven in [11]:

Lemma S4.14 *Assume that (S4.1) describes a reaction network with linear mass-action and Michaelis-Menten dynamics, that is, $f(x) = Ax + N(x)$ where A is Metzler and Hurwitz stable and where $N(x)$ contains the Michaelis-Menten terms. Assume further that the graph of the network is strongly connected and at least one entry of b_0 is positive. Then,*

- (a) *There exists a unique equilibrium point x^* in the positive orthant.*
- (b) *The Jacobian matrix $J(x^*)$ is row diagonally dominant with negative diagonal and is, therefore, Hurwitz stable, which implies that the unique equilibrium point x^* is locally exponentially stable.*

The condition that b_0 is nonzero is here to ensure that there at least one molecular species is constitutively produced. The strong connectedness condition of the graph of the network enforces a "mixing property" guaranteeing that all the species act on each other in a persistent way, making the equilibrium point positive. This latter condition is sufficient only for the positivity of the equilibrium point and weaker ones can be formulated, possibly on a case-by-case basis.

Based on the above result, we can state our main result regarding the control of Michaelis-Menten networks with unimolecular mass-action reactions using an output niAIC:

Theorem S4.15 *Assume that Assumption S4.2 and S4.6 are satisfied for the systems (S4.1) and (S4.2), which represents a Michaelis-Menten reaction networks with $f(x) = Ax + N(x)$ where A Metzler and Hurwitz stable and $N(x)$ contains the nonlinear Michaelis-Menten terms. Assume further that the graph of the network is strongly connected, that $b_0 \neq 0$, that r is admissible (i.e. $r \in \mathcal{Y}$), that $\mathcal{X} \subset \mathbb{R}_{>0}^d$, and that $H_n(0, r) > 0$.*

Then, for all $r \in \mathcal{Y}$ the equilibrium point (S4.18) of the system (S4.17) is locally exponentially stable for all $\eta, k_p > 0$.

Proof : From Lemma S4.14, the matrix $J^*(r)$ is Hurwitz stable for all $r \in \mathcal{Y}$ because it is row diagonally dominant with negative diagonal. This also implies that both $J^*(r) - u_*(r)e_n e_n^T$ and $J_{11}^*(r)$ are row diagonally dominant with negative diagonal. This shows that the conditions in Assumption S4.3 are verified. It remains to show that one of the conditions in Theorem S4.10 is satisfied. The existence of a diagonal matrix $P_1(r)$ is automatically follows from [44, 47] and the fact that the matrix $J_{11}^*(r)$ is row diagonally dominant with

negative diagonal. ◇

S5 Extension to other types of integral controllers

S5.1 Exponential integral controllers

We now consider the following class of exponential integral controller [19, 77, 13]

$$\mathbf{Z} + \mathbf{Y} \xrightarrow{\alpha} \mathbf{Z} + \mathbf{Y} + \mathbf{Z}, \quad \mathbf{Z} \xrightarrow{\alpha r} \mathbf{0} \quad (\text{S5.1})$$

described as

$$\dot{z}(t) = \alpha z(t)(y(t) - r) \quad (\text{S5.2})$$

where $\alpha > 0$ is a positive parameter of the controller and r is the desired set-point. The closed-loop network is given in this case by

$$\begin{aligned} \dot{x}(t) &= Ax(t) - e_n x_n(t) k_p z(t) + b_0 \\ \dot{z}(t) &= \alpha z(t)(y(t) - r). \end{aligned} \quad (\text{S5.3})$$

Similar calculations as in the antithetic case yield the following result:

Proposition S5.1 *The closed-loop network (S5.3) has the following equilibrium points:*

(a) *One positive equilibrium point defined as*

$$x^* = -\bar{A}^{-1}(-e_n k_p r z^* + b_0) \quad \text{and} \quad z^* = \frac{g_0 - r}{g_n r k_p}, \quad (\text{S5.4})$$

where $r < g_0$.

(b) *One zero-equilibrium point given by*

$$x^* = -A^{-1}b_0 \quad \text{and} \quad z^* = 0. \quad (\text{S5.5})$$

It is known from [13] that the zero-equilibrium point is structurally unstable. So, we just need to focus on proving the structural stability of the positive equilibrium point. This is stated in the following result:

Theorem S5.2 *Assume that A is Metzler and Hurwitz stable. Then the unique positive equilibrium point of the system (S5.3) is locally exponentially stable for all $\alpha, k > 0$ and $\mu < g_0$.*

Proof: The linearized dynamics are governed by the matrix

$$\begin{bmatrix} \bar{A} & -e_n k_p \mu \\ \frac{\alpha(g_0 - \mu)}{g_n \mu k_p} e_n^T & 0 \end{bmatrix}. \quad (\text{S5.6})$$

This can be interpreted as the negative interconnection of the transfer function $H_n(s)$ and the integrator $\alpha(g_0 - \mu)/(g_n s)$. By virtue of the previously obtained results, we know that this interconnection is asymptotically stable for all $\alpha, k > 0$ and $\mu < g_0$. This proves the result. ◇

We have the following immediate extension to the case where the matrix A is Metzler and output unstable:

Theorem S5.3 *Assume that A is Metzler, output unstable, and non-singular. Then, the unique positive equilibrium point of the system (S5.3) is locally exponentially stable for all $\mu, \alpha, k > 0$.*

Proof: The proof follows from the same arguments as for the antithetic integral controller. ◇

S5.2 Logistic integral controllers

We consider now the logistic integral controller [13]

$$\dot{z}(t) = \frac{\alpha}{\beta} z(t)(\beta - z(t))(y(t) - r) \quad (\text{S5.7})$$

where $\alpha > 0$ is a parameter of the controller, $\beta > 0$ is the saturation level, and r is the desired set-point. The closed-loop network is given in this case by

$$\begin{aligned} \dot{x}(t) &= Ax(t) - e_n k_p x_n(t) z(t) + b_0 \\ \dot{z}(t) &= \frac{\alpha}{\beta} z(t)(\beta - z(t))(y(t) - r). \end{aligned} \quad (\text{S5.8})$$

We have the following result:

Proposition S5.4 *The closed-loop network (S5.8) has the following equilibrium points:*

- One positive interior equilibrium point given by

$$(x^*, z^*) = \left(-\bar{A}^{-1}(-e_n r z^* + b_0), \frac{g_0 - r}{g_n r} \right), \quad (\text{S5.9})$$

where $r \in (g_0/(1 + \beta k_p g_n), g_0)$.

- One zero-equilibrium point given by

$$(x^*, z^*) = (-A^{-1}b_0, 0). \quad (\text{S5.10})$$

- One positive saturating equilibrium point given by

$$(x^*, z^*) = -((A - e_n e_n^T k_p \beta)^{-1} b_0, \beta). \quad (\text{S5.11})$$

It is known from [13] that the zero and saturating equilibrium points are structurally unstable. Therefore, we just need to focus on proving the structural stability of the positive equilibrium. This is stated in the following result:

Theorem S5.5 *Assume that A is Metzler and Hurwitz stable and that $\beta > 0$. Then the unique positive equilibrium point of the system (S5.8) is locally exponentially stable for all $\alpha > 0$ and all*

$$r \in \left(\frac{g_0}{1 + k_p \beta g_n}, g_0 \right).$$

Proof : The linearized dynamics are governed by the matrix

$$\begin{bmatrix} \bar{A} & -e_n k_p r \\ \frac{\alpha}{\beta} z^* (\beta - z^*) e_n^T & 0 \end{bmatrix}. \quad (\text{S5.12})$$

This can be interpreted as the negative interconnection of the transfer function $H_n(s)$ and the integrator $k\beta z^*(\beta - z^*)/(\beta s)$. Since the gain of the integrator is always positive, then the transfer function is positive real and the previously obtained apply. \diamond

We have the following immediate extension to the case where the matrix A is Metzler and output unstable:

Theorem S5.6 *Assume that A is Metzler, output unstable, and non-singular. Then, the unique positive equilibrium point of the system (S5.8) is locally exponentially stable for all $k > 0$ and all $r > g_0/(1 + \beta k_p g_n)$.*

Proof : The proof follows from the same argument as for the exponential and the antithetic controllers. \diamond

References

- [1] K. J. Åström and T. Häggglund. *PID Controllers: Theory, Design, and Tuning*. Instrument Society of America, Research Triangle Park, North Carolina, USA, 1995.
- [2] U. Alon. Network motifs: theory and experimental approaches. *Nature Review Genetics*, 8:450–461, 2007.
- [3] S. Anastassov, M. Filo, C.-H. Chang, and M. Khammash. A cybergenetic framework for engineering intein-mediated integral feedback control systems. *Nature Communications*, 14:1337, 2023.
- [4] S. Aoki, G. Lillacci, A. Gupta, A. Baumschlager, D. Schweingruber, and M. Khammash. A universal biomolecular integral feedback controller for robust perfect adaptation. *Nature*, 570:533–537, 2019.
- [5] R. Araujo and L. Liotta. Universal structures for adaptation in biochemical reaction networks. *Nature Communications*, 14:2251, 2023.
- [6] R. P. Araujo and L. A. Liotta. The topological requirements for robust perfect adaptation in networks of any size. *Nature Communications*, 9:1757, 2018.
- [7] J. Baillieul and T. Samad, editors. *Encyclopedia of Systems and Control*. Springer London, 2015.
- [8] N. Barkai and S. Leibler. Robustness in simple biochemical networks. *Nature*, 387:913–917, 1997.
- [9] A. Berman and R. J. Plemmons. *Nonnegative matrices in the mathematical sciences*. SIAM, Philadelphia, USA, 1994.
- [10] M. Bin, J. Huang, A. Isidori, L. Marconi, M. Mischiati, and E. Sontag. Internal models in control, bioengineering, and neuroscience. *Annual Review of Control, Robotics, and Autonomous Systems*, 5:55–79, 2022.
- [11] F. Blanchini, D. Breda, G. Giordano, and D. Liessi. Michaelis-Menten networks are structurally stable. *Automatica*, 147:110683, 2023.
- [12] F. Blanchini and G. Giordano. Structural analysis in biology: A control-theoretic approach. *Automatica*, 126:109376, 2021.
- [13] C. Briat. A biology-inspired approach to the positive integral control of positive systems - the antithetic, exponential, and logistic integral controllers. *SIAM Journal on Applied Dynamical Systems*, 19(1):619–664, 2020.
- [14] C. Briat, A. Gupta, and M. Khammash. Antithetic integral feedback ensures robust perfect adaptation in noisy biomolecular networks. *Cell Systems*, 2(1):15–26, 2016.
- [15] C. Briat, A. Gupta, and M. Khammash. Variance reduction for antithetic integral control of stochastic reaction networks. *Journal of the Royal Society: Interface*, 15(143):20180079, 2018.
- [16] C. Briat and M. Khammash. Perfect adaptation and optimal equilibrium productivity in a simple microbial biofuel metabolic pathway using dynamic integral control. *ACS Synthetic Biology*, 7(2):419–431, 2018.
- [17] C. Briat and M. Khammash. Ergodicity, output-controllability, and antithetic integral control of uncertain stochastic reaction networks. *IEEE Transactions on Automatic Control*, 66(5):2087–2098, 2020.
- [18] C. Briat and M. Khammash. Noise in biomolecular systems: Modeling, analysis, and control implications. *Annual Review of Control, Robotics, and Autonomous Systems*, 6:10.1–10.29, 2023.
- [19] C. Briat, C. Zechner, and M. Khammash. Design of a synthetic integral feedback circuit: dynamic analysis and DNA implementation. *ACS Synthetic Biology*, 5(10):1108–1116, 2016.

- [20] B. Brogliato, R. Lozano, B. Maschke, and O. Egeland. *Dissipative Systems Analysis and Control*. Springer-Verlag, 2007.
- [21] W. B. Cannon. Organization for physiological homeostasis. *Physiological Reviews*, 9(3):399–431, 1929.
- [22] D. Chen and A. P. Arkin. Sequestration-based bistability enables tuning of the switching boundaries and design of a latch. *Molecular Systems Biology*, 8(1), 2012.
- [23] C. Cuba Samaniego and E. Franco. Ultrasensitive molecular controllers for quasi-integral feedback. *Cell Systems*, 12:272–288, 2021.
- [24] C. Cuba Samaniego, Y. Qian, K. Carleton, and E. Franco. Building subtraction operators and controllers via molecular sequestration. *IEEE Control Systems Letters*, 7:3361–3366, 2023.
- [25] T. Drengstig, X. Y. Ni, K. Thorsen, L. W. Jolma, and P. Ruoff. Robust adaptation and homeostasis by autocatalysis. *The Journal of Physical Chemistry*, 116:5355–5363, 2012.
- [26] T. Drengstig, H. R. Ueda, and Peter P. Ruoff. Predicting perfect adaptation motifs in reaction kinetic networks. *The Journal of Physical Chemistry B*, 112(51):16752–16758, 2008.
- [27] H. El-Samad, J. P. Goff, and M. Khammash. Calcium homeostasis and parturient hypocalcemia: An integral feedback perspective. *Journal of Theoretical Biology*, 214:17–29, 2002.
- [28] Fages F, G. Le Guludec, O. Bournez, and A. Pouly. Strong turing completeness of continuous chemical reaction networks and compilation of mixed analog-digital programs. In J. Feret and H. Koepl, editors, *Computational Methods in Systems Biology*, pages 108–127, Cham, 2017. Springer International Publishing.
- [29] L. Farina and S. Rinaldi. *Positive Linear Systems: Theory and Applications*. John Wiley & Sons, 2000.
- [30] M. Filo, A. Gupta, and M. Khammash. Anti-windup protection circuits for biomolecular intergal controllers. *BioRxiv: 2023.10.06.561168*, 2023.
- [31] M. Filo and M. Khammash. A class of simple biomolecular antithetic proportional-integral-derivative controllers. *bioRxiv*, 2021.
- [32] M. Filo, S. Kumar, and M. Khammash. A hierarchy of biomolecular proportional-integral-derivative feedback controllers for robust perfect adaptation and dynamic performance. *bioRxiv*, 2021.
- [33] M. Filo, S. Kumar, and M. Khammash. A hierarchy of biomolecular proportional-integral-derivative feedback controllers for robust perfect adaptation and dynamic performance. *Nature Communications*, 13:2119, 2022.
- [34] B. A. Francis and W. M. Wonham. The internal model principle of control theory. *Automatica*, 12:457–465, 1976.
- [35] T. Frei, C.-H. Chang, M. Filo, and M. Khammash. A genetic mammalian proportional–integral feedback control circuit for robust and precise gene regulation. *PNAS*, 199(24):e2122132119, 2022.
- [36] M. Golubitsky and I. Stewart. Homeostasis, singularities, and networks. *Journal of Mathematical Biology*, 74:387–407, 2017.
- [37] J. Goutsias and G. Jenkinson. Markovian dynamics on complex reaction networks. *Physics reports*, 529:199–264, 2013.
- [38] A. Gupta and M. Khammash. An antithetic integral rein controller for bio-molecular networks. In *58th IEEE Conference on Decision and Control*, pages 2808–2813, Nice, France, 2019.

- [39] A. Gupta and M. Khammash. Universal structural requirements for maximal robust perfect adaptation in biomolecular networks. *Proceedings of the National Academy of Sciences*, 119(43):e2207802119, 2022.
- [40] P. Henrici. Sign changes. the rule of descartes. In *Power Series-Integration-Conformal Mapping-Location of Zeros*, volume 1 of *Applied and Computational Complex Analysis*, pages 439–443. Wiley - New York, 1989.
- [41] Y. Hirono, A. Gupta, and M. Khammash. Complete characterization of robust perfect adaptation in biochemical reaction networks. *arXiv:2307.07444*, pages 1–65, 2023.
- [42] F. Jacob and J. Monod. Genetic regulatory mechanisms in the synthesis of proteins. *Journal of Molecular Biology*, 3:318–356, 1961.
- [43] O. Karin, A. Swisa, B. Glaser, Y. Dor, and U. Alon. Dynamical compensation in physiological circuits. *Molecular Systems Biology*, 12:1–7, 2016.
- [44] E. Kaszkurewicz and A. Bhaya. *Matrix diagonal stability in systems and computation*. Springer Science+Business, New York, USA, 2000.
- [45] M. Khammash. Perfect adaptation in biology. *Cell Systems*, 12(6):509–521, 2021.
- [46] M. H. Khammash. Cybergenetics: Theory and applications of genetic control systems. *Proceedings of the IEEE*, 110(5):631–658, 2022.
- [47] O. Y. Kushel. Unifying matrix stability concepts with a view to applications. *SIAM Review*, 61(4):643–729, 2019.
- [48] W. Ma, A. Trusina, H. El-Samad, W. A. Lim, and C. Tang. Defining network topologies that can achieve biochemical adaptation. *Cell*, 138:760–773, 2009.
- [49] J. Monod, J.-P. Changeux, and F. Jacob. Allosteric proteins and cellular control systems. *Journal of Molecular Biology*, 6:306–329, 1963.
- [50] D. Muzzey, C. A. Gómez-Urbe, J. T. Mettetal, and A. van Oudenaarden. A systems-level analysis of perfect adaptation in yeast osmoregulation. *Cell*, 97(9):160–171, 2009.
- [51] A. Nanda, S. S. Nasker, A. Mehra, S. Panda, and S. Nayak. Inteins in science: Evolution to application. *Microorganisms*, 8(12):2004, 2020.
- [52] X. Y. Ni, T. Drengstig, and P. Ruoff. The control of the controller: Molecular mechanisms for robust perfect adaptation and temperature compensation. *Biophysical journal*, 97:1244–1253, 2009.
- [53] K. Oishi and E. Klavins. Biomolecular implementation of linear I/O systems. *IET Systems Biology*, 5(4):252–260, 2010.
- [54] N. Olsman, A.-A. Baetica, F. Xiao, Y. P. Leong, and R. M. Murray. Hard limits and performance tradeoffs in a class of antithetic integral feedback networks. *Cell Systems*, 9:1–15, 2019.
- [55] N. Olsman, F. Xiao, and J. C. Doyle. Architectural principles for characterizing the performance of antithetic integral feedback networks. *iScience*, 14:277–291, 2019.
- [56] T. Plesa, A. Dack, and T. E. Oulridge. Integral feedback in synthetic biology: Negative-equilibrium catastrophe. *Journal of Mathematical Chemistry*, 2023.
- [57] Y. Qian and D. Del Vecchio. Realizing “integral control” in living cells: How to overcome leaky integration due to dilution? *Journal of the Royal Society: Interface*, 15:20170902, 2018.
- [58] Y. Qian and D. Del Vecchio. A singular singular perturbation problem arising from a class of biomolecular feedback controllers. *IEEE Control Systems Letters*, 3(2):236–241, 2019.

- [59] A. Rantzer. On the Kalman-Yakubovich-Popov lemma. *Systems & Control Letters*, 28(1):7–10, 1996.
- [60] D. Richeson and J. Wiseman. A fixed point theorem for bounded dynamical systems. *Illinois Journal of Mathematics*, 46(2):491–495, 2002.
- [61] D. Richeson and J. Wiseman. Addendum to “a fixed point theorem for bounded dynamical systems”. *Illinois Journal of Mathematics*, 48(3):1079–1080, 2004.
- [62] P. T. Saunders, J. H. Koeslag, and J. A. Wessels. Integral rein control in physiology. *Journal of Theoretical Biology*, 194:163–173, 1998.
- [63] R. Scheepers and R. P. Araujo. Robust homeostasis of cellular cholesterol is a consequence of endogenous antithetic integral control. *Frontiers in Cell and Developmental Biology*, 11:1244297, 2023.
- [64] A. P. Seyranian and A. A. Mailybaev. *Multiparameter stability theory with mechanical applications*. World Scientific, Singapore, 2003.
- [65] O. Shoval, U. Alon, and E. Sontag. Symmetry invariance for adapting biological systems. *SIAM Journal on Applied Dynamical Systems*, 10(3):857–886, 2011.
- [66] E. Sontag. Adaptation and regulation with signal detection implies internal model. *Systems & Control Letters*, 50(2):119–126, 2003.
- [67] J. F. Sturm. Using SEDUMI 1.02, a Matlab Toolbox for Optimization Over Symmetric Cones. *Optimization Methods and Software*, 11(12):625–653, 2001.
- [68] L. G. Treviño-Quintanilla, J. A. Freyre-González, and I. Martínez-Flores. Anti-sigma factors in e. coli: Common regulatory mechanisms controlling sigma factors availability. *Current Genomics*, 14:378–387, 2013.
- [69] R. H. Tütüncü, K. C. Toh, and M. J. Todd. Solving semidefinite-quadratic-linear programs using SDPT3. *Mathematical Programming Ser. B*, 95:189–217, 2003.
- [70] A. van der Schaft. *L₂-Gain and Passivity Techniques in Nonlinear Control*. Springer-Verlag, London, 2000.
- [71] E. O. Voit. *Computational Analysis of Biochemical Systems*. Cambridge University Press, 2000.
- [72] S. Walcher. On cooperative systems with respect to arbitrary orderings. *Journal of Mathematical Analysis and Applications*, 263:543–554, 2001.
- [73] H. Wang, .: Wang, B. Zhong, and Z. Dai. Protein splicing of inteins: A powerful tool in synthetic biology. *Frontiers in Bioengineering and Biotechnology*, 10:2022, 2022.
- [74] N. Wiener. *Cybernetics: or the Control and Communication in the Animal and the Machine*. MIT Press, 1961.
- [75] J. C. Willems. Least squares stationary optimal control and algebraic Ricatti equation. *IEEE Transactions on Automatic Control*, 16(6):621–634, 1971.
- [76] F. Xiao and J. C. Doyle. Robust perfect adaptation in biomolecular reaction networks. *BioRxiv*, page 299057, 2018.
- [77] F. Xiao and J. C. Doyle. Robust perfect adaptation in biomolecular reaction networks. In *57th IEEE Conference on Decision and Control*, pages 4345–4352, Miami Beach, FL, USA, 2018.
- [78] J Yang and S. A. Prescott. Homeostatic regulation of neuronal function: importance of degeneracy and pleiotropy. *Frontiers in Neuroscience*, 17:1184563, 2023.

- [79] T.-M. Yi, Y. Huang, M. I. Simon, and J. Doyle. Robust perfect adaptation in bacterial chemotaxis through integral feedback control. *Proceedings of the National Academy of Sciences*, 97(9):4649–4653, 2000.